University of Zululand

University of Zululand
Faculty of Science and Agriculture
Department of Physics

Determination of the Spectroscopic Quadrupole Moment of ^{40}Ar

Elijah Hornam Akakpo

A thesis presented for the degree of
Master of Science in Physics

Supervisor: Prof. S. S. Ntshangase[1]
Co-supervisors: Prof. J. N. Orce[2]
University of Zululand[1]
University of the Western Cape[2]

January 2019

Abstract

Coulomb excitation reorientation effects measurement was performed at the AFRODITE vault of iThemba LABS to determine the $Q_s(2_1^+)$ of ^{40}Ar. A beam of ^{40}Ar at a laboratory energy of 134.94 MeV was Coulomb excited on a ^{194}Pt target at a safe distance between nuclear surfaces of 6.5 fm. The backward scattered ^{40}Ar particles were detected by an S3-CD double sided silicon detector at a distance of 30 mm with an angular range of 130° to 159°. Eight HPGe clover detector array (five at 90° and three at 135° to the beam axis) was employed to detect the de-excited γ-ray energy emitted by the ^{40}Ar particles. The ^{40}Ar particles and their corresponding γ-rays were collected in coincidence and stored. MTsort MIDAS was used in conjunction with an offline sorting code to sort the coincidence data. Coulomb excitation analytical code, GOSIA, was used to extract the diagonal matrix element, $\langle 2_1^+ \| E2 \| 2_1^+ \rangle = 0.00(4)$ eb. From the relation, $\langle 2_1^+ \| E2 \| 2_1^+ \rangle = \frac{Q_s}{0.75793}$, the $Q_s(2_1^+)$ was determined as +0.00(3) eb. This result indicates a spherical shape for ^{40}Ar at the 2_1^+ state.

Acknowledgments

Glory be to God in the highest, through His grace, mercy and love this research has come to fruition. May His holy name be praised.

To Prof J. N. Orce and Prof S. S. Nsthangase for the opportunity afforded me to be a part of your success story, I say thank you and may you continue to be a leading star and inspire more young scientists. One could not have asked for better supervisors.

Dr. M. K. Raju and Dr. K. Kapoor, thank you for your active involvement towards the completion of this work.

To the UWC Coulex group (Craig, Jerry, Kenzo, Mavela, Cebo and Senamile), I appreciate your support and contribution towards my success story. More laurels to us in our future endeavours.

To the department of Physics and Engineering (UNIZULU) and the department of Physics and Astronomy (UWC), I am grateful for all the support I received in completing this research work.

To the Nuclear Physics department of iThemba LABS, your assistance and guidance in running the experiment is much appreciated. Thank you.

To the National Research Foundation for the financial support.

To my beautiful and lovely wife Emmanuella Elikplim Akakpo, your prayers, love and care carried me through tough times. Thank you for all the encouragement and support, You are a rare gem.

And last but not the least, my father (Andreas), mother (Alice) and beloved brothers (Seli, Eli and Edem), I say thanks for all your support and prayers. Without you this journey would have been almost impossible.

Declaration

I declare that apart from the recognized references and help, the dissertation submitted for the Master of Science in Physics to the University of Zululand is my own work and has not been submitted to any other University for a degree.

Elijah Hornam Akakpo

Signed: ..... Date: .....

Contents

List of Figures

List of Tables

Chapter 1

Introduction

The quest to unravel and understand the myths surrounding the structure of the atomic nucleus is like an unquenchable thirst for nuclear physicists. A fundamental goal of the study of nuclear structure physics is to understand the interaction of atomic nucleons through both the long and short range forces and how these affect the properties of the atomic nucleus.

Many theoretical and experimental techniques have been developed to achieve this goal. One such technique is the Coulomb excitation. Coulomb excitation plays a pivotal role in understanding nuclear collectivity. Its main advantage is, if the reaction or interaction is done well below the Coulomb barrier, nuclear effects are negligible and hence the excitation depends solely on the well understood electromagnetic interaction which is a long range force.

Nuclei can be excited through the electromagnetic interaction when the target nucleus is bombarded with energetic charged particles. If the bombarding energy is greater than the Coulomb barrier, a compound nucleus can be formed. This idea was first suggested by Weisskopf in 1938 [1], but the first γ-ray spectroscopic studies were observed in 1953 [2]. The dynamic and

static properties of the low-lying nuclear states are well explained by the collective model of Bohr and Mottelson [3]. The model provides a simplistic understanding of the spin and parity, de-excitation modes and moments [3].

1.1 The Nuclear Atom

The concept of matter consisting of discrete particles surfaced among the ancient Greek philosophers. The concept was utilized by John Dalton in the 1800s to explain the number ratios of the masses of the components of compounds and molecular constitution. This became the first evidence for a theory of the atom [5].

Becquerel in 1896 observed radioactivity by the fogging of photographic plates from radiation emanating from uranium rocks [5]. The atomic structure was described by Thomson in the early 20^{th} century as a positively charged sphere with negative electrons uniformly embedded through it [6]. He discovered the electrons and measured the charge-to-mass ratio of the electron in 1879. Ernst Rutherford and his students in 1910 performed the famous alpha (α) particle scattering experiment shown in Fig. 1.1. Three observations were made;

i Most of the α particles passed through the gold foil unscattered.

ii Few α particles were scattered through small angles.

iii Extremely few α particles were scattered at backward angles.

From these observations, it was concluded that the atom consists of space filled with electrons resulting in most of the α particles passing through it unscattered. The few particles that were scattered through small angles

came close to a positive core that occupies a very small space. Finally, the extremely small number that got scattered backward came head-on with the positively charged core concentrated in a small volume within the atom.

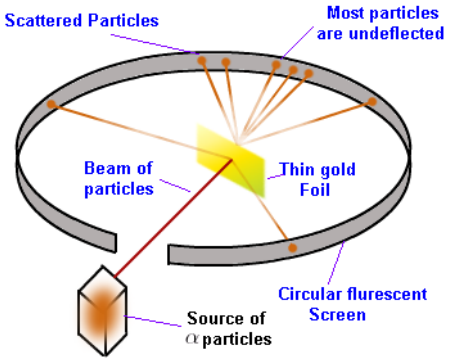

Figure 1.1: Rutherford α particle experiment; A beam of α particles is directed at a thin gold foil [7].

1.2 Argon

There are twenty four known isotopes of argon of which three are stable. The nucleus ^{32}Ar has an isomer at 5600 keV. Of the three stable isotopes (^{36}Ar, ^{38}Ar and ^{40}Ar), ^{40}Ar is the most abundant with a relative abundance of 99.6% on earth. The longest-lived radioactive isotope of argon is ^{39}Ar, with a half-life of 269 years. It is produced by cosmic rays and also decay to ^{39}K through β^- decay. Argon is an inert gas and is mostly used for welding to protect the weld region since it is unreactive. It is also used in the production of titanium and in low-energy bulbs. Arguably, the most significant use of argon in the scientific community is the Ar-Ar or ^{40}Ar/^{39}Ar dating in archaeology and geochronology [8]. This dating technique is an improvement on the previous K-Ar dating and the U-Pb and U-He dating techniques. The ^{40}Ar/^{39}Ar

dating technique can be used to date a wide variety of archaeological artifacts. Every potassium containing rock or mineral can be dated using this advanced $^{40}Ar/^{39}Ar$ dating technique. Additionally, ^{40}Ar is a very stable nucleus (see position on the nuclear chart in Fig. 1.2). Some of the main chemical and physical properties of Ar are listed in Table 1.1.

Table 1.1: Some chemical and physical properties of Argon [9].

Atomic Number	18
Atomic Mass	39.948
Density	1.633×10^{-3}
Melting Point	83.81 K
Boiling Point	87.30 K
State at Room Temperature	Gas

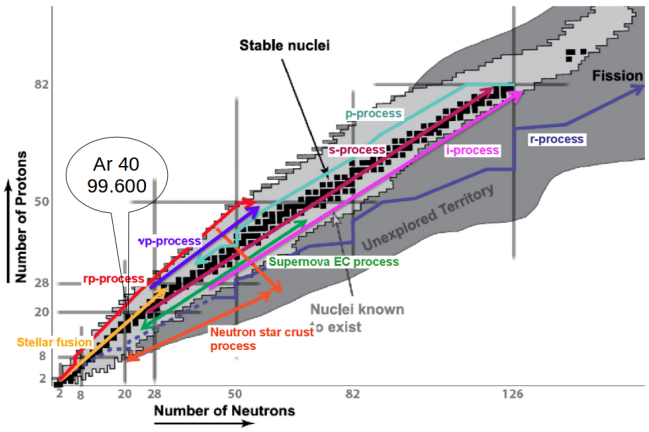

Figure 1.2: Chart of Nuclides with nuclear processes and position of ^{40}Ar [10]

1.3 Quadrupole Moment and Nuclear Shape

The basic shape of a nucleus is a measure of its deviation from a sphere. One of the ways of experimentally measuring the nuclear shape is by measuring its intrinsic (Q_o) or spectroscopic (Q_s) quadrupole moment. An effective and reliable experimental technique used for measuring Q_s is through the reorientation effect in Coulomb excitation [11]. The quadrupole operator for a spherical nucleus is defined as;

$$\langle \hat{Q} \rangle = e(3z^2 - r^2) = er^2(3\cos\theta - 1) = \sqrt{\frac{16\pi}{5}} er^2 Y_{20}(\theta, \phi), \tag{1.1}$$

where $r^2 = x^2 + y^2 + z^2$, and x, y and z are the distances from the center to the surface of the sphere in $\hat{\imath}$, $\hat{\jmath}$, $\hat{k}$ -directions in a Cartesian coordinate system. Y_{20} is a spherical harmonic. Since $3z^2 = r^2$ for a spherical shape, $\langle \hat{Q} \rangle = 0$. The quadrupole moment of a nuclear state is defined as the expectation value of the quadrupole operator in the maximum magnetic substate, M. The quadrupole moment, Q_o, in the intrinsic frame of the nucleus can also be determined by measuring the reduced transition probability, $B(E2)$, of the transition. Q_o and $B(E2)$ values are related by,

$$B(E2, 0_1^+ \rightarrow 2_1^+) = \frac{5}{16\pi} Q_o^2. \tag{1.2}$$

From the rotational model, Q_o and Q_s are related by,

$$Q_s = \frac{3K^2 - J(J+1)}{(2J+3)(J+1)} Q_o, \tag{1.3}$$

where K is the projection of the total angular momentum, J, onto the symmetry axis. For transitions from the ground state to the first 2^+ state, where

$K = 0$ and $J = 2$,

$$Q_s(2_1^+) = -\frac{2}{7}Q_o. \tag{1.4}$$

The nuclear shapes, illustrated in Fig. 1.3, is dependent on the value of Q_o. A positive value ($Q_o > 0$) corresponds to a prolate deformation, $Q_o = 0$ corresponds to a spherical shape, and the third shape ($Q_o < 0$) corresponds to an oblate quadrupole deformation.

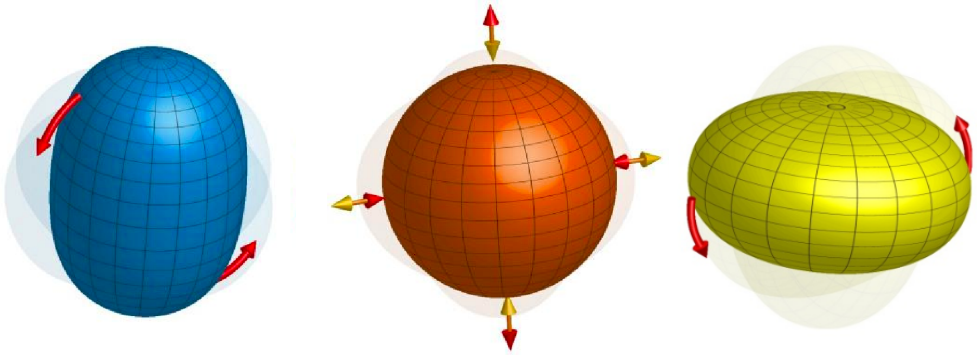

(a) Prolate shape: $Q_s > 0$. (b) Spherical: $Q_s = 0$. (c) Oblate shape: $Q_s < 0$

Figure 1.3: Nuclear shape and its dependence on the sign of the Q_s [12].

1.4 Motivation of the Study

Theoretical models and experimental results have provided us information about the shapes and other properties of the atomic nucleus. Spectroscopic quadrupole moment of the first excited 2_1^+ states, $Q_s(2_1^+)$, of most light nuclei have been extensively studied through Coulomb excitation reorientation effect measurements. The process, Coulomb excitation, employs the well understood electromagnetic interaction which excites collective nuclear states. Many research groups have exploited this process in studying $Q_s(2_1^+)$ values

in the *sd* shells of light even-even nuclei [13]. The results and evaluation of these measurements, shown in Fig. 1.4, reveals an interesting trend. Beginning with an almost spherical shape is ^{18}O. A larger prolate deformation in ^{20}Ne can be observed with a gradual decreasing prolate deformation in ^{26}Mg. A drastic and large oblate deformation is then observed in ^{28}Si and then a nearly spherical shape of ^{30}Si is formed in the middle of the *sd* shell, maintaining this zig-zag pattern to the end of the *sd* shell with another nearly spherical shape in ^{40}Ar.

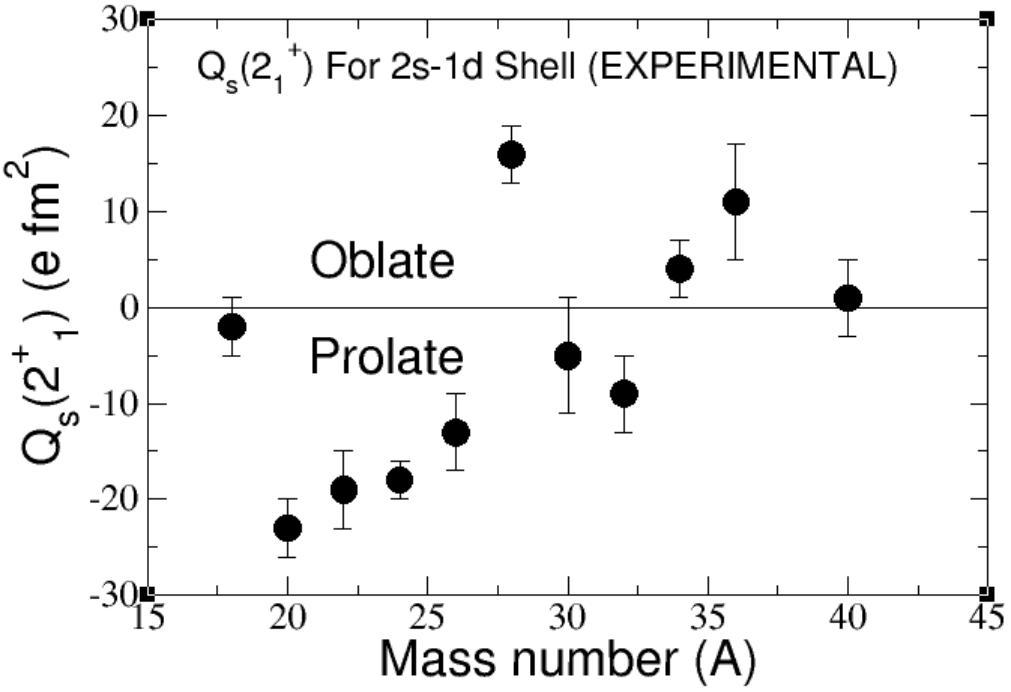

Figure 1.4: Experimental values of $Q_s(2_1^+)$ for some nuclei in the *sd* shell obtained from Coulomb excitation reorientation effect measurements [13].

The $Q_s(2_1^+)$ trend in the *sd* shell also remained relatively unchanged in the various Coulomb excitation reorientation effect measurements carried out at iThemba LABS by Coulomb excitation group at the University of the Western Cape [14, 15].

There is only one reorientation effect measurement, listed in Table 1.2, for ^{40}Ar with $Q_s(2_1^+)_{RE} = +1.0\ (4)$ efm^2 (almost spherical in shape) [16]. In this measurement, an undefined minimum separation between nuclear surfaces, $S(\vartheta)$, was used [13].

$$S(\vartheta) = \frac{0.72 \times Z_t Z_p}{E}(1 + \frac{A_p}{A_t})\Big[1 + cosec(\frac{1}{2}\vartheta)\Big] - 1.25(A_p^{\frac{1}{3}} + A_t^{\frac{1}{3}}), \qquad (1.5)$$

where Z_t and Z_p are the atomic numbers of the target and projectile, A_t and A_p the mass numbers of the target and projectile, E the beam energy and ϑ the center-of-mass scattering angle.

Table 1.2: Experimental determination of Q_s for ^{40}Ar (E_x = 1.461 MeV) through the previous Coulomb excitation reorientation effect measurement [13, 16].

Auther	Year	$Q_s(2_1^+)$ (eb)	Target	Beam energies	$S_{min}(\vartheta)$
Nakai	1970	+0.01(4)	^{120}Sn/^{130}Te/^{206}Pb	unknown	unknown

The bombarding energy used in these measurements was unknown and very little information about the target, ^{206}Pb, was known with an assumed value of $Q_s(2_1^+) = +0.0 \pm 0.5 \mid Q^{rot} \mid$ adopted for the analysis. The value of $Q_s(2_1^+)$ for ^{206}Pb was later determined to be 0.17±0.31 eb [16]. This single measurement of the $Q_s(2_1^+)$ value as seen in Fig. 1.5 and Table 1.2, is still the accepted value in the NNDC database [17]. As stated by Spear, further experimental work with well-defined parameters is clearly desirable [13]. The safe minimum distance, unlike the impact parameter, (perpendicular distance between the direction of approaching particle and the center of the target nucleus), is the minimum distance between the centers of approaching particle and the target just before it scatters to minimize the nuclear effect.

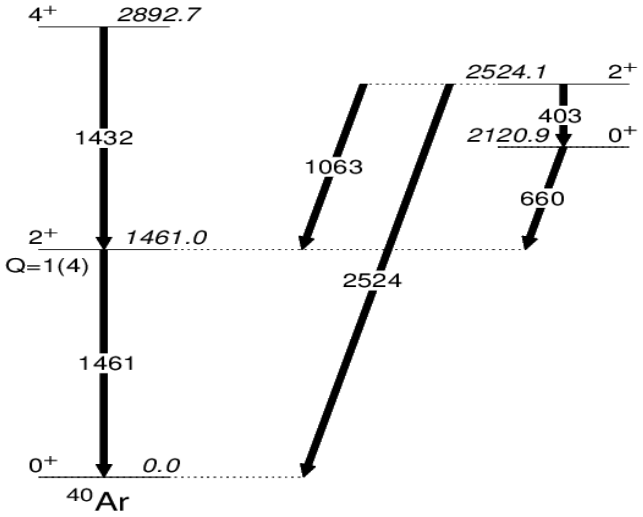

Figure 1.5: Partial level scheme of ^{40}Ar with $Q_s(2_1^+)_{RE} = 1(4)$ e fm^2 [16, 17, 18].

This research projects employed the Coulomb-excitation reorientation effect and the particle-γ coincidence technique to study the $Q_s(2_1^+)$ value in ^{40}Ar. A beam of ^{40}Ar with a charge state of $^+6$ and a safe energy of 134.9(5) MeV bombarded a ^{194}Pt target at a minimum safe distance of $S(\vartheta) = 6.5$ fm. The AFRODITE array of clover detectors at iThemba LABS was used. The de-excitation γ rays were detected using the HPGe clover detectors at angles of 90° and 135°. The excited ^{40}Ar particles were also detected using an S3 CD-type silicon detector at backward scattering angles ranging between 130° to 160° in the laboratory frame. The diagonal matrix element, $\langle 2_1^+ \| \hat{E}2 \| 2_1^+ \rangle$, was extracted using the Coulomb excitation data analysis code, GOSIA [19].

The framework of this thesis consists of the theory of Coulomb excitation and conditions for a safe Coulomb excitation experiment is discussed in Chapter 2, the experimental procedure in Chapter 3 and the data analysis in Chapter 4. The discussion of the result and recommendations are in Chapter 5.

Chapter 2

Literature and Theoretical Review

Many theories and models have been developed and employed to describe the structure and properties of the atomic nuclei. None of the theories available so far could explain the nuclear behavior thoroughly. Coulomb Excitation (CE) is one of these techniques. It is a model-independent probe and is based on the well understood electromagnetic interaction. The process involves the bombardment of target nuclei by projectiles at beam energies well below the Coulomb barrier. The separation distance, $S_\vartheta min$, between the two nuclear surfaces must be ≥ 6.5 fm for light nuclei [13, 20] to excite the nucleus solely through the electromagnetic interaction.

This chapter will discuss the technique and theory of CE as a powerful experimental tool for low-lying collective nuclear structure studies. It will also discuss some nuclear models, conditions and parameters to be considered to perform a successful CE experiment.

2.1 The Liquid Drop Model

One of the earliest nuclear models developed to explain the structure of the atomic nucleus is the Liquid Drop Model (LDM). In this model, the nucleus is likened to a classical liquid drop where the protons and neutrons form an incompressible droplet of liquid [21].

According to the LDM, nucleons inside the droplet should have an analogous interaction. Von Weizsäcker in 1935 used the LDM as the basis to explain the nuclear binding energy and later to formulate the semi-empirical mass formula (SEMF) [21].

$$E_B = a_v A - a_s A^{\frac{2}{3}} - a_c Z \frac{(Z-1)}{A^{\frac{1}{3}}} - a_A \frac{(N-Z)^2}{A} \pm \delta(A,Z), \tag{2.1}$$

where E_B is the binding energy of a given nucleus. $a_v A$, the volume energy term which describes the mass dependence on the nuclear force. The interior nucleons interacts with each other within the range of the nuclear force. The total binding energy is proportional to the number of interacting nucleons and hence proportional to the nuclear volume. The second term is the surface correction term. The effect of the nuclear force on the surface nucleons of the nucleus, compared to interior nucleons is very small. For the nuclear force to be proportional to the nuclear volume, the binding energy must be constant, hence, the surface correction term, $a_s A^{\frac{2}{3}}$, is subtracted from the volume energy term to correct this discrepancy.

Another term that contributes negatively to the binding energy is the Coulomb energy term. This term, $a_c Z \frac{(Z-1)}{A^{\frac{1}{3}}}$, represents the repulsive electromagnetic force that exist between the protons. The symmetry term, $a_A \frac{(N-Z)^2}{A}$, stems from the Pauli exclusion principle and describes the energy lost due to the effective force between unlike nucleons being greater than that between similar nucleons. The final term is the pairing term, $\delta(A,Z)$, which indicates the

contribution of unpaired nucleons to the binding energy of the nucleus. This term employs the Pauli's exclusion principle to increase or decrease the binding energy of the nucleus. For a nucleus with an even A, $\delta(A,Z) > 0$ if $N = Z$ is even and E_b decreases. E_b increases if Z and N are odd ($\delta(A,Z) < 0$) with A even. The binding energy is unaffected by the pairing term if A is odd since $\delta(A,Z) = 0$.

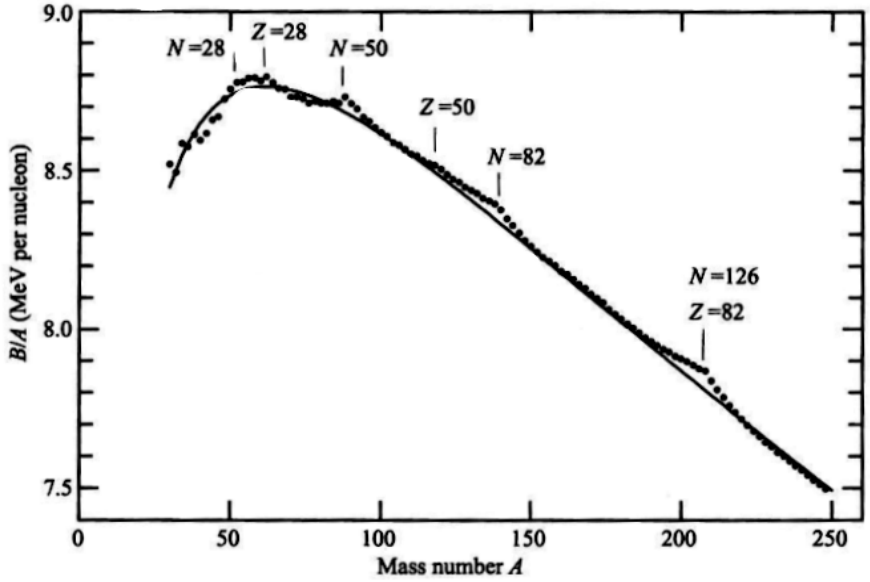

Figure 2.1: Binding energy per nucleon, B/A, as a function of mass number, A. The dotted curve represents experimental values and the smooth curve represents semi-empirical mass formula [21].

Masses calculated using the semi-empirical mass formula agrees with the experimental values in Fig. 2.1 within the mass region of $A \geq 20$. Even though the LDM has succeeded in explaining some collectivity in nuclei, it also have some major limitations. Due to the macroscopic nature of LDM,

many of the microscopic properties gets neglected. In an attempt to get the lost nuclear properties, the Nuclear Shell Model was developed to describe the atomic nuclei at the microscopic level.

2.2 The Shell Model

Fundamentally, the atomic nucleus is made up of nucleons (positively charged protons and neutral neutrons). The nucleus is held together by two competing forces, the long range weak Coulomb force, which causes like charges to repel each other, and the short range strongly attractive nuclear force. The interactions between the nucleons can be approximated using the single-particle potential [22, 27] such as the square well potential or the harmonic oscillator potential. These interactions and approximations are the principles behind the shell model.

The valence nucleons in a nucleus just like electrons in an atom, oscillates and provides a potential within which the nucleons are bound. Given that the potential is assumed to be spherical, the potential can be compared to that of a simple harmonic oscillator, given by,

$$V(x) = \frac{1}{2}Kx^2 = \frac{1}{2}m\omega^2x^2, \tag{2.2}$$

where $\omega^2 = \frac{K}{m}$ and K and m are wave number and mass, respectively. The associated Hamiltonian with the potential is,

$$H = \frac{p^2}{2m} + \frac{1}{2}m\omega^2x^2. \tag{2.3}$$

The wave equation associated to the Hamiltonian for a given energy eigenstate is,

$$\frac{-\hbar^2}{2m}\frac{d^2\psi_{nlm}}{dx^2} + \frac{1}{2}Kx^2\psi_{nlm} = E\psi_{nlm}, \tag{2.4}$$

where ψ_{nlm} represents the wave function with its associated energy eigenvalue given as;

$$E_n = (N + \frac{3}{2})\hbar\omega, \tag{2.5}$$

in 3D space. The wave function, ψ_{nlm} is given by,

$$\psi_{nlm}(x) = (\frac{m\omega}{\pi\hbar})^{\frac{1}{4}} e^{(\frac{-m\omega x^2}{2\hbar})}, \tag{2.6}$$

where N corresponds to the major oscillator quantum number and n, l, m are the principal, orbital momentum and magnetic quantum numbers, respectively.

There is also evidence that suggests extra stability for nuclei with certain proton and neutron numbers [28]. As shown in Fig. 2.1, a spike in the binding energy per nucleon for nuclei with neutron numbers N = 28, 50, 82 and 126 is observed. A similar trend can be seen in Fig. 2.2, where a plot of two-neutron separation energy, as a function of neutron number, shows a sharp rise at neutron numbers N = 2, 8, 20, 28, 50, 82 and 126. These numbers are called magic numbers and nuclei with neutron number equal to these numbers exhibits high stability.

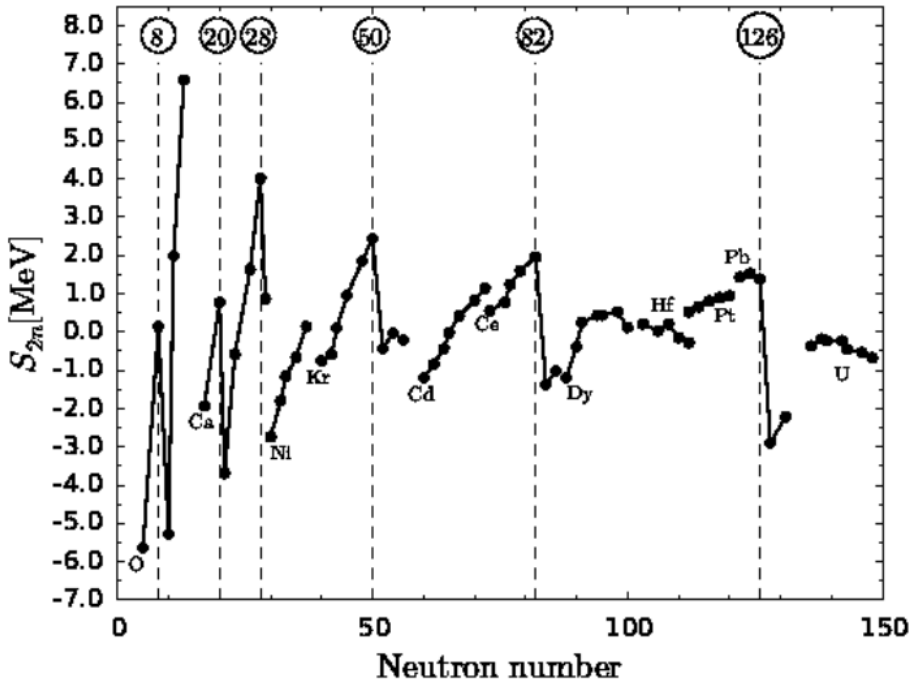

Figure 2.2: A two-neutron separation energy, plotted as a function of neutron number, showing energy spikes at the neutron magic numbers, N=2, 8, 20, 28, 50, 82 and 126 [21].

The energy gaps on the left in Fig. 2.2, could not be observed experimentally. To account for this discrepancy, the term l^2, (orbital angular momentum squared), was introduced into the simple harmonic oscillator potential. The addition of l^2 reduced the dependence of the energy levels with the splitting up of levels where $l > 0$. This however, did not correct the energy gap. A second term, which involves the spin-orbit(SO) interaction, was introduced into the simple harmonic oscillator potential to correct the energy gaps predicted by the shell model. The spin-orbit potential has the form, $-V_{so}(r)l\cdot s$, where l and s are the orbital and angular momenta respectively. The binding energy changes depending on the alignment of l and s, it increases if l and s

are parallel and decreases if anti-parallel. The splitting of the energy levels depends on the SO potential which is proportional to $l \cdot s$. The total angular momentum, j, is given by; $j = l + s$

$$j^2 = (l + s)^2 = l^2 + s^2 + 2l \cdot s, \tag{2.7}$$

where

$$\langle l \cdot s \rangle = \frac{1}{2}[j(j+1) - l(l+1) - s(s+1)]\hbar^2. \tag{2.8}$$

Since $s = \pm\frac{1}{2}$
$\langle l \cdot s \rangle = \frac{1}{2}\hbar^2$ for $s = +\frac{1}{2}$ and $-\frac{1}{2}(l+1)\hbar^2$ for $s = -\frac{1}{2}$ where $l \neq 0$.

The splitting up of the energy level for l is thus proportional to $2l + 1$ for $l > 0$ and predicts the experimental observations in the energy gaps of the magic numbers fairly well as seen in Fig. 2.3. However a better prediction is made with the introduction of the Woods-Saxon potential.

$$V = \frac{V_0}{1 + e^{(\frac{r-R}{a})}}, \tag{2.9}$$

where V_0 is approximately 50 MeV, $R = 1.2A^{\frac{1}{3}}$ fm is the radius of the nucleus and $a \approx 0.60$ fm is the diffuseness parameter [23].

The nuclear shell model provides a significant insight into the structure of the atomic nucleus [24]. However a great deal still remains, especially simplification of the many-body problem. The complexity of the nucleon interaction makes the simplification a daunting task. Since the model did not account for the residual interactions, $\sum_{ij} v(r_i, r_j)$, such as pairing, clustering and neutron-proton interactions that results in shape mixing, shape coexistence or super deformity in nuclei [25, 26], it presents an incomplete collective model. The addition of the potential of the residual interactions to the Hamiltonian of the shell model gives an excellent approximation of nuclear collectivity.

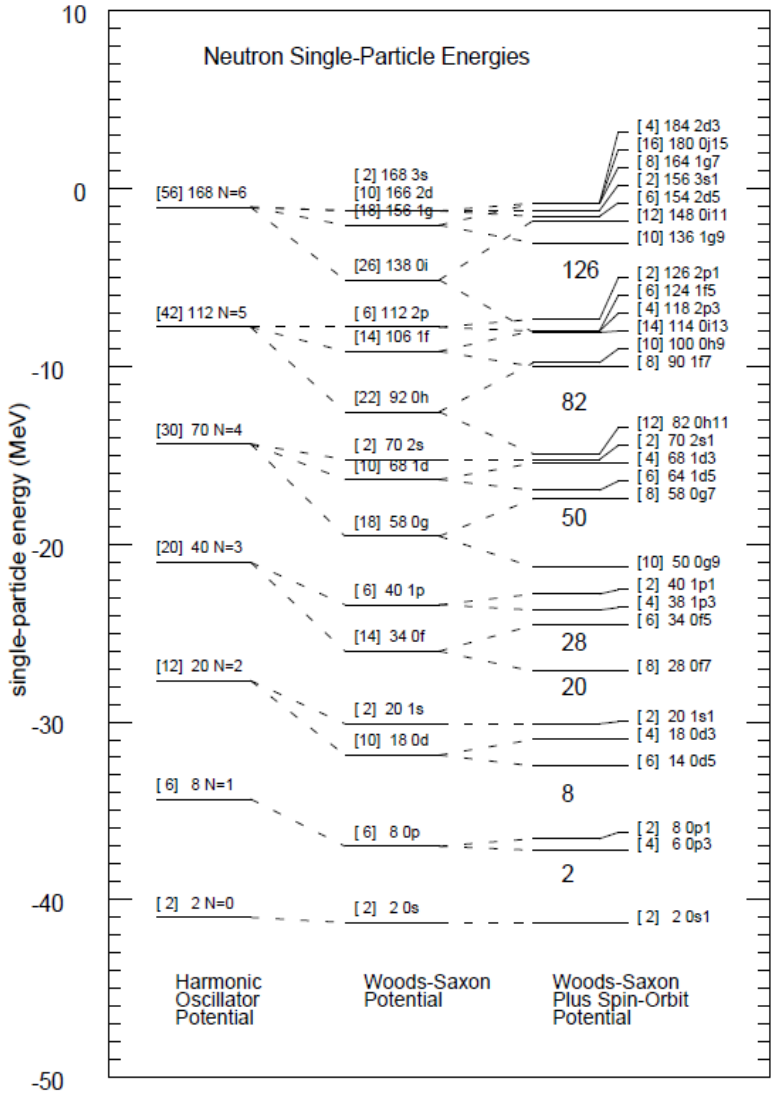

Figure 2.3: Single-particle energy for different Nlj orbits. Numbers in square brackets represents allowable number of protons (or neutrons) in each state and bold numbers represents magic numbers [21]

2.3 Theory of Coulomb Excitation

Coulomb excitation is a powerful tool used to get insight into the nuclear collectivity. This is because the theory is model independent and since the projectile moves in a hyperbolic trajectory, the excitation process is treated semi-classically. The technique is solely based on the electromagnetic field interactions of the nuclei involved. This permits the use of the well-understood electromagnetic field theory to describe the process. For accurate measurements, when semi-classically treated, two assumptions are considered:

i) The particle can be described as a wave with dimensions smaller than the half-distance of closest approach on a head-on collision.

ii) The energy loss by the incident particle is small compared with the bombarding energy.

The accuracy and success of the CE process is based on the implementation of the above mentioned considerations. For consideration **i**), the Sommerfeld parameter, η, defined as a measure of the ratio of half the distance of closest approach, a, to the de-Broglie wavelength, $\frac{2\pi}{\lambda}$, should be much greater than unity; $\eta \gg 1$

$$\eta = \frac{2\pi a}{\lambda} = \frac{Z_T Z_P e^2}{\hbar \nu_\infty} \gg 1, \tag{2.10}$$

where Z_T and Z_P are the atomic numbers of the target and projectile nuclei respectively and ν_∞ is the velocity of the projectile in the laboratory frame.

In fulfilling the second assumption, a heavy target, compared to the projectile, is used and the bombarding energy of the projectile is far below the Coulomb barrier. The implementation of these considerations results in the elimination or minimization of the effect of the nuclear force and makes the technique an advantageous tool for nuclear spectroscopy.

Coulomb excitation is therefore an excellent tool for determining the electromagnetic transition matrix elements and reduced transition probabilities. Diagonal matrix elements are used to calculate the spectroscopic quadrupole moment, an electromagnetic property of the nuclei which plays a monumental role in acquiring significant information on the nuclear shape which, in turn, can be used to benchmark modern nuclear models [29]. The classical treatment involves the movement of the projectile being considered hyperbolic, as seen in Fig. 2.4, since the projectile experiences a repulsive Coulomb force from the target nucleus. The scattering of the projectile obeys the Rutherford scattering equation with a scattering differential cross section given by,

$$d\sigma_R = \frac{1}{4}a^2 sin^{-4}\Big(\frac{\vartheta}{2}\Big)d\Omega, \tag{2.11}$$

where σ_R is the Rutherford cross section, a half the distance of closest approach in a head-on collision and ϑ the center-of-mass scattering angle.

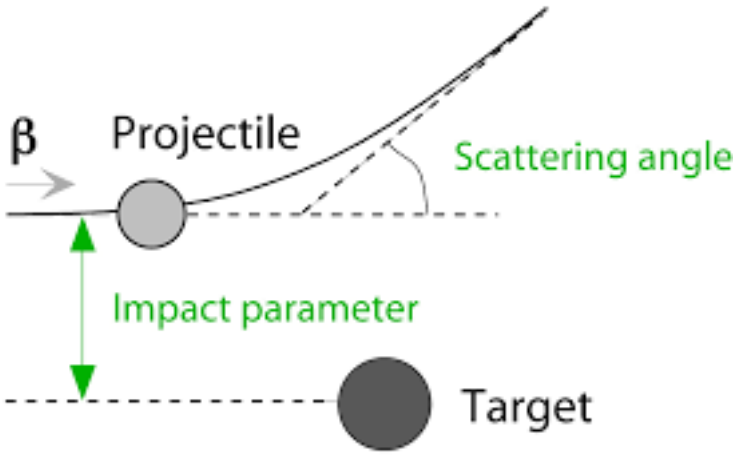

Figure 2.4: Coulomb excitation of a projectile by a target following a classical Rutherford hyperbolic trajectory.

The excitation of either the projectile or the target occurs at the nuclear collision site and assuming that the particle's orbit is not affected by the

excitation, the CE cross section, $d\sigma_{CE}$, can be given by the Rutherford differential cross section multiplied by the excitation probability,P_{i-f},

$$d\sigma_{CE} = P_{i-f} d\sigma_R, \tag{2.12}$$

where P_{i-f} can be expressed in terms of the transition amplitude from the initial $|i\rangle$ or ground state to the final $|f\rangle$ state,

$$P_{i-f} = (2I_i + 1)^{-1} \sum_{m_i m_f} |b_{if}|^2, \tag{2.13}$$

where I_i is the spin of the initial state, b_{if} the excitation amplitude between the initial and final states and m_i and m_f are the initial and final magnetic quantum numbers, respectively.

If the excitation amplitude is very small compared to unity, a first order perturbation theory can be applied to the treatment of the excitation, where b_{if} is defined as,

$$b_{if} = \frac{1}{i\hbar} \int_{-\infty}^{+\infty} \langle f|H_{int}(t)|i\rangle e^{i\omega t} dt, \tag{2.14}$$

and H_{int} is the time-dependent electromagnetic interaction and $\omega = \frac{E_f - E_i}{\hbar}$ is the nuclear frequency. The transition amplitude, b_{if}, for electric multiple transition order, λ, can be separated into orbital and nuclear parts.

$$b_{if}^{(1)} = (-i)(-1)^{I_i - m_i} (2I_i + 1)^{\frac{1}{2}} \chi_{i\to f}^{\lambda} \sum_{\mu} \begin{pmatrix} I_i & \lambda & I_f \\ -m_i & \mu & m_f \end{pmatrix} \mathcal{K}(\vartheta, \xi), \tag{2.15}$$

The strength of the electric transition is measured by the dimensionless quantity,

$$\chi_{i\to f}^{\lambda} = (16\pi)^{\frac{1}{2}} \frac{(\lambda+1)!}{(2\lambda+1)!!} \frac{Ze}{\hbar\varepsilon_\infty} \frac{\langle I_i \| M(E\lambda) \| I_f\rangle}{a^\lambda \sqrt{2I_i + 1}}, \tag{2.16}$$

where $\langle I_i \| M(E\lambda) \| I_f\rangle$ is the reduced transition matrix element and it is related to the reduced transition probability,$B(E\lambda : I_i \to I_f)$, by

$$B(E\lambda : I_i \to I_f) = \frac{1}{2I_i + 1} |\langle I_i \| M(E\lambda) \| I_f\rangle|^2. \tag{2.17}$$

The transition depends on probabilities of the projectile in $\mathcal{K}$ in Eq. 2.14,

$$\mathcal{K}(\theta,\xi) = \sqrt{\pi}\frac{(2\lambda-1)!!}{(\lambda-1)!}Y_{\lambda,\mu}(\frac{\pi}{2},0)I_{\lambda,\mu}(\vartheta,\xi), \tag{2.18}$$

where $Y_{\lambda,\mu}(\frac{\pi}{2},0) = \begin{cases} (\frac{2\lambda+1}{4\pi})^{\frac{1}{2}}\frac{\sqrt{(\lambda-\mu)!(\lambda+\mu)!}}{(\lambda-\mu)!!(\lambda+\mu)!!}(-1)^{\frac{\lambda+\mu}{2}} & if\ \lambda{+}\mu\ is\ even \\ 0 & if\ \lambda{+}\mu\ is\ odd \end{cases}$

and $I_{\lambda,\mu}$ is the orbital integral which depends on the scattering angle, ϑ, and the excitation energy, ΔE through ξ, the adiabaticy parameter, which is a ratio of the collision time (τ_c) to the nuclear period (τ_n),

$$\xi = \frac{\tau_c}{\tau_n} = \frac{\Delta E}{\hbar}\frac{a}{\nu_\infty}. \tag{2.19}$$

To achieve an optimum CE, the collision time must be much less than the nuclear period ($\xi \ll 1$). The final excitation probability, combining equations 2.12, 2.14 and 2.17, yields

$$P_{i\to f} = [\chi^{\lambda}_{i\to f}]^2(2\lambda+1)^{-1}\sum_{\mu}[\mathcal{K}_{\lambda\mu}(\vartheta,\xi)]^2. \tag{2.20}$$

In case of a sudden impact head-on collision where $\vartheta = 180$ and $\xi = 0$ [33, 31], the orbital integral reduces and the excitation probability becomes;

$$P_{i\to f} = [\chi^{(\lambda)}_{i\to f}]^2. \tag{2.21}$$

If $\chi \ll 1$, the excitation process can be described using first-order perturbation theory.

Since the advent of advanced accelerators, energetic heavy-ion beams can be produced and accelerated and the value of χ can be of the order greater than unity. In situations where $\chi >> 1$, first order perturbation approximation no longer holds, and higher order, such as second order, perturbation is required to solve the time-dependent amplitude of the transition [29, 30, 31, 32]. The state of interest $|I_f\rangle$, maybe populated from the initial state $|I_i>$, through an intermediate state $|I_n>$ and the excitation probability is

determined using the multiple CE theory [29, 30]. The transition is not only influenced by the initial and final states, but also the intermediate state as well as the static properties of $|I_f>$ [29], where the matrix element of the quadrupole operator between the various magnetic substates are the diagonal and off-diagonal with respect to the magnetic quantum number m_f [21]. The schematic diagram shown in Fig. 2.5, shows the reorientation effect of a nucleus where the transition from $|I_i>$ to $|I_f\rangle$ splits up into different magnetic substates.

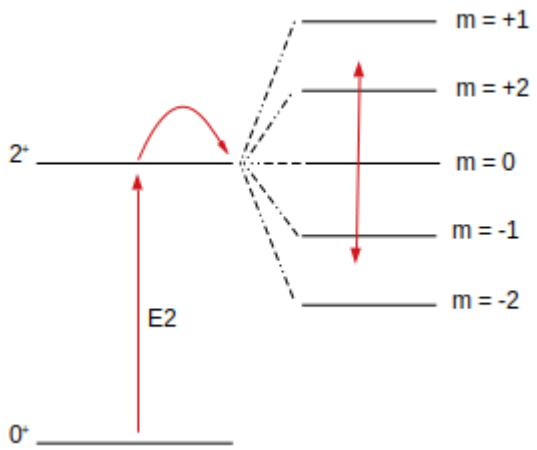

Figure 2.5: Reorientation effect of a nucleus transitioning from 0^+ ground state to 2^+ excited state.

Since the second-order perturbation theory offers a good approximation for the analysis of the experimental data for larger $\chi_{i\to f}$ [32], the semi-classical theory to the second order was employed [33].

$$d\sigma = d\sigma^{(1)} + d\sigma^{(1,2)} + d\sigma^{(2)} \tag{2.22}$$

The term $d\sigma^{(1)}$, is the excitation cross section of the first-order, $d\sigma^{(2)}$ is the second-order excitation cross section and $d\sigma^{(1,2)}$ corresponds to the interference between the first- and second-order excitations.

2.4 Coulomb Excitation Analytical Tool: GOSIA

Coulomb excitation as a tool for probing the nuclear structure was well recognized in the early 1950's [19]. The analysis of CE experiments involves vigorous mathematics and computational power. The first multiple CE computer code was developed by Winther and deBoer in 1986 [34]. The code, GOSIA, has been tremendously improved to fix ≈ 3000 matrix elements [19]. This improvement was made possible due to the inception of sensitive high resolution 4π γ ray detectors coupled to particle detectors such as Gammasphere and CHICO, HIE-ISOLDE and AFRODITE and has also increased the efficiency of γ-particle coincidence data collection.

For given set of matrix elements, GOSIA provides a strong computational skills to fit a χ^2 curve and evaluate the excitation amplitudes and the γ-decay yields [19]. The discussion of the GOSIA code will be limited to the scope of this work. The input files in appendix B will be briefly discussed.

The current research work involves the extraction of the diagonal matrix element, $\langle 2_1^+ \| \hat{E}2 \| 2_1^+ \rangle$, γ-ray integrated yields, as well as the excitation probability. GOSIA is designed for the analysis of particle-γ coincidence and γ yields for CE experiments. To reproduce the γ yields observed in the CE experiment, an interaction over the energy range of the scattering particles and the scattering (detection) angular range are required. Assuming that the scattering angle of the projectile in the laboratory frame θ_p, and the bombarding energy E, remains constant, the point and integrated yields are given by,

$$Y_{point}(I_i \rightarrow I_f) = sin\theta_p \int_{\phi} \frac{d^2\sigma(I_i \rightarrow I_f)}{d\Omega_\gamma d\Omega_p} d\phi_p \tag{2.23}$$

and

$$Y_{int}(I_i \rightarrow I_f) = \int_E dE \frac{1}{\frac{dE}{dx}} \int_{\theta_p} Y_{point}(I_i \rightarrow I_f) d\theta_p \tag{2.24}$$

respectively. The solid angle factor is $sin(\theta)$. GOSIA uses both the Y_{point}, Y_{int} to transform the experimental yields to corrected experimental yields through the transformation relation;

$$Y^{c}_{exp}(I_i \rightarrow I_f) = Y_{exp}(I_i \rightarrow I_f)\frac{Y_{point(I_i \rightarrow I_f)}}{Y_{int}(I_i \rightarrow I_f)} \tag{2.25}$$

where c represents the corrected value.

2.4.1 Calculation of observables: Absolute coincident particle-γ yields

The integration of the coincident γ ray yields ($Y(I_i \rightarrow I_f)$ defined by Eqs. 2.22 $-$2.24 is done by an OP,INTI command (discussed in the subsequent section) in the GOSIA input file. The detection efficiency for both γ rays (ε_γ) and particle (ε_p) are however not included in the OP,INTI computations. The total coincident γ rays detected is given by the expression,

$$N_i = 10^{-30}\Big[\frac{Q}{\hat{q}e}\Big]\Big[\frac{N_A}{A}\Big]Y(I_i \rightarrow I_f)\varepsilon_p\kappa_{p\gamma}\varepsilon_\gamma(E_\gamma)\Delta\Omega_\gamma, \tag{2.26}$$

where Q is the beam charge, $\hat{q}$ the average charge state of the beam, e the proton charge, N_A the Avogadro number, A the atomic mass of the target, $\kappa_p\gamma$ the $p-\gamma$ live time efficiency factor that corrects the dead time due to pileup rejection during data acquisition and $\varepsilon_\gamma(E_\gamma)$ the energy dependency γ ray peak efficiency over a unit solid angle $\Delta\Omega$. The total detected particles that elastically scatter, $N_{singles}$, is given by Eq. 2.27 below,

$$N_{singles} = 10^{-30}\Big[\frac{Q}{\hat{q}e}\Big]\Big[\frac{N_A}{A}\Big]Y_{singles}\varepsilon_p\kappa_p. \tag{2.27}$$

To normalize the experimental data of the p-γ coincident events in the projectile to the target, a ratio of the projectile (N^P_i) to the target (N^T_i) given by Eq. 2.28 is used.

$$\frac{N^P_i}{N^T_i} = \frac{Y^P(I^P_i \rightarrow I^P_f)}{Y^T(I^T_i \rightarrow I^T_f)}\frac{\varepsilon_\gamma(E^P_\gamma)}{\varepsilon_\gamma(E^P_\gamma)}, \tag{2.28}$$

where the ratio $\frac{\varepsilon_\gamma(E_\gamma^P)}{\varepsilon_\gamma(E_\gamma^P)}$ is the factor that converts the GOSIA output into observables. Some of the observables in CE experiments are transition strengths (B(E2) and B(M1)), static E2 moments of excited states, static M1 moments and rotational invariants.

2.5 GOSIA Input Files For This Work

Two input files were created to analyze the CE experimental data (One for the projectile ^{40}Ar and the other for the target nucleus ^{194}Pt). The GOSIA code is executed by an input file that specifies command options in the form 'OP, followed by a four character name' [19]. A summary of the command options used for the analysis of this work is briefly discussed below.

2.5.1 OP,FILE

The OP,FILE command option permit one to assign file names to jobs in the output file.

2.5.2 OP,GOSI

This option fits matrix elements to the CE experimental data. It requires other suboptions such as,

- LEVE: Reads the level scheme of the nucleus under investigation.
- ME: This suboption allows one to input the matrix element information about the different transitions in the nucleus of interest.

- EXPT: Under this suboption, atomic properties such as the atomic masses and numbers of both the projectile and target, bombarding energy, as well as the detector type, are all defined for the fitting by the OP,GOSI. The number of experiments (number of rings on the particle detector) is also required for this option.

- CONT: The CONT command allows us to override the GOSIA default settings. One can then control and specify the running of the code to suit the experimental needs.

The option also requires information about the branching ratios, mixing ratios, life times and known matrix elements for the fitting.

2.5.3 OP,YIEL

This option permits one to input the experimental data needed to calculate the γ ray de-excitation of the investigated nucleus. It also fits the matrix elements to the γ ray yields. OP,YIEL uses inputs from the OP,GOSI to calculate the de-excitations of the γ rays [19].

2.5.4 OP,RAW

The OP,RAW option command allows one to input uncorrected γ ray yields from the CE experiment [19]. This option in essential for the analysis of data from multidetector arrays. It allows the user to combine Doppler corrected yields with the raw data from γ detectors collected in coincidence with recoil particles. This results in the minimization of the data sets and improves the statistics of the data to be analyzed [19].

Chapter 3

Experimental Techniques and Equipment

Two different sets of semiconductor detectors were used for the Coulomb excitation experimental research work. The detectors were an S3 double-sided CD silicon particle detector and a High Purity Germanium (HPGe) gamma detector array. African Omnipurpose Detector for Innovative Techniques and Experiments (AFRODITE) facility of iThemba Laboratory for accelerator Based Sciences (LABS) was used to carry out the CE experiment.

AFRODITE is a medium size detector array. The AFRODITE frame and target chamber are rhombi cuboctahedron by design. The array accommodates a maximum of thirteen clovers and eight LEPS, totaling sixteen gamma detectors. The target chamber houses a maximum of two particle detectors (for detection of both forward and backward scattered particles) and a target ladder. Details of the the S3 and clover detectors used for this experimental work are discussed in subsequent sections.

3.1 S3 CD-type Double-sided Silicon Detector

Double sided S3 silicon detector was employed for the detection of ^{40}Ar in the Coulomb excitation experiment. The S3 CD-type detector was manufactured by Micron Semiconductors in the United Kingdom and purposely designed for Coulomb excitation studies involving radioactive ion beams. The S3 CD-type silicon detector is a segmented microstrip detector based on ion implantation technology. Each segmentation comprises of 24 rings on one side (junction) and 32 sectors on the other side (ohmic) electrically separated. The microstrip segmentation enables the detection of energy deposition by the particle as well as position of the particle. A picture of the S3 detector is shown in Fig. 3.1 with its schematics in Fig. 3.2 below.

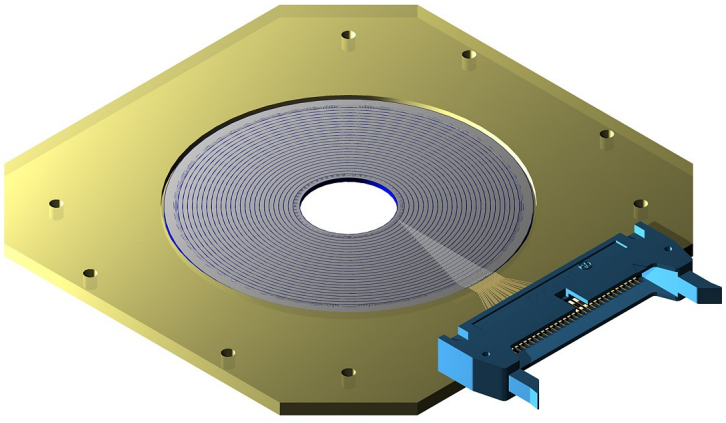

Figure 3.1: The S3 CD-type double sided silicon detector used for the detection of recoil particles in the CE experiment [37].

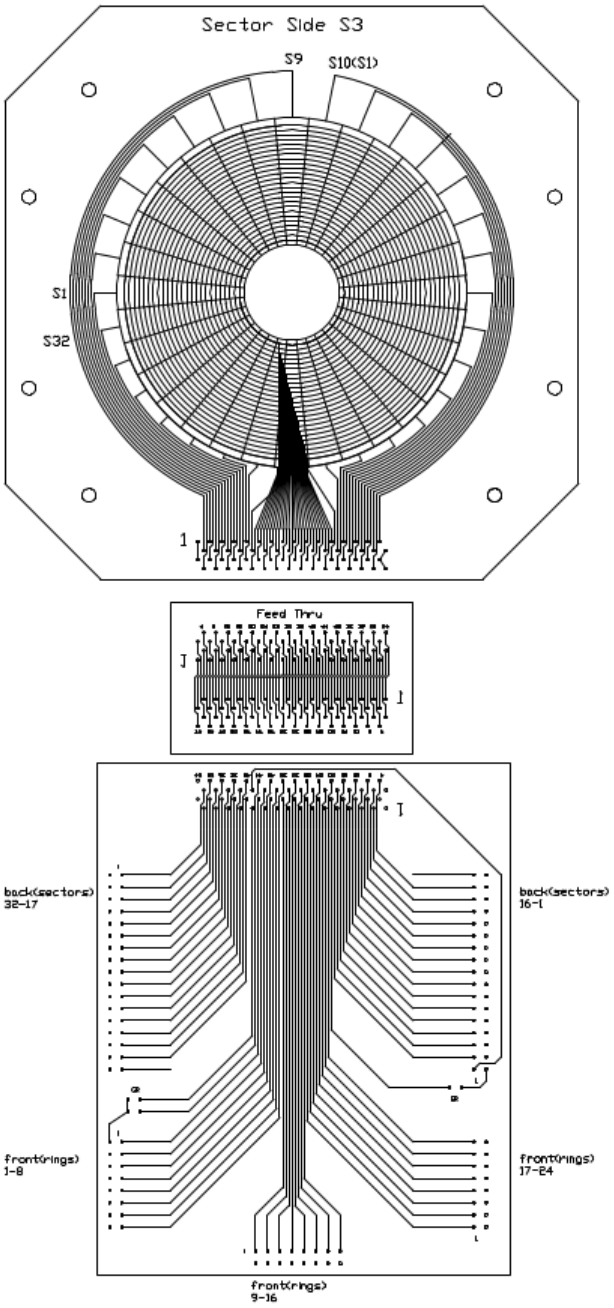

Figure 3.2: Schematic of the S3 CD-type double-sided silicon detector

The S3 CD-type double-sided silicon detector has an inner diameter of 22 mm and an outer diameter of 70 mm. It consists of 32 sectors of equal size on the ohmic side and 24 concentric rings of width, 0.866 mm, at the junction side. The dimensions of the rings on the S3 detector are tabulated in Table 3.1 [37]. The energy resolution of rings at 7.68 MeV of 226Ra source is 85 keV and sectors it is 80 keV for the experiment.

Table 3.1: Geometry of the S3 CD-type double-sided silicon detector: From ring 1 (inner-most ring) to ring 24 (outer-most ring) [37]

Ring	Inner Radius(mm)	Outer Radius(mm)	Ring Width(mm)
1	11.480	12.366	0.866
2	12.466	13.352	0.866
3	13.452	14.338	0.866
4	14.438	15.324	0.866
5	15.424	16.310	0.866
6	16.410	17.296	0.866
7	17.396	18.282	0.866
8	18.382	19.268	0.866
9	19.368	20.254	0.866
10	20.354	21.240	0.866
11	21.340	22.226	0.866
12	22.326	23.212	0.866
13	23.312	24.198	0.866
14	24.298	25.184	0.866
15	25.284	26.170	0.866
16	26.270	27.156	0.866
17	27.256	28.142	0.866
18	28.242	29.128	0.866
19	29.228	30.114	0.866
20	30.214	31.100	0.866
21	31.200	32.086	0.866
22	32.186	33.072	0.866
23	33.172	34.058	0.866
24	34.158	35.044	0.866

3.2 The HPGe Clover Detectors

The clover detectors are High Purity Germanium (HPGe) crystal detectors with high efficiency. Clover detectors were first developed by Camberra in collaboration with Eurogam [38]. Gamma detectors used for the detection of gamma ray energy in the Coulomb excitation of ^{40}Ar on ^{194}Pt target were clover detectors (with a maximum efficiency for the ^{40}Ar(^{194}Pt, ^{194}Pt*)^{40}Ar* of 2470.19 ± 29.02 at 121.78 using ^{152}Eu source). The design, consisting of four n-type germanium crystals arranged like a four leaf clover, improves the efficiency and resolution of the detector.

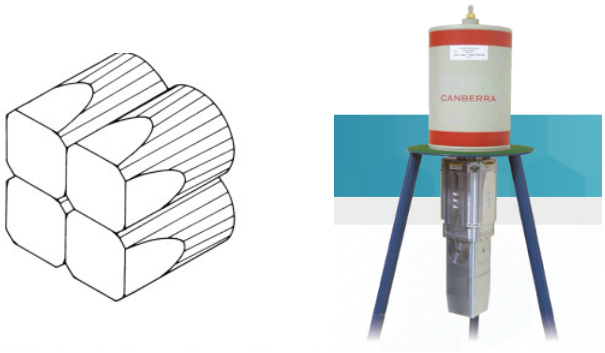

(a) Germanium crystals. (b) Clover on a stand.

Figure 3.3: Schematic of the HPGe Clover detector (left) and a typical clover for the AFRODITE array (right) [38]

To reduce the amount of material around the crystal and improve the peak-to-background ratio, the crystal is held on a minimized crystal holder [38]. The four crystals are mounted on a common cryostat with a square shaped end cap. The crystal-cap distance is reduced to a minimum for the improvement of efficiency and solid angle. Each crystal is 70 mm long and 50 mm in diameter [38]. The signals from the crystals are obtained via a coupling capacitance connected to a high ground voltage.

3.3 Detector Set-up And Electronics

The AFRODITE detector array at iThemba LABS, shown in Fig. 3.4, was used for the Coulomb excitation of ^{40}Ar on ^{194}Pt target.

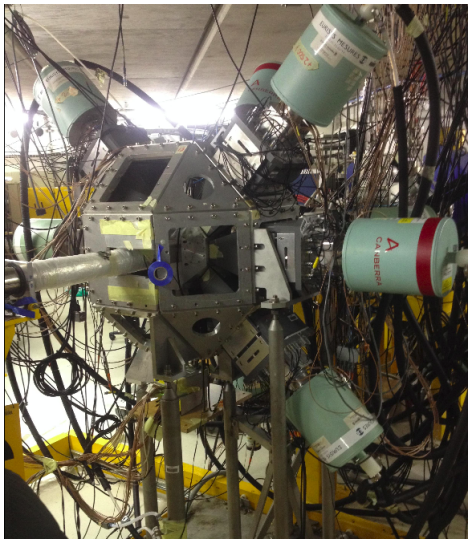

Figure 3.4: AFRODITE array at iThemba LABS, with clover detectors.

The enriched ^{194}Pt target was mounted on a target ladder in the target chamber of the AFRODITE experimental vault. The chamber also houses the S3 detector connected to a 64-way R/A Yamaichi connector.

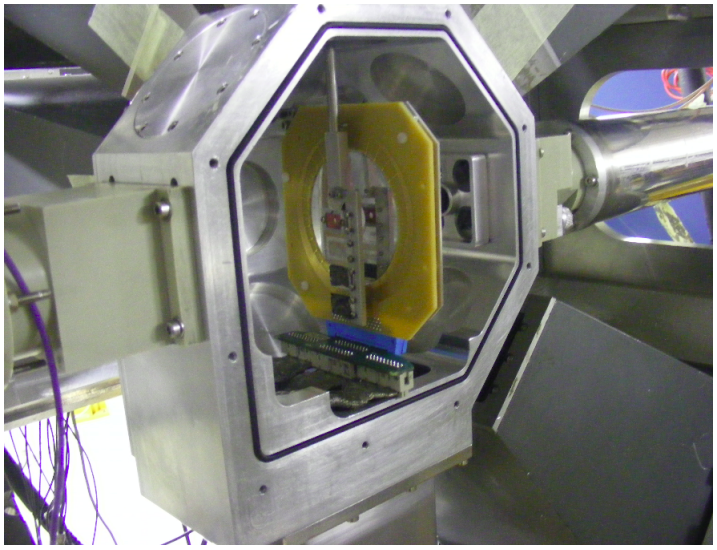

Figure 3.5: The target chamber housing the target on a target ladder and the S3 detector connected to a 64-way R/A Yamaichi connector.

Mesytec mesh-shielded cables (labelled S1, S2, R1 and R2) were used to transport signals from the twenty four rings and thirty two sectors through the 64-way connector. The sector signals were transported by the S1 and S2 cables while signals from the rings were transported by the R1 and R2 cables. Each cable accommodates a maximum of 16 signal channels.

The signals from the S1, S2, R1 and R2 served as input to the Mesytec MPR-32 multichannel preamplifiers, shown in Fig. 3.6, for boosting and pulse shaping [39]. The MPR-32 are then connected to the MHV-4 bias unit (Fig. 3.7). The MHV-4 was used to bias the S3 detector and the MPR-32 [39, 40]. It was also used for the monitoring of the leakage current during the CE measurement and adjusting the S3 detector voltage. The output of the preamplifiers were input to the array patch panel as illustrated in the schematic diagram in Fig. 3.8. The S1, S2, R1 and R2 were then sent to the XIA modules connected to the Digital Data Acquisition System (DDAS) shown in Fig. 3.8.

The XIA modules used in this experiment was a digital system consisting of two PXI crates. The two crates housed six 16-channel DGF PIXIE-16 modules. Two of the DGF PIXIE-16 modules received 32 amplified data signals from the clover detectors. The remaining four, received 56 (32 sectors and 24 rings) digitised signals from the S3 detector. The data from both detectors, consisted of 48 bit time-stamped energy signals and were collected in coincidence at a frequency of 100 MHz [41, 42]. The collected data was store on a server computer. MTsort [43] and MIDAS (multi-instance data acquisition software) [44], were used to control the experiment, sort and store the data. Fig. 3.8 shows Schematic diagram of the electronic set-up for the experiment.

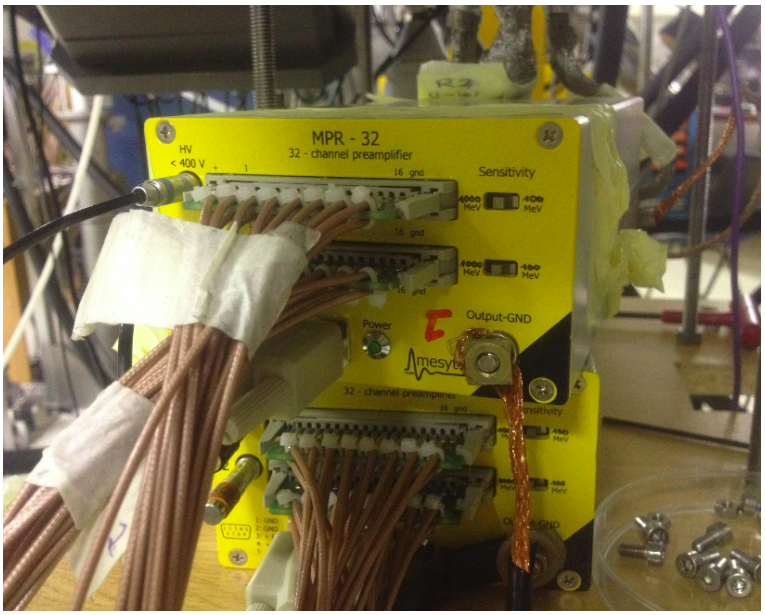

Figure 3.6: R1, R2, S1 and S2 connected to MPR-32 multichannel preamplifiers.

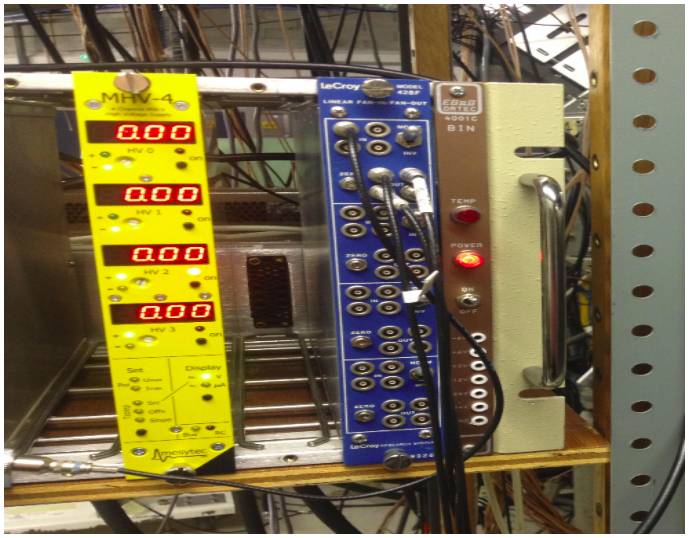

Figure 3.7: MHV-4 bias unit used to bias the silicon detector and monitor current leakage. The bias voltage for the CE experiment was 105V with a leakage current of 0.86μA.

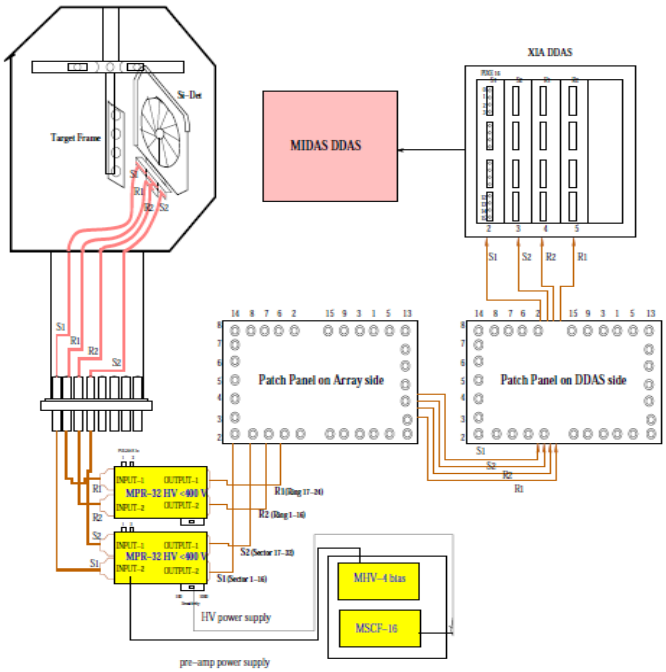

Figure 3.8: Schematic diagram of the S3 CD-type detector systems to the AFRODITE patch panels and the DDAS.

3.4 Experimental Conditions

For a successful Coulomb excitation experiment, the experimental conditions must be chosen carefully to avoid or minimize the effect of the nuclear force. The conditions for this work are listed in Table 3.3.

Table 3.2: Experimental conditions for ^{40}Ar(^{194}Pt, ^{194}Pt*)^{40}Ar* interaction

Target	^{194}Pt
Target thickness	1 mg/cm^2
Beam	^{40}Ar^{6+}
Beam current	1nA
Beam energy	134.94 MeV
Safe distance	6.5 fm

3.4.1 Safe Bombarding Energy

The safe bombarding energy is calculated for the chosen target and projectile based on safe Coulomb excitation conditions such as the Sommerfeld parameter ($\eta = 120 \gg 1$, for this research) [19]. Then the maximum safe bombarding energy ($E_{(max)}$) is given by;

$$E_{(max)}(MeV) = 1.44\frac{A_P + A_T}{A_T} \cdot \frac{Z_P Z_T}{1.25(A_P^{1/3} + A_T^{1/3}) + 6.5}, \tag{3.1}$$

$$E_{(max)} = 147.6 \text{ MeV}.$$

Where $E_{(max)}$ is maximum safe interaction or bombarding energy, Z_T and A_T are the atomic and mass number of the target, Z_P and A_P are the atomic and mass number of the projectile. The bombarding energy for a safe and successful Coulomb excitation experiment, must be far below the Coulomb barrier. The Coulomb barrier, $V_c = \frac{Z_T Z_P e^2}{4\pi\varepsilon_o(R_T+R_P)}$, of ^{40}Ar and ^{194}Pt is 182.95 MeV. Where R_T and R_P are the respective target and projectile radii.

3.4.2 Safe Minimum Distance

The safe minimum distance was calculated from the safe bombarding energy using Eq. 1.5.

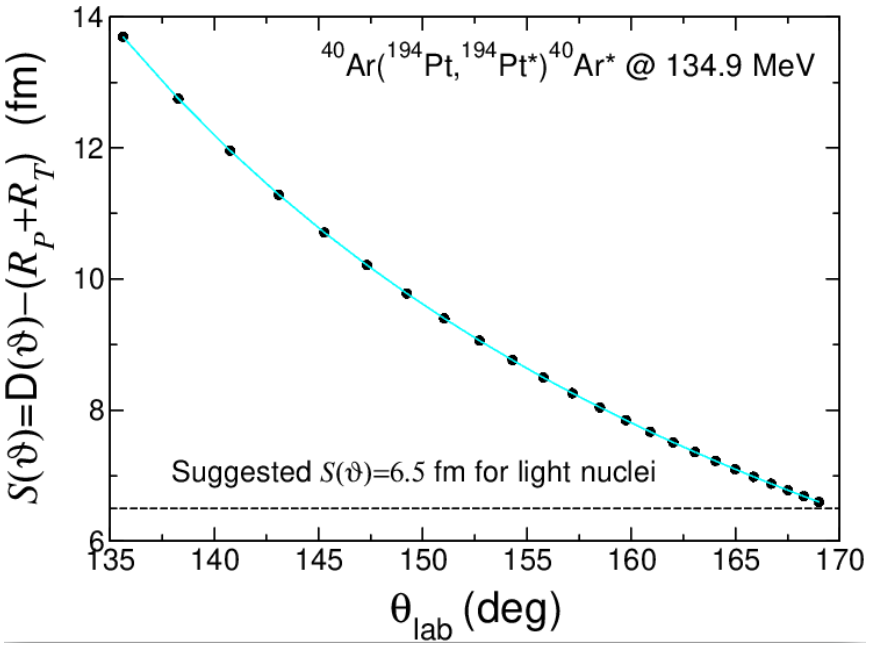

Figure 3.9: Distance between nuclear surfaces, $S(\vartheta_{cm})$, as a function of projectile scattering angle in the laboratory frame for ^{40}Ar(^{194}Pt, ^{194}Pt*)^{40}Ar* reaction at 134.9 MeV

3.5 The ^{40}Ar Coulomb Excitation Experiment

The ^{194}Pt(^{40}Ar,^{40}Ar*)^{194}Pt* CE experiment was carried out over a period of one weekend in March 2016 at iThemba LABS. ^{40}Ar beam was produced by the Solid-Pole injector Cyclotron (SPC2) and pre-accelerated to 8 MeV. The 8 MeV ^{40}Ar beam was then transported to the Separated Sector Cyclotron (SSC) for acceleration to the required 134.9 MeV energy. The 134.9 MeV

$^{40}Ar^{6+}$ beam was Coulomb excited on an enriched ^{194}Pt target of 1.0 mg.cm^{-2} thickness. The detection of the γ rays was done using the AFRODITE array consisting of eight clovers (five at 90° and three at 135°) as shown in Figs. 3.3 and 3.4. The de-excitation ^{40}Ar particles were detected by the S3 detector (Fig. 3.1). A safe distance of 6.5 fm between the nuclear surfaces along with a Sommerfeld parameter, $\eta = 120$, indicating that the semiclassical approximation requirement is satisfied. The clovers were calibrated using a standard ^{152}Eu source while the calibration of the S3 was done by a standard ^{266}Ra source. The S3 was calibrated before the CE measurement while the clovers were done before and after the measurement. The geometric positions of the clovers in the laboratory frame during the measurement are illustrated in Table 3.3.

Table 3.3: Clover detector geometry configuration (taken from the center of each clover) for the $^{194}Pt(^{40}Ar,^{40}Ar^*)^{194}Pt^*$ CE measurement

Clover	θ (°)	ϕ (°)
1	90	45
2	90	90
3	90	135
4	90	315
5	90	0
6	135	90
7	135	225
8	135	270

Chapter 4

Data Analysis and results

4.1 Projectile Energy Loss

When charged energetic particles (Projectile) traveling at velocity v_t ($v_t << c$), interacts with matter (target) during the course of a Coulomb excitation reaction, the projectile loses energy due to nuclei and atomic electrons interactions as it travels through the target. The energy loss can be minimized, if the mass of the projectile, m_P, is small in comparison to the target mass m_T ($m_P < m_T$). When a target with higher atomic number compared to that of a projectile is used in Coulomb excitation experiments, the number of collisions per unit length increases significantly and so does the projectile energy loss. The amount of energy loss to the target is small compared to the projectile energy under safe energy and distance conditions [46]. The energy loss per unit length due to these interactions is known as the stopping power. To compute the stopping power, $\frac{dE}{dx}$, the Bethe-Bloch formula given by

$$-\frac{dE}{dx} = \Big(\frac{Z_p e^2}{4\pi\varepsilon_o}\Big)^2 \Big(\frac{4\pi Z_t \rho_t N_A}{A_t M_e v^2}\Big)\Big[ln\Big(\frac{2M_e v^2}{I_E}\Big) - ln\Big(1-\beta^2\Big) - \beta^2\Big], \quad (4.1)$$

is used. A_t, ρ_t and Z_t are atomic number, density and mass number of the target, Z_p the atomic number of the projectile, M_e and I_E the electron mass and the mean ionization energy of the target respectively, and β is given by $\sqrt{1-\frac{v}{c}}$. A significant feature from Eq. 4.1 is that the energy loss, $\frac{dE}{dx}$, is directly proportional to the square of the atomic number of the projectile, Z_p. The energy of the projectile after scattering, E_f, is

$$E_f = E_p - \frac{dE}{dx}dx, \tag{4.2}$$

where E_p is the energy of the projectile in the laboratory frame. The SRIM (Stopping and Range of Ions in Matter) program [47] was employed in calculating the energy loss of the projectile as shown in Fig. 4.1. The path traveled by the projectile is hyperbolic, but since the target is thin, a straight path is assumed and used in SRIM for the calculations.

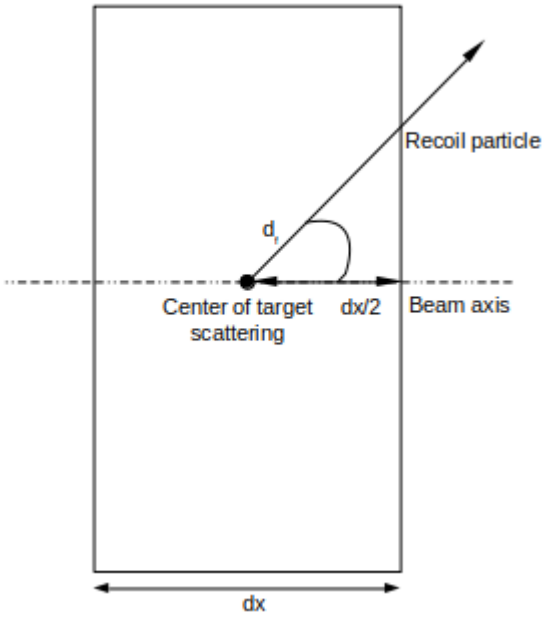

Figure 4.1: Trajectory of projectile in a target of thickness dx, scattering through a distance d_f, at an angle of φ. There we assume the center-of-target scattering

For the purposes of this research study where a thin target was used, we assume that the scattering occurs at the center of the target. Letting $dx = dx_{ap}$, to be the apparent thickness, the total distance traveled by the projectile in the target can be given as,

$$dx_{ap} = \frac{dx}{2} + d_f, \tag{4.3}$$

where $d_f = \frac{dx}{2} cos\varphi$.

$$dx_{ap} = \frac{dx}{2} + \frac{dx}{2} cos\varphi = \frac{dx}{2}(1 + cos\varphi). \tag{4.4}$$

The final energy of the projectile after scattering given in Eq. 4.2, becomes

$$E_f = E_p - \frac{dE}{dx} dx_{ap} = \frac{dE}{dx}\Big(\frac{dx}{2}(1 + cos\varphi)\Big). \tag{4.5}$$

The energy loss calculated from SRIM was 6.80 MeV and the final energy after, E_f was 128.14 MeV.

4.2 Intensity and Efficiency Calibration

The intensities of the detected γ rays and the Gamma Ray Efficiency Measurement and Line INtensity calculation (GREMLIN), developed at Rochester in 1987 by Kavka [19], was used to calculate the efficiency of the HPGe clover detectors as well as the intensities of the γ-ray peaks . The GREMLIN program performs two operations [19];

i) Least-squares fit of a γ-ray detection efficiency-calibration function to a set of peak areas from γ-ray calibration spectra.

ii) Calculation of detection-efficiency corrected γ-ray intensities from peak areas, using the fitted efficiency function for the Doppler shift corrected γ-ray energy.

4.3 HPGe Clover Efficiency Calibration

The efficiency of the High Purity Germanium (HPGe) clover detectors was done by placing the ^{152}Eu calibration source (spectra in Fig. 4.2) at target position. The data was collected before and after the experiment. An input file, shown in Table 4.1, consisting of energy, (E), energy uncertainty, (ΔE), intensity, (I) and intensity uncertainty, (ΔI) was created from the ^{152}Eu source.

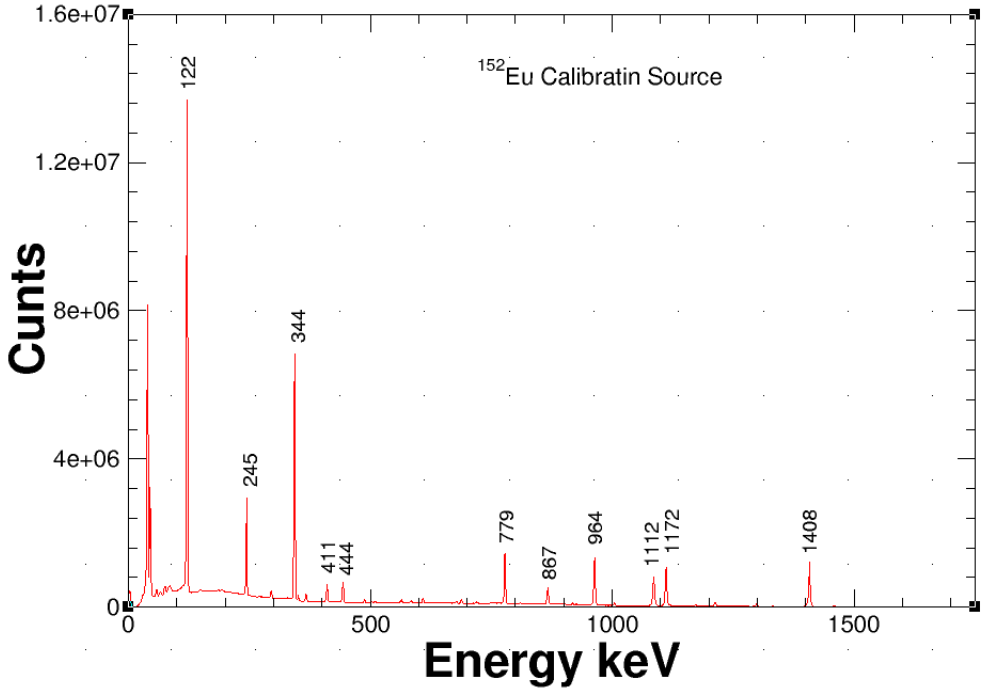

Figure 4.2: The ^{152}Eu source spectrum used for energy calibration with the calibration peaks labeled.

Table 4.1: Table of energies, intensities and areas of peaks of the ^{152}Eu source used for the clover calibration.

E(KeV)	I($KeVm^{-2}$)	ΔI($KeVm^{-2}$)	A(m^2)	ΔA(m^2)
121.783	13620	160	33643987	6388
244.692	3590	60	6581861	3387
344.276	12750	90	17213750	4687
411.115	1070	10	1331228	1855
443.976	1480	20	1684718	1909
778.903	6190	80	4644124	2538
867.388	1990	40	1422947	1634
964.131	6920	90	4508587	2312
1112.116	6490	90	3762433	2105
1299.124	780	10	377285	798
1408.011	10000	30	4883428	2253

For every line in Table 4.1, the relative efficiency as well as the root-mean-square error was calculated by GREMLIN using equations;

$$\varepsilon = \frac{A}{I}, \tag{4.6}$$

and

$$\Delta\varepsilon = \varepsilon\sqrt{\left(\frac{\Delta A}{A}\right)^2 + \left(\frac{\Delta I}{I}\right)^2}. \tag{4.7}$$

The efficiency was then fitted using the transformation;

$$x \equiv log\frac{E}{E_0}, \tag{4.8}$$

and

$$y \equiv log\varepsilon. \tag{4.9}$$

The error in y is,

$$\Delta y = \frac{\Delta\varepsilon}{\varepsilon}, \tag{4.10}$$

where $E_0 = 50$ keV and the logarithms are to the base e.

To obtain a good fit, GREMLIN uses a complex function, Eq. 4.11 comprising of four individual functions that accounts for the γ-ray absorption, electronic thresholds, higher and lower energy detection efficiencies separately.

$$\varepsilon(E) = A(E)P(E; a_1...a_n)F(E; f)W(E; b, c), \tag{4.11}$$

where the parameters $a_1...a_n$, f, b and c are determined. The individual terms, $A(E)$, $P(E; a_1...a_n)$, $F(E; f)$ and $W(E; b, c)$ in Eq. 4.11 represent the attenuation factor, the polynomial factor, low energy function and the Woods-Saxon factor respectively.

Using the data from *Appendix C* and Eq. 4.11, GREMLIN fitted the efficiency curve and the result is plotted in Fig. 4.3.

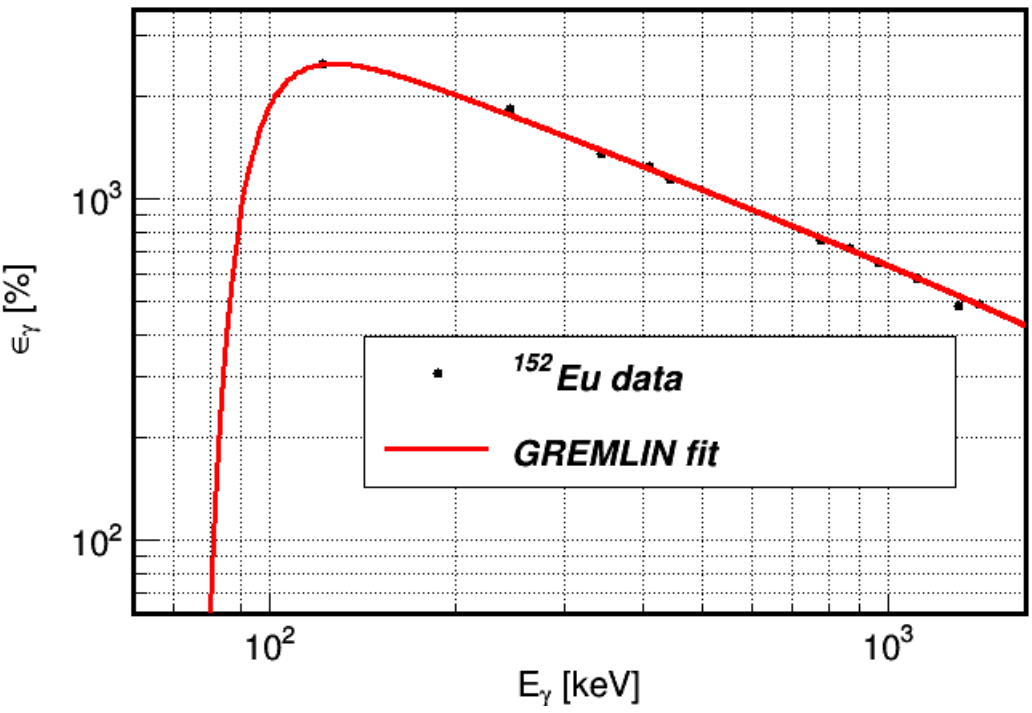

Figure 4.3: Clover detector efficiency calibration using the ^{152}Eu source.

4.3.1 The Attenuation Factor

The attenuation factor is a factor that accounts for the γ ray absorption rate in materials. When an absorber used in an experiment consists of different materials or layers, their effect on the detected γ rays are accounted for when determining the efficiency of the detectors. The attenuation factor is given by the expression;

$$A(E) = exp\Big[- \sum_{t=1}^{m} \mu_i(E) d_i \Big], \tag{4.12}$$

where $A(E)$ is the absorption of m different absorber materials placed in front of the detector, d_i is the thickness of the i^{th} absorber material and μ_i represents the attenuation coefficients. The data statements in GREMLIN, contains attenuation coefficient for the absorber materials (C, Al, Si, Fe, Cu, Cd, Sn, Ta and Pb) for γ energies ranging from 30 keV to 4000 keV. A cubic spline curve interpolation of two energy mesh points (88.004 and 67.416 keV) of the K-edges from Pb and Ta respectively is done, keeping the curves below and above the edges. The spline curves are plotted using the variables $x = log\frac{E}{E_0}$ and $y = log\frac{\mu}{m\mu_0}$, where $\mu_0 = 1$ cm^{-1}. The attenuation coefficients can be calculated using the total cross-section from reference [48], and equation 4.13.

$$\mu = \frac{\rho N_A \sigma}{M} = 0.602 \frac{\rho \sigma}{M}, \tag{4.13}$$

where M, ρ, N_A and σ are atomic weight, density, Avogadro's number and the total cross-section.

4.3.2 The Polynomial Factor

The efficiency curve is a polynomial fit of the degree $n \leq 3$. The factor, given by the relation,

$$P(E; a_1...a_n) = exp\Big[\sum_{k=0}^{n} a_k \Big(log\frac{E}{E_0}\Big)^k\Big], \tag{4.14}$$

represents the decrease in efficiency as the γ energy increases. An optimum initial value for a_k is determined by GREMLIN, by fitting an n^{th} degree (chosen by user) polynomial, where $P(E)$ dominates above 220 keV region.

4.3.3 Low-Energy Slope

To fit the low energy region of the efficiency curve, $f < 0$ and $N > 0$, chosen arbitrary, is used to describe the inverse-power factor.

$$F(E; a_1...a_n) = exp\Big[f(log\frac{E}{E_0})^{-N}\Big]. \tag{4.15}$$

For the Woods-Saxon factor, b and $c > 0$, also arbitrarily chosen are used.

$$W(E; b, c) = \frac{1}{1 + exp\frac{b-E}{c}}, \tag{4.16}$$

are optional for the efficiency fit. In this work, $W = 0$, since it also describes the low-energy slope of the fit. A value of $N = 5$ was used for the fitting which produced a good chi-square(χ^2) fit.

The final efficiency curve was plotted using values from Table 4.1 and after five iterations, GREMLIN generated the best χ^2 parameters(*Appendix C*) for the fit.

4.4 γ-Ray Intensity Calculations

The GREMLIN program fits the function $\varepsilon(E)$ from the file generated in *section* 4.2.1 (*Appendix* C). To fit the function perfectly, the kinematics of the experiment (projectile and target masses, angle of excited particle(θ, ϕ) beam energy, and the position of detectors$(\theta_\gamma, \phi_\gamma)$) must be specified to calculate the Doppler-shifted γ energies from the equation;

$$E'_\gamma = \frac{E_\gamma}{1 - \frac{\nu}{c} cos\alpha} \tag{4.17}$$

and

$$cos\alpha = sin\theta sin\theta_\gamma cos(\phi - \phi_\gamma) + cos\theta cos\theta_\gamma, \tag{4.18}$$

where α is the angle between the γ-ray and the excited particle and ν is the kinematic velocity.

To calculate the relative intensities and uncertainties in the peaks of the transition energies E, GREMLIN requires the peak areas(A) and uncertainties (ΔA) using the equation;

$$I = \frac{A}{\varepsilon(E')} \tag{4.19}$$

and

$$\left(\frac{\Delta I}{I}\right)^2 = \left(\frac{\Delta A}{A}\right)^2 + \left(\frac{\Delta \varepsilon}{\varepsilon}\right)^2, \tag{4.20}$$

where the estimation of $(\Delta\varepsilon)$ is given by;

$$(\Delta\varepsilon)^2 = \Sigma_{j=1}^{p} \Sigma_{k=1}^{p} \frac{\delta\varepsilon}{\delta\alpha_j} \frac{\delta\varepsilon}{\delta\alpha_k} C_{ij}, \tag{4.21}$$

and $a_j (j = 1...p)$ are the fit parameters and C is a correlation matrix. The calculated relative efficiencies and intensities with their respective uncertainties for both ^{40}Ar and ^{194}Pt are listed in the Table 4.2.

Table 4.2: Table of efficiencies and intensities of the first excited states of ^{40}Ar (1460.895 keV) and ^{194}Pt (328.646 keV) from the CE experiment.

E(keV)	I(keVm^{-2})	ΔI(keVm^{-2})	ε	$\Delta\varepsilon$
1460.849	34.895	0.486	473.516	5.379
328.464	954.870	15.875	1427.418	23.696

4.5 Particle Detector Calibration

The particle detector used in this experimental work was S3 CD-type double sided silicon detector as described in Chapter 2. It has 24 rings on the junction side and 32 sectors on the ohmic side. The detector was biased such that each side reads opposite signal. The particle detector calibration was done by utilizing an α peak (7.8 MeV) from the ^{226}Ra calibration source and a simulated 135 MeV GEANT4 peak in a two point calibration [50]. The calibration gains and offset coefficients of the 24 rings and 32 sectors were then used as part of the input parameters for an offline sort code to generate the calibrated particle energy spectra in Fig. 4.4.

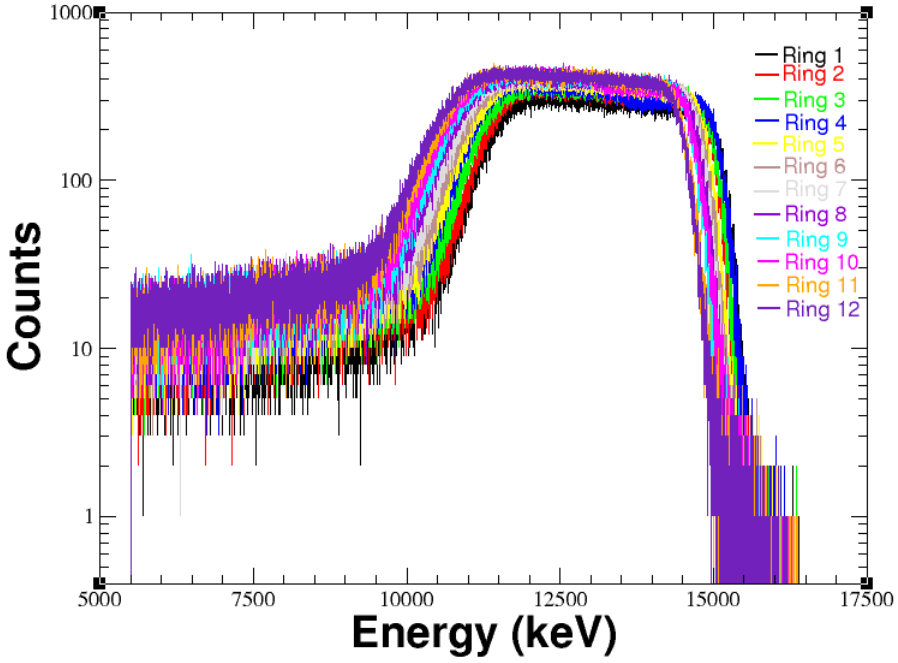

Figure 4.4: Calibrated ^{40}Ar particle spectra showing the first 12 rings, where ring 1 is the outer-most-ring.

4.6 Data Analysis and Discussion

To sort the experimental data for analysis, an offline sorting code, was developed. The code was designed to extract statistics on the de-excitation γ-ray from the de-exciting ^{40}Ar particles. To obtain the desired statistics for the analysis and reduce the background γ-rays, various conditions were implemented. The code was ran using the MIDAS package in MTsort to sort the data [44, 43]. The conditions implemented in the code are discussed in the following section.

4.6.1 Particle Coincidence Condition

During the experiment, many particles were excited having different excitation energies. These particles were detected by the S3 detector and their corresponding de-excitation γ-rays were detected by the clovers. The particle coincidence condition allowed the selection of detected particles with energies of interest.

The condition, once implemented, permitted the code to register events between the rings and sectors that fell within a chosen energy and time window. This requires two hits, simultaneously, on the rings and sectors of the S3 detector within a certain chosen time window, Δt. A broad energy gate, ranging between the inner-most ring and the outer-most ring, is applied to the coincidence particles detected. All other events are considered background. The broad energy and time gates for this condition is illustrated in Fig. 4.5 and Fig. 4.6 respectively.

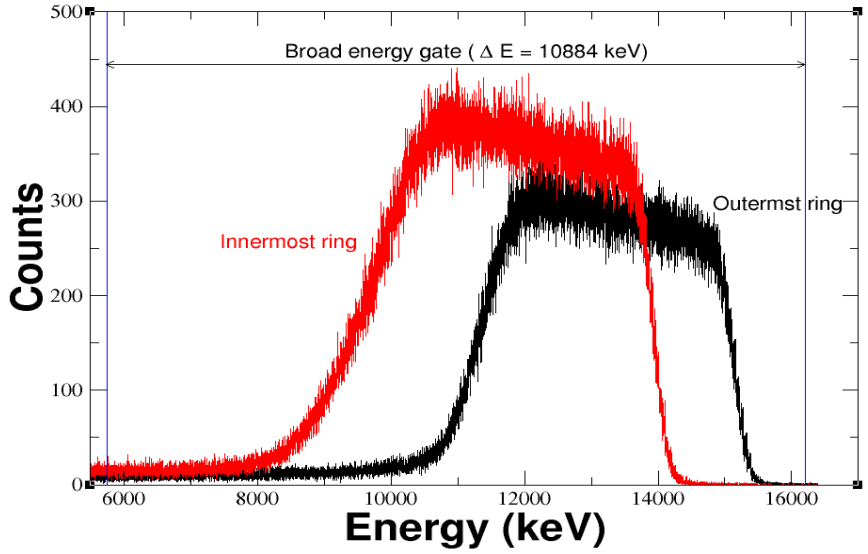

Figure 4.5: Broad energy gate (inner-most (red) and outer-most (black) rings) used for the particle coincidence with ΔE=10884 keV.

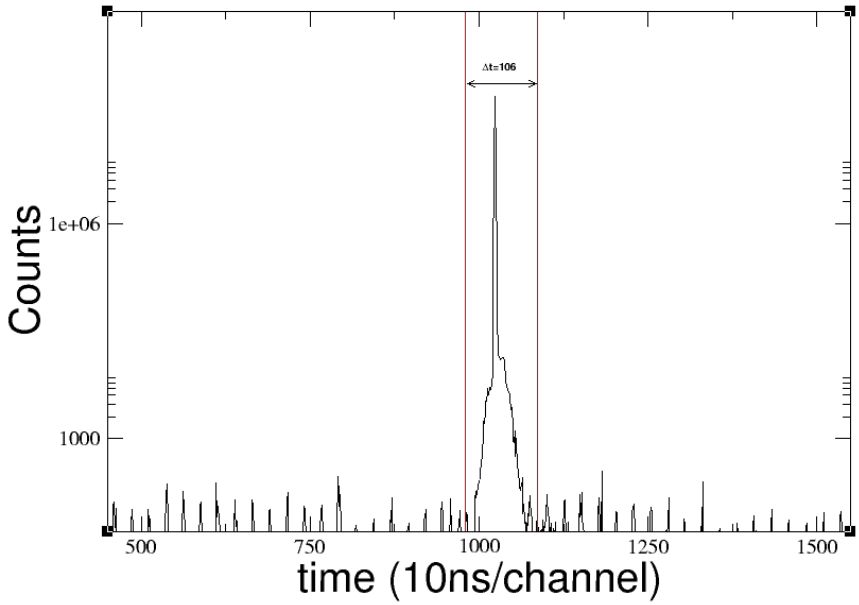

Figure 4.6: Time window for the particle coincidence with Δt = 106 ns.

4.6.2 Particle-γ Coincidence Condition

This condition was set up in the sort code such that the registered de-excitation γ-rays in the clovers were in coincidence with a simultaneous hit in the rings and sectors of the S3 detector [49]. Just as in the particle coincidence condition, a time window was also required for this condition. The chosen time window for the condition in this experiment was $\Delta t_\gamma = 106$ ns as shown in Fig. 4.7. This condition ensures that only the γ rays hitting clovers within this time frame were recorded and stored.

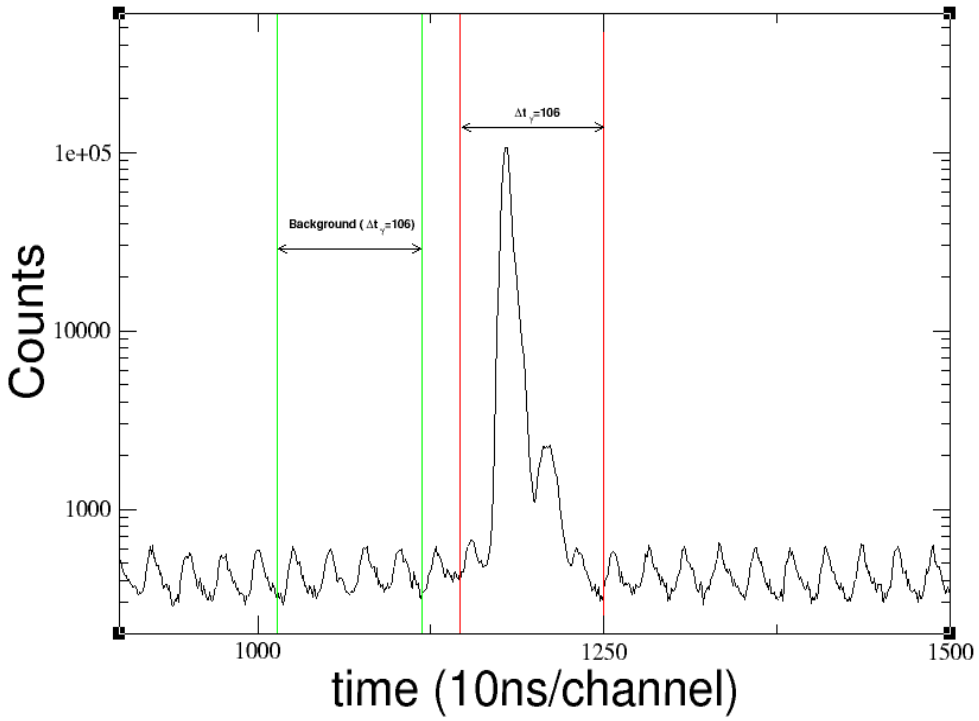

Figure 4.7: Time window for the particle-γ coincidence with $\Delta t_\gamma = 106$ ns and background with same time interval as Δt_γ.

All other γ rays and particles (^{40}Ar* and ^{194}Pt*) registering outside Δt_γ are considered as background events. These events were then subtracted from the coincidence time window using the 'adding-up' function in MIDAS [44].

The particle-γ coincidence condition resulted in a spectrum with the peak (1461 keV) and background as seen in Fig. 4.8.

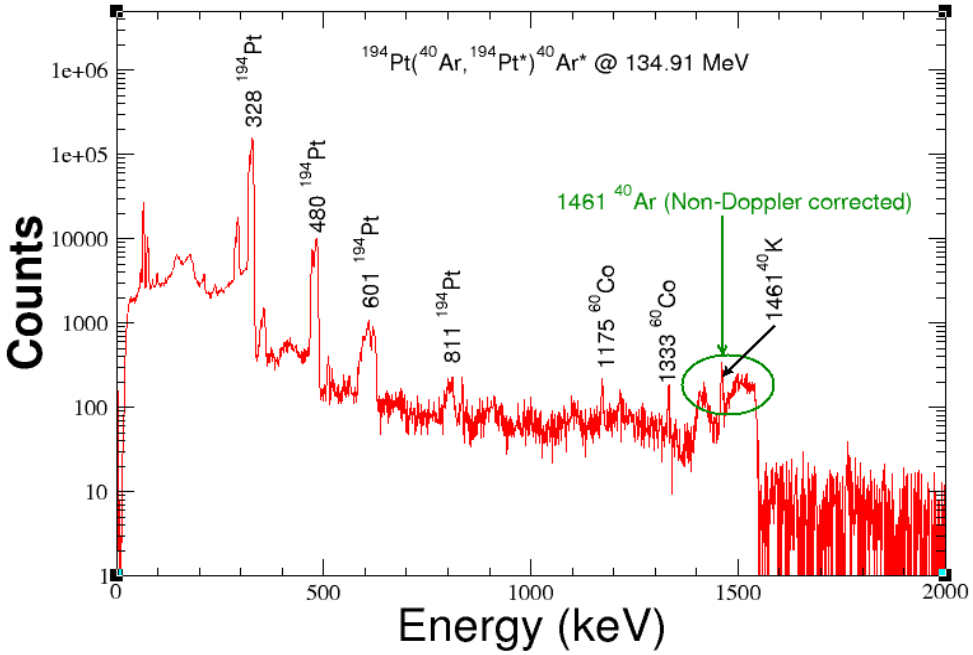

Figure 4.8: Non-Doppler corrected spectrum with labeled background energy peaks.

4.6.3 Energy Sharing Condition

In addition to the particle and particle-γ coincidence conditions, the background can be reduced further. An energy sharing condition was implemented to achieve this goal. When charged particles deposit energy on the S3 detector, the energy is sometimes shared between a sector (or a ring) and its adjoining dead layer. A dead layer of a detector is the inactive layer between two adjacent rings or sectors. Since the full energy is not deposited on the ring or sector, it is registered as background. By plotting a 2D histogram of energies of sectors as a function rings, an optimum energy gate for this condition is chosen. The energy difference, $|E_{sector} - E_{ring}|$, was incremented in steps of 100 keV to get the boundaries of the 2D histogram. By

implementing this condition the spectrum was clean from background and the elastic peak of the 2_1^+ of ^{40}Ar at 1461 keV was clearly identified. After the implementation of all the above discussed conditions, a background free spectrum without Doppler shifted energy was obtained as shown in Fig. 4.9.

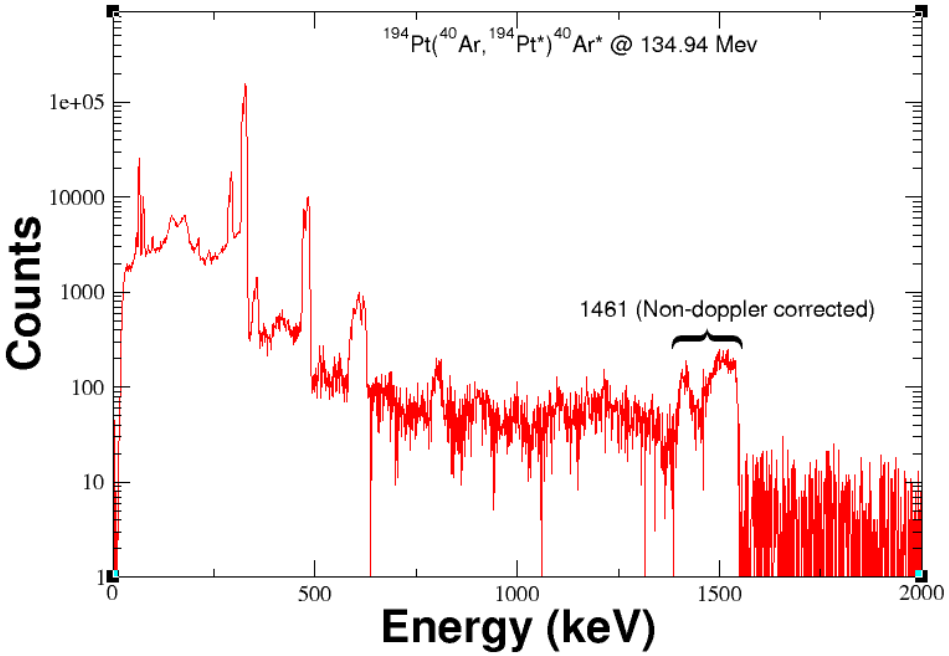

Figure 4.9: Non-Doppler corrected γ-ray spectrum with the labeled 1461 keV peak and other Coulomb excited transitions.

The final step in the data sorting required the 1461 keV peak to be doppler corrected.

4.6.4 Doppler Correction

The γ rays from the de-exciting nuclei were detected by the clovers at varying angles. This resulted in the Doppler broadening of the peaks in the spectrum.

The relativistic Doppler-shift equation is given by [51],

$$E_\gamma = \frac{E_0\sqrt{1-(\frac{v}{c})^2}}{1-\frac{v}{c}\cos\theta_{p\gamma}}, \tag{4.22}$$

where E_γ is measured γ energy, E_0 is the energy of the transition and v is the beam velocity. The angle between the de-exciting particle and the corresponding γ ray it emits is $\theta_{p\gamma}$ and $v < 10\%$ of c for this experiment Hence $(\frac{v}{c})^2 \approx 0$ and Eq. 4.22 reduces to ;

$$E_\gamma = E_0(1-\frac{v}{c}\cos\theta_{p\gamma}). \tag{4.23}$$

From the relationship between the 3D cartesian coordinate and spherical polar coordinate systems, illustrated in Fig. 4.10,

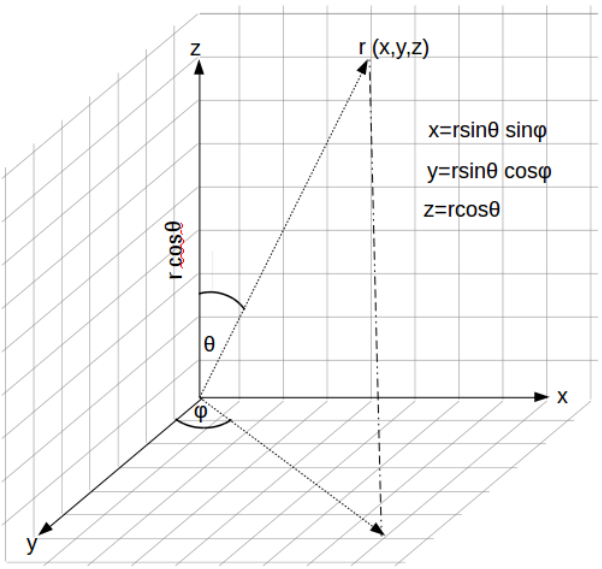

Figure 4.10: The transformation relation between spherical coordinate and polar coordinate systems.

$\theta_{p\gamma}$ can be expressed as;

$$\cos\theta_{p\gamma} = \frac{\vec{r_p}.\vec{r_\gamma}}{|r_p||r_\gamma|}. \tag{4.24}$$

Redefining $\vec{r}$ in terms of x, y and z in Fig. 4.9, Eq. 4.24 can be rewritten as;

$$\cos\theta_{p\gamma} = \frac{x_p x_\gamma + y_p y_\gamma + z_p z_\gamma}{|r_p||r_\gamma|}. \tag{4.25}$$

Replacing x, y and z with their geometrical components and substituting Eq. 4.25 into 4.23, the Doppler shift equation becomes;

$$E_\gamma = E_0\Big[1 - \frac{v}{c}(\sin\theta_p \sin\theta_\gamma \cos(\varphi_p - \varphi_\gamma) + \cos\theta_p \cos\theta_\gamma)\Big]. \tag{4.26}$$

Using Eq. 4.26 to correct the broadening of the 1461 keV peak in Fig. 4.9, a final spectrum (displaced in Fig. 4.11) is obtained.

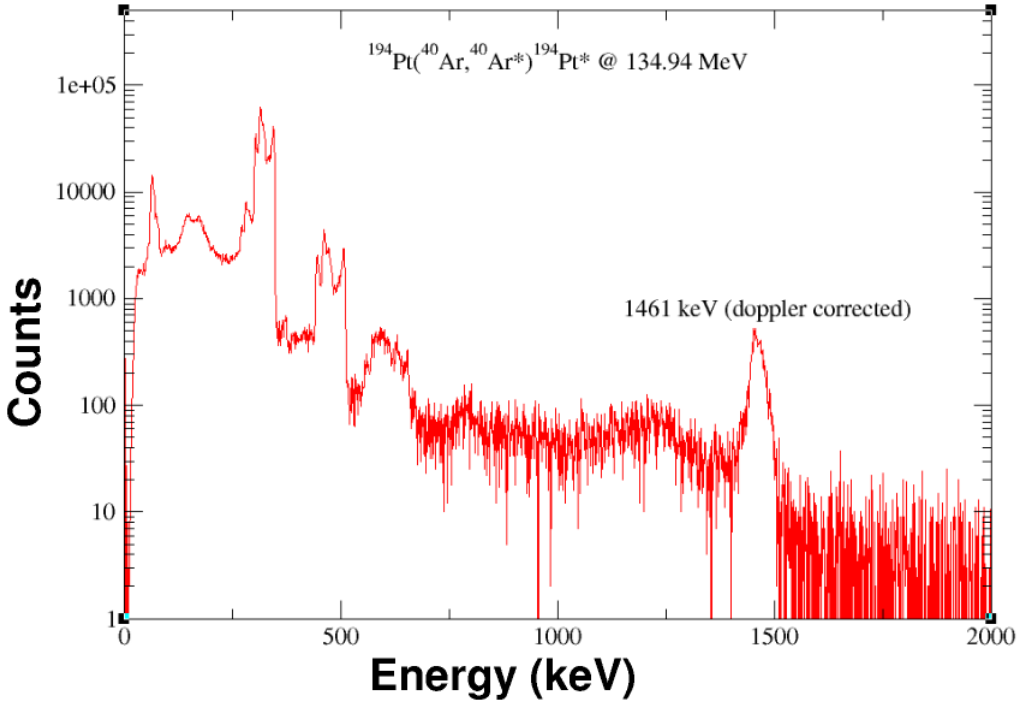

Figure 4.11: Doppler corrected γ-ray spectrum with the labeled 1461 keV peak Coulomb excited in ^{40}Ar.

Chapter 5

Discussion and Conclusion

5.1 GOSIA Simulation and Matrix Element Extraction

The $Q_s(2_1^+)$ was evaluated using the matrix element extracted from the GOSIA simulations. Two GOSIA input files were created to extract the diagonal matrix element for the 2_1^+ state in ^{40}Ar, one for the target nuclei and the second for the projectile. Information such as the level energies, life times, branching ratios and the reduced transition probabilities were obtained from the National Nuclear Data Center (NNDC) and Häusser *et al.* [17, 32, 52].

Fig. 1.5 in Chapter 1 and Fig. 5.1 show partial level schemes of ^{40}Ar and ^{194}Pt, and shows some states with corresponding properties used as inputs for the GOSIA simulations.

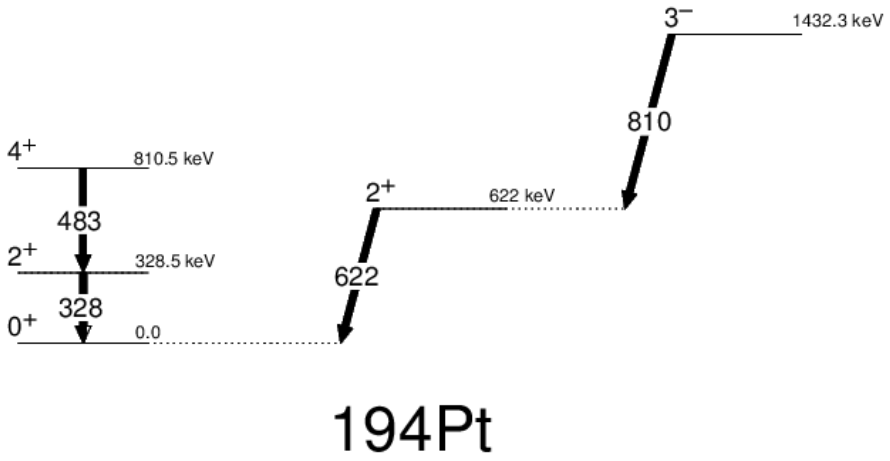

Figure 5.1: Partial level schemes of ^{194}Pt [17, 53].

Information such as detector geometry, beam energy, particle detection angular ranges and the kinematics of the experiment were also included in the input files. The comprehensive input file for ^{40}Ar and ^{194}Pt is shown in Appendix B.

To determine $\langle 2_1^+ \| \hat{E}2 \| 2_1^+ \rangle$ in ^{40}Ar, the normalization method employed in Ref. [49] was used, where a graph of $\langle 2_1^+ \| \hat{E}2 \| 2_1^+ \rangle$ as a function of $\langle 0_1^+ \| \hat{E}2 \| 2_1^+ \rangle$ was plotted. The transition matrix element, $\langle 0_1^+ \| \hat{E}2 \| 2_1^+ \rangle$, was fixed in steps of 0.01 eb and the diagonal matrix element, $\langle 2_1^+ \| \hat{E}2 \| 2_1^+ \rangle$, was varied till the integrated yields converged. The point of convergence is obtained from the intensity ratio of the projectile to the target given by;

$$\frac{\sigma_{E2}^T W(\vartheta)^T}{\sigma_{E2}^P W(\vartheta)^P} = \frac{1}{0.965} \frac{N_\gamma^P \varepsilon_\gamma^T}{N_\gamma^T \varepsilon_\gamma^P} = 1.036 \frac{I_\gamma^T}{I_\gamma^P}, \tag{5.1}$$

where $W(\vartheta)^T$ and $W(\vartheta)^P$ are the integrated angular distribution of the de-excitation γ-rays of the target and projectile respectively, σ_{E2}^T is the Coulomb

excitation cross-section of the target, σ_{E2}^{P} is the Coulomb excitation cross-section of the projectile. N_{γ}^{T} and N_{γ}^{P} are the total count from target and projectile. I_{γ}^{T} and I_{γ}^{P} the γ-ray intensities of the target and projectile respectively, while $\frac{1}{0.965} = 1.036$ was the target enrichment factor.

^{194}Pt with well-known B(E2) values (matrix elements), was used to normalize the ^{40}Ar data to minimize pile-up rejection and dead time effects. Total counts of $N_{\gamma}^{T} = 1375223 \pm 1219$ and $N_{\gamma}^{P} = 15054 \pm 147$, and absolute efficiencies of $\varepsilon_{\gamma}^{T} = 1427.418 \pm 42.834$ and $\varepsilon_{\gamma}^{P} = 475.516 \pm 9.470$ yielded intensities of $I_{\gamma}^{T} = 963.4 \pm 28.9$ and $I_{\gamma}^{P} = 31.8 \pm 0.7$ respectively. The GOSIA simulations resulted in the Coulomb excitation diagonal band plotted in Fig. 5.2. For the error estimation, the systematic error was considered to be negligible since the data was normalized to well known gamma peaks in the platinum target. Emphasis was placed on the statistical errors from independent measurement in quadrature. The statistical error on $\langle 2_1^+ \| \hat{E}2 \| 2_1^+ \rangle$ was obtained from the crossing of the life time (B(E2) value) with the errors on the diagonal matrix element and the diagonal matrix element with the errors on the life time. $\Delta\langle 2_1^+ \| \hat{E}2 \| 2_1^+ \rangle = \sqrt{0.02^2 + 0.02^2 + 0.02^2 + 0.02^2} = 0.04$ eb. From Eq. 5.2,

$$\langle 2_1^+ \| \hat{E}2 \| 2_1^+ \rangle = \frac{Q_s}{0.75793} \ (eb), \tag{5.2}$$

which relates the diagonal matrix element, $\langle 2_1^+ \| \hat{E}2 \| 2_1^+ \rangle$, to the spectroscopic quadrupole moment, Q_s, hence the $Q_s(2_1^+)$ of ^{40}Ar was determined as 0.00±0.04 eb.

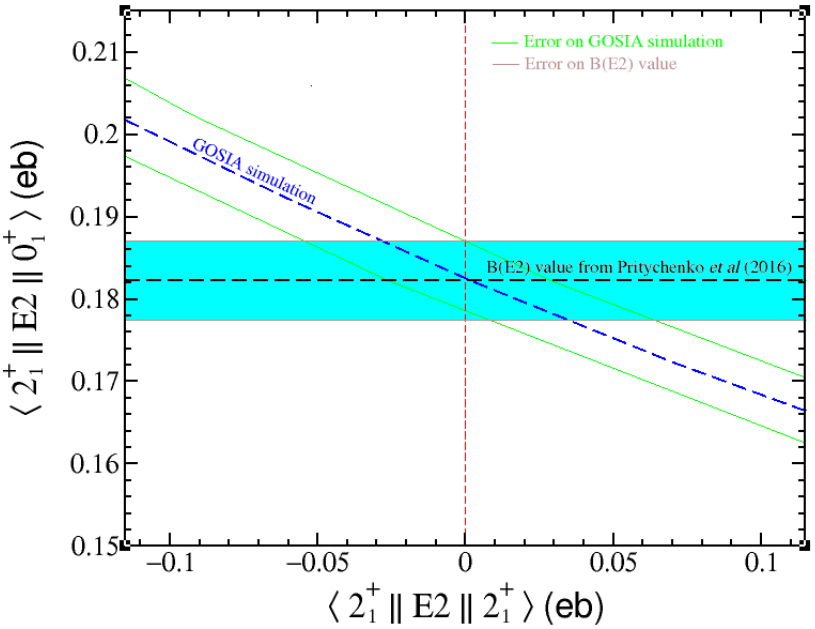

Figure 5.2: The $\langle 0_1^+ \| \hat{E}2 \| 2_1^+ \rangle$ as a function of $\langle 2_1^+ \| \hat{E}2 \| 2_1^+ \rangle$ for the 2_1^+ state in ^{40}Ar. The black dashed line represent the transition matrix element adopted from Pritychenko's table of B(E2) values [53]. The shaded region is the error on the transition matrix element, while the dashed blue line represents the diagonal matrix element for the GOSIA simulations. The green lines are the respective errors (minimum and maximum) on the diagonal matrix elements.

5.2 Conclusion

Coulomb excitation experimental work aimed to determine $Q_s(2_1^+)$ of ^{40}Ar was performed using the AFRODITE array at iThemba LABS. The process involved the extraction of diagonal matrix element by measuring de-excitation γ-ray energies of the excited ^{40}Ar particles from the 2_1^+ to the ground state. The normalization nuclide, ^{194}Pt, was chosen since its transi-

tion energies, B(E2) values, life times and branching ratios are well known [17, 53].

Results from Nakai *et al.* and Spear *et al.*, in agreement with Rowe's argument of the shape of light nuclei, shed light on the shape and behaviour of the *sd*-shell nuclei. Nakai *et al.* found $Q_s(2_1^+) = +1(4)$ for ^{40}Ar [16] indicating a nearly spherical shape and $Q_s(2_1^+)$ of other *sd*-shells nuclei compiled by Spear [13, 15, 16], in Table 5.1 agrees with Rowe's explanation.

Table 5.1: Adopted experimental values of $Q_s(2_1^+)$ for different nuclei [13].

nuclei	Adopted $Q_s(2_1^+)$ (e fm^2)
^{18}O	-2(3)
^{22}Ne	-19(4)
^{24}Mg	-18(2)
^{30}Si	-5(6)
^{32}Si	-9(4)
^{36}Ar	+11(6)
^{40}Ar	+1(4)

The rapidly changing shape of the *sd*-shell nuclei, is due to a competition between aligned and pair coupling schemes [54]. Recent measurements done at iThemba LABS by University of the Western Cape Coulex group also agrees with the shape changing argued by Rowe and reported by Spear and Nakai [13, 15, 16, 54], as shown in Table 5.1 and Fig.5.3.

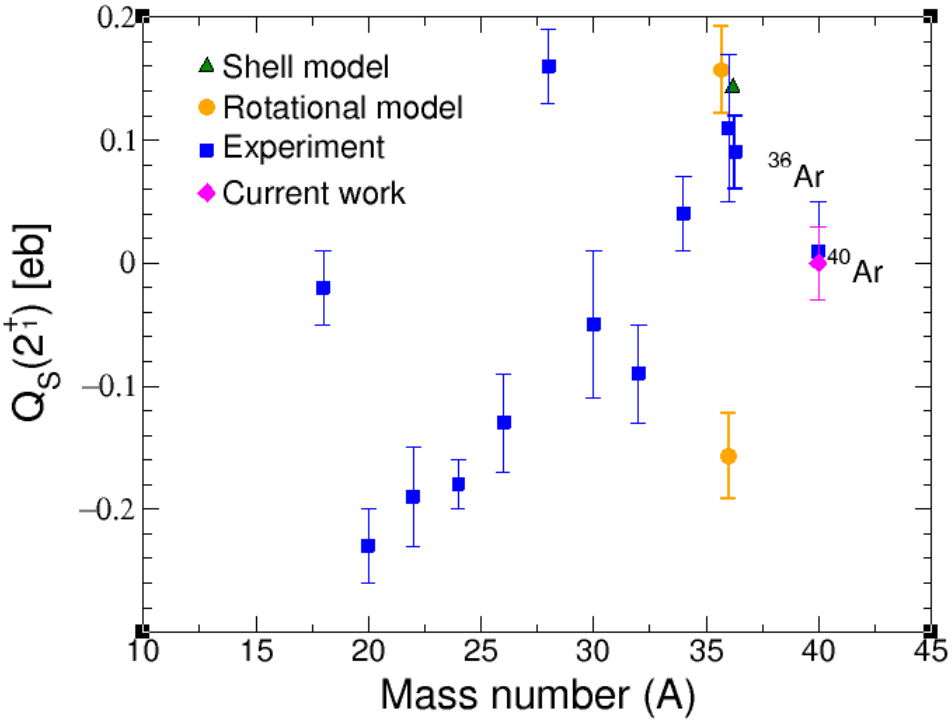

Figure 5.3: Previous and current experimental measurement of $Q_s(2_1^+)$ compared to theory in the *sd* shell [13, 15, 16, 49].

The Coulomb excitation experiment for this research work where a 134.94 MeV ^{40}Ar beam was Coulomb excited on a ^{194}Pt target with angular coverage of 130° to 159° resulted in the extraction of the diagonal matrix ($2_1^+ \longrightarrow 2_1^+$) as 0.00(0.04) eb and a subsequent value of $Q_s(2_1^+) = +0.00(0.03)$ eb. The result also suggested a spherical shape with a better error approximation than from previous studies.

Appendix A

A.1 Rutherford Cross Section

The Coulomb excitation theory considers that an incident nucleus can scatter if its electromagnetic field interacts with the field of the target nucleus. This form of interaction was first observed by Rutherford in the famous alpha particle scattering experiment (see Chapter 1). If conditions such as safe energy, safe distance and the Sommerfield parameter are carefully considered, the effect of the nuclear force can be greatly minimized to an extent that the excitation can be assumed to be solely electromagnetic. Assuming that an incident particle with charge $Z_i e$ approaches a target nucleus of charge $Z_t e$ on a head-on collision, the distance of closest approach before scattering is the point at which the kinetic energy equals the Coulomb potential energy of the system in the center-of-mass frame,

$$T_{CM} = V_{CM} = \frac{1}{2}\mu\nu_o^2 = \frac{Z_i Z_t e^2}{4\pi\varepsilon_o d} \tag{A.1}$$

and

$$F_c = \frac{Z_i Z_t e^2}{4\pi\varepsilon_o r^2}, \tag{A.2}$$

where μ is the reduced mass, ν_o is initial projectile velocity in the laboratory frame, d and r are the distance of closest approach and position vector with

angle ϑ (in the center-of-mass frame) to the z-axis respectively. The angular momentum of the system is also conserved.

$$\mu_o \nu_o b = mr^2 \frac{d\vartheta}{dt}. \tag{A.3}$$

where b is the impact parameter and if the path of the incident particle is assumed to be symmetric about the x-axis, the initial and final momenta are equal and opposite in direction,

$$p_i = +\mu_o v_o sin\Big(\frac{\theta}{2}\Big), \tag{A.4}$$

$$p_f = -\mu_o v_o sin\Big(\frac{\theta}{2}\Big), \tag{A.5}$$

and the change in momentum, Δp, is given by,

$$\Delta p = 2\mu_o v_o sin\Big(\frac{\theta}{2}\Big). \tag{A.6}$$

From Newton's second law of motion, Δp is defined as;

$$\Delta p = \int F cos\vartheta dt = \int F\Big(\frac{dt}{d\vartheta}\Big) d\vartheta. \tag{A.7}$$

Defining $(\frac{dt}{d\vartheta})$ from Eq. (A.3), substituting (A.2) into (A.7) and integrating within the limits of $-\vartheta$ and ϑ yields,

$$\Delta p = \frac{Z_i Z_t e^2}{4\pi\varepsilon_o v_o b} \int_{-\vartheta}^{\vartheta} cos\vartheta d\vartheta = \frac{Z_i Z_t e^2}{2\pi\varepsilon_o v_o b} cos\Big(\frac{\theta}{2}\Big), \tag{A.8}$$

given that $\vartheta = \frac{\pi-\theta}{2}$. To obtain the relation between b and θ, Eq. (A.6) and (A.8) are combined,

$$b = \frac{Z_i Z_t e^2}{4\pi\varepsilon_o \mu_o v_o} cot\Big(\frac{\theta}{2}\Big). \tag{A.9}$$

In the above, we assuming azimuthal symmetry about the beam axis for the scattering (incident) particle, with impact parameter ranging from b to $b+db$.

If the particle scatters into an angular range of θ and $\theta + d\theta$ with the area of db given by, $2\pi bdb$, The intensity of the scattering particle within the given impact parameter can be expressed as a function of its flux, Φ.

$$dR = 2\pi bdb\Phi, \tag{A.10}$$

$$dR = \Phi\pi d^2 \frac{cos\left(\frac{\theta}{2}\right)}{4sin\left(\frac{\theta}{2}\right)} d\theta. \tag{A.11}$$

Eq. (A.11) represents the rate at which the particles are scattered into a solid angle $d\Omega = 2\pi sin\theta d\theta$. The differential cross section of the scattered particles is given by the expression,

$$\frac{d\sigma}{d\Omega} = \frac{1}{\Phi}\frac{dR}{d\Omega} = \left(\frac{Z_i Z_t e^2}{8\pi\varepsilon_o m_o v^2}\right)^2 \frac{cos\left(\frac{\theta}{2}\right)}{sin^3\left(\frac{\theta}{2}\right)} \frac{1}{2sin\theta d\theta}, \tag{A.12}$$

$$\frac{d\sigma}{d\Omega} = \left(\frac{Z_i Z_t e^2}{8\pi\varepsilon_o \mu_o v_o^2}\right)^2 \frac{1}{sin^4\left(\frac{\theta}{2}\right)} \tag{A.13}$$

Give that the kinetic energy of the incident particle is $T = \frac{1}{2}\mu_o v_o^2$, Eq. (A.13) can also be expressed as,

$$\frac{d\sigma}{d\Omega} = \left(\frac{Z_i Z_t e^2}{16\pi\varepsilon_o E}\right)^2 \frac{1}{sin^4\left(\frac{\theta}{2}\right)}. \tag{A.14}$$

Defining the kinetic energy of the incident particle in terms of the distance of closest approach in a head-on collision as from Eq. (A.1) and substituting into Eq. (A.14), the differential cross section becomes

$$\frac{d\sigma}{d\Omega} = \left(\frac{d}{4}\right)^2 \frac{1}{sin^4\left(\frac{\theta}{2}\right)}. \tag{A.15}$$

Appendix B

GOSIA Input Files

B.1 ^{40}Ar Input File (Projectile)

```
OP,FILE
22,3,1
40Ar.out
9,3,1
det40Ar.gdt
8,3,1
det40Ar.raw
0,0,0
OP,TITL
40Ar+194Pt@134.94 Mev beam excitation
OP,GOSI
LEVE !Excitation energies
1,1,0,0
2,1,2,1.461
3,1,4,2.893
4,1,0,2.1209
5,1,2,2.5241
0,0,0,0
ME !Matrix elements
2,0,0,0,0
1,2,0.14,-1,2
1,5,0.0695,-0.1,1
2,2,0.36656,-1,1.8 !¡2+——E2——2+¿=Qs/0.75793;Qs=1
2,3,0.2077,-0.4,1.3
2,4,0.06563,-0.3,1.1
2,5,0.2704,-0.5,1.5
3,5,0.6047,-0.4,1.6
7,0,0,0,0
2,5,0.5755,-0.2,1.9
0,0,0,0,0
```

```
EXPT !Experimental details
24,18,40
-78,194,134.94,130.9,4,1,0,0,360,0,1 !R1
-78,194,134.94,131.8,4,1,0,0,360,0,2 !R2
-78,194,134.94,132.6,4,1,0,0,360,0,3 !R3
-78,194,134.94,133.5,4,1,0,0,360,0,4 !R4
-78,194,134.94,134.4,4,1,0,0,360,0,5 !R5
-78,194,134.94,135.3,4,1,0,0,360,0,6 !R6
-78,194,134.94,136.3,4,1,0,0,360,0,7 !R7
-78,194,134.94,137.3,4,1,0,0,360,0,8 !R8
-78,194,134.94,138.3,4,1,0,0,360,0,9 !R9
-78,194,134.94,139.4,4,1,0,0,360,0,10 !R10
-78,194,134.94,140.5,4,1,0,0,360,0,11 !R11
-78,194,134.94,141.6,4,1,0,0,360,0,12 !R12
-78,194,134.94,142.8,4,1,0,0,360,0,13 !R13
-78,194,134.94,144.0,4,1,0,0,360,0,14 !R14
-78,194,134.94,145.3,4,1,0,0,360,0,15 !R15
-78,194,134.94,146.6,4,1,0,0,360,0,16 !R16
-78,194,134.94,147.9,4,1,0,0,360,0,17 !R17
-78,194,134.94,149.3,4,1,0,0,360,0,18 !R18
-78,194,134.94,150.7,4,1,0,0,360,0,19 !R19
-78,194,134.94,152.1,4,1,0,0,360,0,20 !R20
-78,194,134.94,153.6,4,1,0,0,360,0,21 !R21
-78,194,134.94,155.2,4,1,0,0,360,0,22 !R22
-78,194,134.94,156.7,4,1,0,0,360,0,23 !R23
-78,194,134.94,158.3,4,1,0,0,360,0,24 !R24
CONT
SPL,1.
INT,24.
1,1000
2,1000
3,1000
4,1000
5,1000
6,1000
7,1000
8,1000
9,1000
10,1000
11,1000
12,1000
13,1000
14,1000
15,1000
16,1000
17,1000
18,1000
19,1000
20,1000
21,1000
22,1000
23,1000
24,1000
PRT,0.
1,-1
2,0
4,0
5,1
11,1
12,0
```

```
14,0
16,0
18,1
0,0
END,


OP,YIEL
0
8,1
1.0,1.5,2.0,2.5,3.0,3.5,4.0,4.5 !Energy mesh points
2
0.0000677,0.0001155,0.000330,0.000568,0.000972,0.000998,0.001175,0.001346 !Electron conversion coefficients
32,32,32,32,32,32,32,32,32,32,32,32,32,32,32,32,32,32,32,32,32,32,32,32 ! 24 experiments and 32 gamma detectors per ex-
periment
1,1,1,1,1,1,1,1,1,1,1,1,1,1,1,1,1,1,1,1,1,1,1,1,1,1,1,1,1,1,1,1 ! up to 32
84.8,95.1,95.1,84.8,84.8,95.1,95.1,84.8,84.8,95.1,95.1,84.8,84.8,95.1,95.1,84.8,130.1,140.4,140.4,
130.1,130.1,140.4,140.4,130.1,130.1,140.4,140.4,130.1,84.8,95.1,95.1,84.8 !theta angles
95.1,95.1,84.8,84.8,49.8,49.8,39.5,39.5,230.3,230.3,220.0,220.0,320.3,320.3,310.0,310.0,5.2,5.2,
354.7,354.7,275.0,275.0,264.7,264.7,49.8,49.8,39.5,39.5,275.0,275.0,264.7,264.7 !phi angles
1,1,1,1,1,1,1,1,1,1,1,1,1,1,1,1,1,1,1,1,1,1,1,1,1,1,1,1,1,1,1,1
84.8,95.1,95.1,84.8,84.8,95.1,95.1,84.8,84.8,95.1,95.1,84.8,84.8,95.1,95.1,84.8,130.1,140.4,140.4,
130.1,130.1,140.4,140.4,130.1,130.1,140.4,140.4,130.1,84.8,95.1,95.1,84.8
95.1,95.1,84.8,84.8,49.8,49.8,39.5,39.5,230.3,230.3,220.0,220.0,320.3,320.3,310.0,310.0,5.2,5.2,
354.7,354.7,275.0,275.0,264.7,264.7,49.8,49.8,39.5,39.5,275.0,275.0,264.7,264.7
1,1,1,1,1,1,1,1,1,1,1,1,1,1,1,1,1,1,1,1,1,1,1,1,1,1,1,1,1,1,1,1
84.8,95.1,95.1,84.8,84.8,95.1,95.1,84.8,84.8,95.1,95.1,84.8,84.8,95.1,95.1,84.8,130.1,140.4,140.4,
130.1,130.1,140.4,140.4,130.1,130.1,140.4,140.4,130.1,84.8,95.1,95.1,84.8
95.1,95.1,84.8,84.8,49.8,49.8,39.5,39.5,230.3,230.3,220.0,220.0,320.3,320.3,310.0,310.0,5.2,5.2,
354.7,354.7,275.0,275.0,264.7,264.7,49.8,49.8,39.5,39.5,275.0,275.0,264.7,264.7
1,1,1,1,1,1,1,1,1,1,1,1,1,1,1,1,1,1,1,1,1,1,1,1,1,1,1,1,1,1,1,1
84.8,95.1,95.1,84.8,84.8,95.1,95.1,84.8,84.8,95.1,95.1,84.8,84.8,95.1,95.1,84.8,130.1,140.4,140.4,
130.1,130.1,140.4,140.4,130.1,130.1,140.4,140.4,130.1,84.8,95.1,95.1,84.8
95.1,95.1,84.8,84.8,49.8,49.8,39.5,39.5,230.3,230.3,220.0,220.0,320.3,320.3,310.0,310.0,5.2,5.2,
354.7,354.7,275.0,275.0,264.7,264.7,49.8,49.8,39.5,39.5,275.0,275.0,264.7,264.7
1,1,1,1,1,1,1,1,1,1,1,1,1,1,1,1,1,1,1,1,1,1,1,1,1,1,1,1,1,1,1,1
84.8,95.1,95.1,84.8,84.8,95.1,95.1,84.8,84.8,95.1,95.1,84.8,84.8,95.1,95.1,84.8,130.1,140.4,140.4,
130.1,130.1,140.4,140.4,130.1,130.1,140.4,140.4,130.1,84.8,95.1,95.1,84.8
95.1,95.1,84.8,84.8,49.8,49.8,39.5,39.5,230.3,230.3,220.0,220.0,320.3,320.3,310.0,310.0,5.2,5.2,
354.7,354.7,275.0,275.0,264.7,264.7,49.8,49.8,39.5,39.5,275.0,275.0,264.7,264.7
1,1,1,1,1,1,1,1,1,1,1,1,1,1,1,1,1,1,1,1,1,1,1,1,1,1,1,1,1,1,1,1
84.8,95.1,95.1,84.8,84.8,95.1,95.1,84.8,84.8,95.1,95.1,84.8,84.8,95.1,95.1,84.8,130.1,140.4,140.4,
130.1,130.1,140.4,140.4,130.1,130.1,140.4,140.4,130.1,84.8,95.1,95.1,84.8
95.1,95.1,84.8,84.8,49.8,49.8,39.5,39.5,230.3,230.3,220.0,220.0,320.3,320.3,310.0,310.0,5.2,5.2,
354.7,354.7,275.0,275.0,264.7,264.7,49.8,49.8,39.5,39.5,275.0,275.0,264.7,264.7
1,1,1,1,1,1,1,1,1,1,1,1,1,1,1,1,1,1,1,1,1,1,1,1,1,1,1,1,1,1,1,1
84.8,95.1,95.1,84.8,84.8,95.1,95.1,84.8,84.8,95.1,95.1,84.8,84.8,95.1,95.1,84.8,130.1,140.4,140.4,
130.1,130.1,140.4,140.4,130.1,130.1,140.4,140.4,130.1,84.8,95.1,95.1,84.8
95.1,95.1,84.8,84.8,49.8,49.8,39.5,39.5,230.3,230.3,220.0,220.0,320.3,320.3,310.0,310.0,5.2,5.2,
354.7,354.7,275.0,275.0,264.7,264.7,49.8,49.8,39.5,39.5,275.0,275.0,264.7,264.7
1,1,1,1,1,1,1,1,1,1,1,1,1,1,1,1,1,1,1,1,1,1,1,1,1,1,1,1,1,1,1,1
84.8,95.1,95.1,84.8,84.8,95.1,95.1,84.8,84.8,95.1,95.1,84.8,84.8,95.1,95.1,84.8,130.1,140.4,140.4,
130.1,130.1,140.4,140.4,130.1,130.1,140.4,140.4,130.1,84.8,95.1,95.1,84.8
95.1,95.1,84.8,84.8,49.8,49.8,39.5,39.5,230.3,230.3,220.0,220.0,320.3,320.3,310.0,310.0,5.2,5.2,
354.7,354.7,275.0,275.0,264.7,264.7,49.8,49.8,39.5,39.5,275.0,275.0,264.7,264.7
1,1,1,1,1,1,1,1,1,1,1,1,1,1,1,1,1,1,1,1,1,1,1,1,1,1,1,1,1,1,1,1
84.8,95.1,95.1,84.8,84.8,95.1,95.1,84.8,84.8,95.1,95.1,84.8,84.8,95.1,95.1,84.8,130.1,140.4,140.4,
130.1,130.1,140.4,140.4,130.1,130.1,140.4,140.4,130.1,84.8,95.1,95.1,84.8
95.1,95.1,84.8,84.8,49.8,49.8,39.5,39.5,230.3,230.3,220.0,220.0,320.3,320.3,310.0,310.0,5.2,5.2,
```

```
354.7,354.7,275.0,275.0,264.7,264.7,49.8,49.8,39.5,39.5,275.0,275.0,264.7,264.7
1,1,1,1,1,1,1,1,1,1,1,1,1,1,1,1,1,1,1,1,1,1,1,1,1,1,1,1,1,1,1,1
84.8,95.1,95.1,84.8,84.8,95.1,95.1,84.8,84.8,95.1,95.1,84.8,84.8,95.1,95.1,84.8,130.1,140.4,140.4,
130.1,130.1,140.4,140.4,130.1,130.1,140.4,140.4,130.1,84.8,95.1,95.1,84.8
95.1,95.1,84.8,84.8,49.8,49.8,39.5,39.5,230.3,230.3,220.0,220.0,320.3,320.3,310.0,310.0,5.2,5.2,
354.7,354.7,275.0,275.0,264.7,264.7,49.8,49.8,39.5,39.5,275.0,275.0,264.7,264.7
1,1,1,1,1,1,1,1,1,1,1,1,1,1,1,1,1,1,1,1,1,1,1,1,1,1,1,1,1,1,1,1
84.8,95.1,95.1,84.8,84.8,95.1,95.1,84.8,84.8,95.1,95.1,84.8,84.8,95.1,95.1,84.8,130.1,140.4,140.4,
130.1,130.1,140.4,140.4,130.1,130.1,140.4,140.4,130.1,84.8,95.1,95.1,84.8
95.1,95.1,84.8,84.8,49.8,49.8,39.5,39.5,230.3,230.3,220.0,220.0,320.3,320.3,310.0,310.0,5.2,5.2,
354.7,354.7,275.0,275.0,264.7,264.7,49.8,49.8,39.5,39.5,275.0,275.0,264.7,264.7
1,1,1,1,1,1,1,1,1,1,1,1,1,1,1,1,1,1,1,1,1,1,1,1,1,1,1,1,1,1,1,1
84.8,95.1,95.1,84.8,84.8,95.1,95.1,84.8,84.8,95.1,95.1,84.8,84.8,95.1,95.1,84.8,130.1,140.4,140.4,
130.1,130.1,140.4,140.4,130.1,130.1,140.4,140.4,130.1,84.8,95.1,95.1,84.8
95.1,95.1,84.8,84.8,49.8,49.8,39.5,39.5,230.3,230.3,220.0,220.0,320.3,320.3,310.0,310.0,5.2,5.2,
354.7,354.7,275.0,275.0,264.7,264.7,49.8,49.8,39.5,39.5,275.0,275.0,264.7,264.7
1,1,1,1,1,1,1,1,1,1,1,1,1,1,1,1,1,1,1,1,1,1,1,1,1,1,1,1,1,1,1,1
84.8,95.1,95.1,84.8,84.8,95.1,95.1,84.8,84.8,95.1,95.1,84.8,84.8,95.1,95.1,84.8,130.1,140.4,140.4,
130.1,130.1,140.4,140.4,130.1,130.1,140.4,140.4,130.1,84.8,95.1,95.1,84.8
95.1,95.1,84.8,84.8,49.8,49.8,39.5,39.5,230.3,230.3,220.0,220.0,320.3,320.3,310.0,310.0,5.2,5.2,
354.7,354.7,275.0,275.0,264.7,264.7,49.8,49.8,39.5,39.5,275.0,275.0,264.7,264.7
1,1,1,1,1,1,1,1,1,1,1,1,1,1,1,1,1,1,1,1,1,1,1,1,1,1,1,1,1,1,1,1
84.8,95.1,95.1,84.8,84.8,95.1,95.1,84.8,84.8,95.1,95.1,84.8,84.8,95.1,95.1,84.8,130.1,140.4,140.4,
130.1,130.1,140.4,140.4,130.1,130.1,140.4,140.4,130.1,84.8,95.1,95.1,84.8,
95.1,95.1,84.8,84.8,49.8,49.8,39.5,39.5,230.3,230.3,220.0,220.0,320.3,320.3,310.0,310.0,5.2,5.2,
354.7,354.7,275.0,275.0,264.7,264.7,49.8,49.8,39.5,39.5,275.0,275.0,264.7,264.7
1,1,1,1,1,1,1,1,1,1,1,1,1,1,1,1,1,1,1,1,1,1,1,1,1,1,1,1,1,1,1,1
84.8,95.1,95.1,84.8,84.8,95.1,95.1,84.8,84.8,95.1,95.1,84.8,84.8,95.1,95.1,84.8,130.1,140.4,140.4,
130.1,130.1,140.4,140.4,130.1,130.1,140.4,140.4,130.1,84.8,95.1,95.1,84.8
95.1,95.1,84.8,84.8,49.8,49.8,39.5,39.5,230.3,230.3,220.0,220.0,320.3,320.3,310.0,310.0,5.2,5.2,
354.7,354.7,275.0,275.0,264.7,264.7,49.8,49.8,39.5,39.5,275.0,275.0,264.7,264.7
1,1,1,1,1,1,1,1,1,1,1,1,1,1,1,1,1,1,1,1,1,1,1,1,1,1,1,1,1,1,1,1
84.8,95.1,95.1,84.8,84.8,95.1,95.1,84.8,84.8,95.1,95.1,84.8,84.8,95.1,95.1,84.8,130.1,140.4,140.4,
130.1,130.1,140.4,140.4,130.1,130.1,140.4,140.4,130.1,84.8,95.1,95.1,84.8
95.1,95.1,84.8,84.8,49.8,49.8,39.5,39.5,230.3,230.3,220.0,220.0,320.3,320.3,310.0,310.0,5.2,5.2,
354.7,354.7,275.0,275.0,264.7,264.7,49.8,49.8,39.5,39.5,275.0,275.0,264.7,264.7
1,1,1,1,1,1,1,1,1,1,1,1,1,1,1,1,1,1,1,1,1,1,1,1,1,1,1,1,1,1,1,1
84.8,95.1,95.1,84.8,84.8,95.1,95.1,84.8,84.8,95.1,95.1,84.8,84.8,95.1,95.1,84.8,130.1,140.4,140.4,
130.1,130.1,140.4,140.4,130.1,130.1,140.4,140.4,130.1,84.8,95.1,95.1,84.8
95.1,95.1,84.8,84.8,49.8,49.8,39.5,39.5,230.3,230.3,220.0,220.0,320.3,320.3,310.0,310.0,5.2,5.2,
354.7,354.7,275.0,275.0,264.7,264.7,49.8,49.8,39.5,39.5,275.0,275.0,264.7,264.7
1,1,1,1,1,1,1,1,1,1,1,1,1,1,1,1,1,1,1,1,1,1,1,1,1,1,1,1,1,1,1,1
84.8,95.1,95.1,84.8,84.8,95.1,95.1,84.8,84.8,95.1,95.1,84.8,84.8,95.1,95.1,84.8,130.1,140.4,140.4,
130.1,130.1,140.4,140.4,130.1,130.1,140.4,140.4,130.1,84.8,95.1,95.1,84.8
95.1,95.1,84.8,84.8,49.8,49.8,39.5,39.5,230.3,230.3,220.0,220.0,320.3,320.3,310.0,310.0,5.2,5.2,
354.7,354.7,275.0,275.0,264.7,264.7,49.8,49.8,39.5,39.5,275.0,275.0,264.7,264.7
1,1,1,1,1,1,1,1,1,1,1,1,1,1,1,1,1,1,1,1,1,1,1,1,1,1,1,1,1,1,1,1
84.8,95.1,95.1,84.8,84.8,95.1,95.1,84.8,84.8,95.1,95.1,84.8,84.8,95.1,95.1,84.8,130.1,140.4,140.4,
130.1,130.1,140.4,140.4,130.1,130.1,140.4,140.4,130.1,84.8,95.1,95.1,84.8
95.1,95.1,84.8,84.8,49.8,49.8,39.5,39.5,230.3,230.3,220.0,220.0,320.3,320.3,310.0,310.0,5.2,5.2,
354.7,354.7,275.0,275.0,264.7,264.7,49.8,49.8,39.5,39.5,275.0,275.0,264.7,264.7
1,1,1,1,1,1,1,1,1,1,1,1,1,1,1,1,1,1,1,1,1,1,1,1,1,1,1,1,1,1,1,1
84.8,95.1,95.1,84.8,84.8,95.1,95.1,84.8,84.8,95.1,95.1,84.8,84.8,95.1,95.1,84.8,130.1,140.4,140.4,
130.1,130.1,140.4,140.4,130.1,130.1,140.4,140.4,130.1,84.8,95.1,95.1,84.8
95.1,95.1,84.8,84.8,49.8,49.8,39.5,39.5,230.3,230.3,220.0,220.0,320.3,320.3,310.0,310.0,5.2,5.2,
354.7,354.7,275.0,275.0,264.7,264.7,49.8,49.8,39.5,39.5,275.0,275.0,264.7,264.7
1,1,1,1,1,1,1,1,1,1,1,1,1,1,1,1,1,1,1,1,1,1,1,1,1,1,1,1,1,1,1,1
84.8,95.1,95.1,84.8,84.8,95.1,95.1,84.8,84.8,95.1,95.1,84.8,84.8,95.1,95.1,84.8,130.1,140.4,140.4,
130.1,130.1,140.4,140.4,130.1,130.1,140.4,140.4,130.1,84.8,95.1,95.1,84.8
95.1,95.1,84.8,84.8,49.8,49.8,39.5,39.5,230.3,230.3,220.0,220.0,320.3,320.3,310.0,310.0,5.2,5.2,
```

354.7,354.7,275.0,275.0,264.7,264.7,49.8,49.8,39.5,39.5,275.0,275.0,264.7,264.7
1,1,1,1,1,1,1,1,1,1,1,1,1,1,1,1,1,1,1,1,1,1,1,1,1,1,1,1,1,1,1,1
84.8,95.1,95.1,84.8,84.8,95.1,95.1,84.8,84.8,95.1,95.1,84.8,84.8,95.1,95.1,84.8,130.1,140.4,140.4,
130.1,130.1,140.4,140.4,130.1,130.1,140.4,140.4,130.1,84.8,95.1,95.1,84.8
95.1,95.1,84.8,84.8,49.8,49.8,39.5,39.5,230.3,230.3,220.0,220.0,320.3,320.3,310.0,310.0,5.2,5.2,
354.7,354.7,275.0,275.0,264.7,264.7,49.8,49.8,39.5,39.5,275.0,275.0,264.7,264.7
1,1,1,1,1,1,1,1,1,1,1,1,1,1,1,1,1,1,1,1,1,1,1,1,1,1,1,1,1,1,1,1
84.8,95.1,95.1,84.8,84.8,95.1,95.1,84.8,84.8,95.1,95.1,84.8,84.8,95.1,95.1,84.8,130.1,140.4,140.4,
130.1,130.1,140.4,140.4,130.1,130.1,140.4,140.4,130.1,84.8,95.1,95.1,84.8
95.1,95.1,84.8,84.8,49.8,49.8,39.5,39.5,230.3,230.3,220.0,220.0,320.3,320.3,310.0,310.0,5.2,5.2,
354.7,354.7,275.0,275.0,264.7,264.7,49.8,49.8,39.5,39.5,275.0,275.0,264.7,264.7
1,1,1,1,1,1,1,1,1,1,1,1,1,1,1,1,1,1,1,1,1,1,1,1,1,1,1,1,1,1,1,1
84.8,95.1,95.1,84.8,84.8,95.1,95.1,84.8,84.8,95.1,95.1,84.8,84.8,95.1,95.1,84.8,130.1,140.4,140.4,
130.1,130.1,140.4,140.4,130.1,130.1,140.4,140.4,130.1,84.8,95.1,95.1,84.8
95.1,95.1,84.8,84.8,49.8,49.8,39.5,39.5,230.3,230.3,220.0,220.0,320.3,320.3,310.0,310.0,5.2,5.2,
354.7,354.7,275.0,275.0,264.7,264.7,49.8,49.8,39.5,39.5,275.0,275.0,264.7,264.7
2,1
1
1111. !1
1
1
1111. !2
1
1
1111. !3
1
1
1111. !4
1
1
1111. !5
1
1
1111. !6
1
1
1111. !7
1
1
1111. !8
1
1
1111. !9
1
1
1111. !10
1
1
1111. !11
1
1
1111. !12
1
1
1111. !13
1
1
1111. !14
1
1

1111. !15
1
1
1111. !16
1
1
1111. !17
1
1
1111. !18
1
1
1111. !19
1
1
1111. !20
1
1
1111. !21
1
1
1111. !22
1
1
1111. !23
1
1
1111. !24
1
0
0,0
3,1.0 !Lifetimes
2,1.659,0.072

3,2.813,0.404
4,981.033,30.297
0,0
0,0
OP,RAW
1
0 0 0 0 0 0 0 0
0 0 0 0 0 0 0 0
0 0 0 0 0 0 0 0
0 0 0 0 0 0 0 0
0 0 0 0 0 0 0 0
0 0 0 0 0 0 0 0
0 0 0 0 0 0 0 0
0 0 0 0 0 0 0 0
0 0 0 0 0 0 0 0
0 0 0 0 0 0 0 0
0 0 0 0 0 0 0 0
0 0 0 0 0 0 0 0
0 0 0 0 0 0 0 0
0 0 0 0 0 0 0 0
0 0 0 0 0 0 0 0
0 0 0 0 0 0 0 0
0 0 0 0 0 0 0 0
0 0 0 0 0 0 0 0

```
0 0 0 0 0 0 0 0 0
0 0 0 0 0 0 0 0 0
0 0 0 0 0 0 0 0 0
0 0 0 0 0 0 0 0 0
0 0 0 0 0 0 0 0 0
0 0 0 0 0 0 0 0 0
0 0 0 0 0 0 0 0 0
0 0 0 0 0 0 0 0 0
0 0 0 0 0 0 0 0 0
0 0 0 0 0 0 0 0 0
0 0 0 0 0 0 0 0 0
0 0 0 0 0 0 0 0 0
0 0 0 0 0 0 0 0 0
0 0 0 0 0 0 0 0 0
1
32
1,2,3,4,5,6,7,8,9,10,11,12,13,14,15,16,17,18,19,20,21,22,23,24,25,26,27,28,29,30,31,32
2
0 0 0 0 0 0 0 0 0
0 0 0 0 0 0 0 0 0
0 0 0 0 0 0 0 0 0
0 0 0 0 0 0 0 0 0
0 0 0 0 0 0 0 0 0
0 0 0 0 0 0 0 0 0
0 0 0 0 0 0 0 0 0
0 0 0 0 0 0 0 0 0
0 0 0 0 0 0 0 0 0
0 0 0 0 0 0 0 0 0
0 0 0 0 0 0 0 0 0
0 0 0 0 0 0 0 0 0
0 0 0 0 0 0 0 0 0
0 0 0 0 0 0 0 0 0
0 0 0 0 0 0 0 0 0
0 0 0 0 0 0 0 0 0
0 0 0 0 0 0 0 0 0
0 0 0 0 0 0 0 0 0
0 0 0 0 0 0 0 0 0
0 0 0 0 0 0 0 0 0
0 0 0 0 0 0 0 0 0
0 0 0 0 0 0 0 0 0
0 0 0 0 0 0 0 0 0
0 0 0 0 0 0 0 0 0
0 0 0 0 0 0 0 0 0
0 0 0 0 0 0 0 0 0
0 0 0 0 0 0 0 0 0
0 0 0 0 0 0 0 0 0
0 0 0 0 0 0 0 0 0
0 0 0 0 0 0 0 0 0
0 0 0 0 0 0 0 0 0
0 0 0 0 0 0 0 0 0
1
32
1,2,3,4,5,6,7,8,9,10,11,12,13,14,15,16,17,18,19,20,21,22,23,24,25,26,27,28,29,30,31,32
3
0 0 0 0 0 0 0 0 0
0 0 0 0 0 0 0 0 0
0 0 0 0 0 0 0 0 0
0 0 0 0 0 0 0 0 0
0 0 0 0 0 0 0 0 0
0 0 0 0 0 0 0 0 0
```

```
0 0 0 0 0 0 0 0 0
0 0 0 0 0 0 0 0 0
0 0 0 0 0 0 0 0 0
0 0 0 0 0 0 0 0 0
0 0 0 0 0 0 0 0 0
0 0 0 0 0 0 0 0 0
0 0 0 0 0 0 0 0 0
0 0 0 0 0 0 0 0 0
0 0 0 0 0 0 0 0 0
0 0 0 0 0 0 0 0 0
0 0 0 0 0 0 0 0 0
0 0 0 0 0 0 0 0 0
0 0 0 0 0 0 0 0 0
0 0 0 0 0 0 0 0 0
0 0 0 0 0 0 0 0 0
0 0 0 0 0 0 0 0 0
0 0 0 0 0 0 0 0 0
0 0 0 0 0 0 0 0 0
0 0 0 0 0 0 0 0 0
0 0 0 0 0 0 0 0 0
0 0 0 0 0 0 0 0 0
0 0 0 0 0 0 0 0 0
0 0 0 0 0 0 0 0 0
0 0 0 0 0 0 0 0 0
0 0 0 0 0 0 0 0 0
0 0 0 0 0 0 0 0 0
1
32
1,2,3,4,5,6,7,8,9,10,11,12,13,14,15,16,17,18,19,20,21,22,23,24,25,26,27,28,29,30,31,32
4
0 0 0 0 0 0 0 0 0
0 0 0 0 0 0 0 0 0
0 0 0 0 0 0 0 0 0
0 0 0 0 0 0 0 0 0
0 0 0 0 0 0 0 0 0
0 0 0 0 0 0 0 0 0
0 0 0 0 0 0 0 0 0
0 0 0 0 0 0 0 0 0
0 0 0 0 0 0 0 0 0
0 0 0 0 0 0 0 0 0
0 0 0 0 0 0 0 0 0
0 0 0 0 0 0 0 0 0
0 0 0 0 0 0 0 0 0
0 0 0 0 0 0 0 0 0
0 0 0 0 0 0 0 0 0
0 0 0 0 0 0 0 0 0
0 0 0 0 0 0 0 0 0
0 0 0 0 0 0 0 0 0
0 0 0 0 0 0 0 0 0
0 0 0 0 0 0 0 0 0
0 0 0 0 0 0 0 0 0
0 0 0 0 0 0 0 0 0
0 0 0 0 0 0 0 0 0
0 0 0 0 0 0 0 0 0
0 0 0 0 0 0 0 0 0
0 0 0 0 0 0 0 0 0
0 0 0 0 0 0 0 0 0
0 0 0 0 0 0 0 0 0
0 0 0 0 0 0 0 0 0
0 0 0 0 0 0 0 0 0
```

```
0 0 0 0 0 0 0 0
0 0 0 0 0 0 0 0
1
32
1,2,3,4,5,6,7,8,9,10,11,12,13,14,15,16,17,18,19,20,21,22,23,24,25,26,27,28,29,30,31,32
5
0 0 0 0 0 0 0 0
0 0 0 0 0 0 0 0
0 0 0 0 0 0 0 0
0 0 0 0 0 0 0 0
0 0 0 0 0 0 0 0
0 0 0 0 0 0 0 0
0 0 0 0 0 0 0 0
0 0 0 0 0 0 0 0
0 0 0 0 0 0 0 0
0 0 0 0 0 0 0 0
0 0 0 0 0 0 0 0
0 0 0 0 0 0 0 0
0 0 0 0 0 0 0 0
0 0 0 0 0 0 0 0
0 0 0 0 0 0 0 0
0 0 0 0 0 0 0 0
0 0 0 0 0 0 0 0
0 0 0 0 0 0 0 0
0 0 0 0 0 0 0 0
0 0 0 0 0 0 0 0
0 0 0 0 0 0 0 0
0 0 0 0 0 0 0 0
0 0 0 0 0 0 0 0
0 0 0 0 0 0 0 0
0 0 0 0 0 0 0 0
0 0 0 0 0 0 0 0
0 0 0 0 0 0 0 0
0 0 0 0 0 0 0 0
0 0 0 0 0 0 0 0
0 0 0 0 0 0 0 0
0 0 0 0 0 0 0 0
0 0 0 0 0 0 0 0
1
32
1,2,3,4,5,6,7,8,9,10,11,12,13,14,15,16,17,18,19,20,21,22,23,24,25,26,27,28,29,30,31,32
6
0 0 0 0 0 0 0 0
0 0 0 0 0 0 0 0
0 0 0 0 0 0 0 0
0 0 0 0 0 0 0 0
0 0 0 0 0 0 0 0
0 0 0 0 0 0 0 0
0 0 0 0 0 0 0 0
0 0 0 0 0 0 0 0
0 0 0 0 0 0 0 0
0 0 0 0 0 0 0 0
0 0 0 0 0 0 0 0
0 0 0 0 0 0 0 0
0 0 0 0 0 0 0 0
0 0 0 0 0 0 0 0
0 0 0 0 0 0 0 0
0 0 0 0 0 0 0 0
0 0 0 0 0 0 0 0
0 0 0 0 0 0 0 0
```

```
0 0 0 0 0 0 0 0 0
0 0 0 0 0 0 0 0 0
0 0 0 0 0 0 0 0 0
0 0 0 0 0 0 0 0 0
0 0 0 0 0 0 0 0 0
0 0 0 0 0 0 0 0 0
0 0 0 0 0 0 0 0 0
0 0 0 0 0 0 0 0 0
0 0 0 0 0 0 0 0 0
0 0 0 0 0 0 0 0 0
0 0 0 0 0 0 0 0 0
0 0 0 0 0 0 0 0 0
0 0 0 0 0 0 0 0 0
0 0 0 0 0 0 0 0 0
1
32
1,2,3,4,5,6,7,8,9,10,11,12,13,14,15,16,17,18,19,20,21,22,23,24,25,26,27,28,29,30,31,32
7
0 0 0 0 0 0 0 0 0
0 0 0 0 0 0 0 0 0
0 0 0 0 0 0 0 0 0
0 0 0 0 0 0 0 0 0
0 0 0 0 0 0 0 0 0
0 0 0 0 0 0 0 0 0
0 0 0 0 0 0 0 0 0
0 0 0 0 0 0 0 0 0
0 0 0 0 0 0 0 0 0
0 0 0 0 0 0 0 0 0
0 0 0 0 0 0 0 0 0
0 0 0 0 0 0 0 0 0
0 0 0 0 0 0 0 0 0
0 0 0 0 0 0 0 0 0
0 0 0 0 0 0 0 0 0
0 0 0 0 0 0 0 0 0
0 0 0 0 0 0 0 0 0
0 0 0 0 0 0 0 0 0
0 0 0 0 0 0 0 0 0
0 0 0 0 0 0 0 0 0
0 0 0 0 0 0 0 0 0
0 0 0 0 0 0 0 0 0
0 0 0 0 0 0 0 0 0
0 0 0 0 0 0 0 0 0
0 0 0 0 0 0 0 0 0
0 0 0 0 0 0 0 0 0
0 0 0 0 0 0 0 0 0
0 0 0 0 0 0 0 0 0
0 0 0 0 0 0 0 0 0
0 0 0 0 0 0 0 0 0
0 0 0 0 0 0 0 0 0
0 0 0 0 0 0 0 0 0
1
32
1,2,3,4,5,6,7,8,9,10,11,12,13,14,15,16,17,18,19,20,21,22,23,24,25,26,27,28,29,30,31,32
8
0 0 0 0 0 0 0 0 0
0 0 0 0 0 0 0 0 0
0 0 0 0 0 0 0 0 0
0 0 0 0 0 0 0 0 0
0 0 0 0 0 0 0 0 0
0 0 0 0 0 0 0 0 0
```

```
0 0 0 0 0 0 0 0 0
0 0 0 0 0 0 0 0 0
0 0 0 0 0 0 0 0 0
0 0 0 0 0 0 0 0 0
0 0 0 0 0 0 0 0 0
0 0 0 0 0 0 0 0 0
0 0 0 0 0 0 0 0 0
0 0 0 0 0 0 0 0 0
0 0 0 0 0 0 0 0 0
0 0 0 0 0 0 0 0 0
0 0 0 0 0 0 0 0 0
0 0 0 0 0 0 0 0 0
0 0 0 0 0 0 0 0 0
0 0 0 0 0 0 0 0 0
0 0 0 0 0 0 0 0 0
0 0 0 0 0 0 0 0 0
0 0 0 0 0 0 0 0 0
0 0 0 0 0 0 0 0 0
0 0 0 0 0 0 0 0 0
0 0 0 0 0 0 0 0 0
0 0 0 0 0 0 0 0 0
0 0 0 0 0 0 0 0 0
0 0 0 0 0 0 0 0 0
0 0 0 0 0 0 0 0 0
0 0 0 0 0 0 0 0 0
0 0 0 0 0 0 0 0 0
1
32
1,2,3,4,5,6,7,8,9,10,11,12,13,14,15,16,17,18,19,20,21,22,23,24,25,26,27,28,29,30,31,32
9
0 0 0 0 0 0 0 0 0
0 0 0 0 0 0 0 0 0
0 0 0 0 0 0 0 0 0
0 0 0 0 0 0 0 0 0
0 0 0 0 0 0 0 0 0
0 0 0 0 0 0 0 0 0
0 0 0 0 0 0 0 0 0
0 0 0 0 0 0 0 0 0
0 0 0 0 0 0 0 0 0
0 0 0 0 0 0 0 0 0
0 0 0 0 0 0 0 0 0
0 0 0 0 0 0 0 0 0
0 0 0 0 0 0 0 0 0
0 0 0 0 0 0 0 0 0
0 0 0 0 0 0 0 0 0
0 0 0 0 0 0 0 0 0
0 0 0 0 0 0 0 0 0
0 0 0 0 0 0 0 0 0
0 0 0 0 0 0 0 0 0
0 0 0 0 0 0 0 0 0
0 0 0 0 0 0 0 0 0
0 0 0 0 0 0 0 0 0
0 0 0 0 0 0 0 0 0
0 0 0 0 0 0 0 0 0
0 0 0 0 0 0 0 0 0
0 0 0 0 0 0 0 0 0
0 0 0 0 0 0 0 0 0
0 0 0 0 0 0 0 0 0
0 0 0 0 0 0 0 0 0
0 0 0 0 0 0 0 0 0
```

```
0 0 0 0 0 0 0 0 0
0 0 0 0 0 0 0 0 0
1
32
1,2,3,4,5,6,7,8,9,10,11,12,13,14,15,16,17,18,19,20,21,22,23,24,25,26,27,28,29,30,31,32
10
0 0 0 0 0 0 0 0 0
0 0 0 0 0 0 0 0 0
0 0 0 0 0 0 0 0 0
0 0 0 0 0 0 0 0 0
0 0 0 0 0 0 0 0 0
0 0 0 0 0 0 0 0 0
0 0 0 0 0 0 0 0 0
0 0 0 0 0 0 0 0 0
0 0 0 0 0 0 0 0 0
0 0 0 0 0 0 0 0 0
0 0 0 0 0 0 0 0 0
0 0 0 0 0 0 0 0 0
0 0 0 0 0 0 0 0 0
0 0 0 0 0 0 0 0 0
0 0 0 0 0 0 0 0 0
0 0 0 0 0 0 0 0 0
0 0 0 0 0 0 0 0 0
0 0 0 0 0 0 0 0 0
0 0 0 0 0 0 0 0 0
0 0 0 0 0 0 0 0 0
0 0 0 0 0 0 0 0 0
0 0 0 0 0 0 0 0 0
0 0 0 0 0 0 0 0 0
0 0 0 0 0 0 0 0 0
0 0 0 0 0 0 0 0 0
0 0 0 0 0 0 0 0 0
0 0 0 0 0 0 0 0 0
0 0 0 0 0 0 0 0 0
0 0 0 0 0 0 0 0 0
0 0 0 0 0 0 0 0 0
0 0 0 0 0 0 0 0 0
0 0 0 0 0 0 0 0 0
1
32
1,2,3,4,5,6,7,8,9,10,11,12,13,14,15,16,17,18,19,20,21,22,23,24,25,26,27,28,29,30,31,32
11
0 0 0 0 0 0 0 0 0
0 0 0 0 0 0 0 0 0
0 0 0 0 0 0 0 0 0
0 0 0 0 0 0 0 0 0
0 0 0 0 0 0 0 0 0
0 0 0 0 0 0 0 0 0
0 0 0 0 0 0 0 0 0
0 0 0 0 0 0 0 0 0
0 0 0 0 0 0 0 0 0
0 0 0 0 0 0 0 0 0
0 0 0 0 0 0 0 0 0
0 0 0 0 0 0 0 0 0
0 0 0 0 0 0 0 0 0
0 0 0 0 0 0 0 0 0
0 0 0 0 0 0 0 0 0
0 0 0 0 0 0 0 0 0
0 0 0 0 0 0 0 0 0
0 0 0 0 0 0 0 0 0
```

```
0 0 0 0 0 0 0 0
0 0 0 0 0 0 0 0
0 0 0 0 0 0 0 0
0 0 0 0 0 0 0 0
0 0 0 0 0 0 0 0
0 0 0 0 0 0 0 0
0 0 0 0 0 0 0 0
0 0 0 0 0 0 0 0
0 0 0 0 0 0 0 0
0 0 0 0 0 0 0 0
0 0 0 0 0 0 0 0
0 0 0 0 0 0 0 0
0 0 0 0 0 0 0 0
0 0 0 0 0 0 0 0
1
32
1,2,3,4,5,6,7,8,9,10,11,12,13,14,15,16,17,18,19,20,21,22,23,24,25,26,27,28,29,30,31,32
12
0 0 0 0 0 0 0 0
0 0 0 0 0 0 0 0
0 0 0 0 0 0 0 0
0 0 0 0 0 0 0 0
0 0 0 0 0 0 0 0
0 0 0 0 0 0 0 0
0 0 0 0 0 0 0 0
0 0 0 0 0 0 0 0
0 0 0 0 0 0 0 0
0 0 0 0 0 0 0 0
0 0 0 0 0 0 0 0
0 0 0 0 0 0 0 0
0 0 0 0 0 0 0 0
0 0 0 0 0 0 0 0
0 0 0 0 0 0 0 0
0 0 0 0 0 0 0 0
0 0 0 0 0 0 0 0
0 0 0 0 0 0 0 0
0 0 0 0 0 0 0 0
0 0 0 0 0 0 0 0
0 0 0 0 0 0 0 0
0 0 0 0 0 0 0 0
0 0 0 0 0 0 0 0
0 0 0 0 0 0 0 0
0 0 0 0 0 0 0 0
0 0 0 0 0 0 0 0
0 0 0 0 0 0 0 0
0 0 0 0 0 0 0 0
0 0 0 0 0 0 0 0
0 0 0 0 0 0 0 0
0 0 0 0 0 0 0 0
0 0 0 0 0 0 0 0
1
32
1,2,3,4,5,6,7,8,9,10,11,12,13,14,15,16,17,18,19,20,21,22,23,24,25,26,27,28,29,30,31,32
13
0 0 0 0 0 0 0 0
0 0 0 0 0 0 0 0
0 0 0 0 0 0 0 0
0 0 0 0 0 0 0 0
0 0 0 0 0 0 0 0
0 0 0 0 0 0 0 0
```

```
0 0 0 0 0 0 0 0 0
0 0 0 0 0 0 0 0 0
0 0 0 0 0 0 0 0 0
0 0 0 0 0 0 0 0 0
0 0 0 0 0 0 0 0 0
0 0 0 0 0 0 0 0 0
0 0 0 0 0 0 0 0 0
0 0 0 0 0 0 0 0 0
0 0 0 0 0 0 0 0 0
0 0 0 0 0 0 0 0 0
0 0 0 0 0 0 0 0 0
0 0 0 0 0 0 0 0 0
0 0 0 0 0 0 0 0 0
0 0 0 0 0 0 0 0 0
0 0 0 0 0 0 0 0 0
0 0 0 0 0 0 0 0 0
0 0 0 0 0 0 0 0 0
0 0 0 0 0 0 0 0 0
0 0 0 0 0 0 0 0 0
0 0 0 0 0 0 0 0 0
0 0 0 0 0 0 0 0 0
0 0 0 0 0 0 0 0 0
0 0 0 0 0 0 0 0 0
0 0 0 0 0 0 0 0 0
0 0 0 0 0 0 0 0 0
0 0 0 0 0 0 0 0 0
1
32
1,2,3,4,5,6,7,8,9,10,11,12,13,14,15,16,17,18,19,20,21,22,23,24,25,26,27,28,29,30,31,32
14
0 0 0 0 0 0 0 0 0
0 0 0 0 0 0 0 0 0
0 0 0 0 0 0 0 0 0
0 0 0 0 0 0 0 0 0
0 0 0 0 0 0 0 0 0
0 0 0 0 0 0 0 0 0
0 0 0 0 0 0 0 0 0
0 0 0 0 0 0 0 0 0
0 0 0 0 0 0 0 0 0
0 0 0 0 0 0 0 0 0
0 0 0 0 0 0 0 0 0
0 0 0 0 0 0 0 0 0
0 0 0 0 0 0 0 0 0
0 0 0 0 0 0 0 0 0
0 0 0 0 0 0 0 0 0
0 0 0 0 0 0 0 0 0
0 0 0 0 0 0 0 0 0
0 0 0 0 0 0 0 0 0
0 0 0 0 0 0 0 0 0
0 0 0 0 0 0 0 0 0
0 0 0 0 0 0 0 0 0
0 0 0 0 0 0 0 0 0
0 0 0 0 0 0 0 0 0
0 0 0 0 0 0 0 0 0
0 0 0 0 0 0 0 0 0
0 0 0 0 0 0 0 0 0
0 0 0 0 0 0 0 0 0
0 0 0 0 0 0 0 0 0
0 0 0 0 0 0 0 0 0
0 0 0 0 0 0 0 0 0
```

```
0 0 0 0 0 0 0 0 0
0 0 0 0 0 0 0 0 0
1
32
1,2,3,4,5,6,7,8,9,10,11,12,13,14,15,16,17,18,19,20,21,22,23,24,25,26,27,28,29,30,31,32
15
0 0 0 0 0 0 0 0 0
0 0 0 0 0 0 0 0 0
0 0 0 0 0 0 0 0 0
0 0 0 0 0 0 0 0 0
0 0 0 0 0 0 0 0 0
0 0 0 0 0 0 0 0 0
0 0 0 0 0 0 0 0 0
0 0 0 0 0 0 0 0 0
0 0 0 0 0 0 0 0 0
0 0 0 0 0 0 0 0 0
0 0 0 0 0 0 0 0 0
0 0 0 0 0 0 0 0 0
0 0 0 0 0 0 0 0 0
0 0 0 0 0 0 0 0 0
0 0 0 0 0 0 0 0 0
0 0 0 0 0 0 0 0 0
0 0 0 0 0 0 0 0 0
0 0 0 0 0 0 0 0 0
0 0 0 0 0 0 0 0 0
0 0 0 0 0 0 0 0 0
0 0 0 0 0 0 0 0 0
0 0 0 0 0 0 0 0 0
0 0 0 0 0 0 0 0 0
0 0 0 0 0 0 0 0 0
0 0 0 0 0 0 0 0 0
0 0 0 0 0 0 0 0 0
0 0 0 0 0 0 0 0 0
0 0 0 0 0 0 0 0 0
0 0 0 0 0 0 0 0 0
0 0 0 0 0 0 0 0 0
0 0 0 0 0 0 0 0 0
0 0 0 0 0 0 0 0 0
1
32
1,2,3,4,5,6,7,8,9,10,11,12,13,14,15,16,17,18,19,20,21,22,23,24,25,26,27,28,29,30,31,32
16
0 0 0 0 0 0 0 0 0
0 0 0 0 0 0 0 0 0
0 0 0 0 0 0 0 0 0
0 0 0 0 0 0 0 0 0
0 0 0 0 0 0 0 0 0
0 0 0 0 0 0 0 0 0
0 0 0 0 0 0 0 0 0
0 0 0 0 0 0 0 0 0
0 0 0 0 0 0 0 0 0
0 0 0 0 0 0 0 0 0
0 0 0 0 0 0 0 0 0
0 0 0 0 0 0 0 0 0
0 0 0 0 0 0 0 0 0
0 0 0 0 0 0 0 0 0
0 0 0 0 0 0 0 0 0
0 0 0 0 0 0 0 0 0
0 0 0 0 0 0 0 0 0
0 0 0 0 0 0 0 0 0
```

```
0 0 0 0 0 0 0 0 0
0 0 0 0 0 0 0 0 0
0 0 0 0 0 0 0 0 0
0 0 0 0 0 0 0 0 0
0 0 0 0 0 0 0 0 0
0 0 0 0 0 0 0 0 0
0 0 0 0 0 0 0 0 0
0 0 0 0 0 0 0 0 0
0 0 0 0 0 0 0 0 0
0 0 0 0 0 0 0 0 0
0 0 0 0 0 0 0 0 0
0 0 0 0 0 0 0 0 0
0 0 0 0 0 0 0 0 0
0 0 0 0 0 0 0 0 0
1
32
1,2,3,4,5,6,7,8,9,10,11,12,13,14,15,16,17,18,19,20,21,22,23,24,25,26,27,28,29,30,31,32
17
0 0 0 0 0 0 0 0 0
0 0 0 0 0 0 0 0 0
0 0 0 0 0 0 0 0 0
0 0 0 0 0 0 0 0 0
0 0 0 0 0 0 0 0 0
0 0 0 0 0 0 0 0 0
0 0 0 0 0 0 0 0 0
0 0 0 0 0 0 0 0 0
0 0 0 0 0 0 0 0 0
0 0 0 0 0 0 0 0 0
0 0 0 0 0 0 0 0 0
0 0 0 0 0 0 0 0 0
0 0 0 0 0 0 0 0 0
0 0 0 0 0 0 0 0 0
0 0 0 0 0 0 0 0 0
0 0 0 0 0 0 0 0 0
0 0 0 0 0 0 0 0 0
0 0 0 0 0 0 0 0 0
0 0 0 0 0 0 0 0 0
0 0 0 0 0 0 0 0 0
0 0 0 0 0 0 0 0 0
0 0 0 0 0 0 0 0 0
0 0 0 0 0 0 0 0 0
0 0 0 0 0 0 0 0 0
0 0 0 0 0 0 0 0 0
0 0 0 0 0 0 0 0 0
0 0 0 0 0 0 0 0 0
0 0 0 0 0 0 0 0 0
0 0 0 0 0 0 0 0 0
0 0 0 0 0 0 0 0 0
0 0 0 0 0 0 0 0 0
0 0 0 0 0 0 0 0 0
1
32
1,2,3,4,5,6,7,8,9,10,11,12,13,14,15,16,17,18,19,20,21,22,23,24,25,26,27,28,29,30,31,32
18
0 0 0 0 0 0 0 0 0
0 0 0 0 0 0 0 0 0
0 0 0 0 0 0 0 0 0
0 0 0 0 0 0 0 0 0
0 0 0 0 0 0 0 0 0
0 0 0 0 0 0 0 0 0
```

```
0 0 0 0 0 0 0 0 0
0 0 0 0 0 0 0 0 0
0 0 0 0 0 0 0 0 0
0 0 0 0 0 0 0 0 0
0 0 0 0 0 0 0 0 0
0 0 0 0 0 0 0 0 0
0 0 0 0 0 0 0 0 0
0 0 0 0 0 0 0 0 0
0 0 0 0 0 0 0 0 0
0 0 0 0 0 0 0 0 0
0 0 0 0 0 0 0 0 0
0 0 0 0 0 0 0 0 0
0 0 0 0 0 0 0 0 0
0 0 0 0 0 0 0 0 0
0 0 0 0 0 0 0 0 0
0 0 0 0 0 0 0 0 0
0 0 0 0 0 0 0 0 0
0 0 0 0 0 0 0 0 0
0 0 0 0 0 0 0 0 0
0 0 0 0 0 0 0 0 0
0 0 0 0 0 0 0 0 0
0 0 0 0 0 0 0 0 0
0 0 0 0 0 0 0 0 0
0 0 0 0 0 0 0 0 0
0 0 0 0 0 0 0 0 0
0 0 0 0 0 0 0 0 0
1
32
1,2,3,4,5,6,7,8,9,10,11,12,13,14,15,16,17,18,19,20,21,22,23,24,25,26,27,28,29,30,31,32
19
0 0 0 0 0 0 0 0 0
0 0 0 0 0 0 0 0 0
0 0 0 0 0 0 0 0 0
0 0 0 0 0 0 0 0 0
0 0 0 0 0 0 0 0 0
0 0 0 0 0 0 0 0 0
0 0 0 0 0 0 0 0 0
0 0 0 0 0 0 0 0 0
0 0 0 0 0 0 0 0 0
0 0 0 0 0 0 0 0 0
0 0 0 0 0 0 0 0 0
0 0 0 0 0 0 0 0 0
0 0 0 0 0 0 0 0 0
0 0 0 0 0 0 0 0 0
0 0 0 0 0 0 0 0 0
0 0 0 0 0 0 0 0 0
0 0 0 0 0 0 0 0 0
0 0 0 0 0 0 0 0 0
0 0 0 0 0 0 0 0 0
0 0 0 0 0 0 0 0 0
0 0 0 0 0 0 0 0 0
0 0 0 0 0 0 0 0 0
0 0 0 0 0 0 0 0 0
0 0 0 0 0 0 0 0 0
0 0 0 0 0 0 0 0 0
0 0 0 0 0 0 0 0 0
0 0 0 0 0 0 0 0 0
0 0 0 0 0 0 0 0 0
0 0 0 0 0 0 0 0 0
0 0 0 0 0 0 0 0 0
```

```
0 0 0 0 0 0 0 0 0
0 0 0 0 0 0 0 0 0
1
32
1,2,3,4,5,6,7,8,9,10,11,12,13,14,15,16,17,18,19,20,21,22,23,24,25,26,27,28,29,30,31,32
20
0 0 0 0 0 0 0 0 0
0 0 0 0 0 0 0 0 0
0 0 0 0 0 0 0 0 0
0 0 0 0 0 0 0 0 0
0 0 0 0 0 0 0 0 0
0 0 0 0 0 0 0 0 0
0 0 0 0 0 0 0 0 0
0 0 0 0 0 0 0 0 0
0 0 0 0 0 0 0 0 0
0 0 0 0 0 0 0 0 0
0 0 0 0 0 0 0 0 0
0 0 0 0 0 0 0 0 0
0 0 0 0 0 0 0 0 0
0 0 0 0 0 0 0 0 0
0 0 0 0 0 0 0 0 0
0 0 0 0 0 0 0 0 0
0 0 0 0 0 0 0 0 0
0 0 0 0 0 0 0 0 0
0 0 0 0 0 0 0 0 0
0 0 0 0 0 0 0 0 0
0 0 0 0 0 0 0 0 0
0 0 0 0 0 0 0 0 0
0 0 0 0 0 0 0 0 0
0 0 0 0 0 0 0 0 0
0 0 0 0 0 0 0 0 0
0 0 0 0 0 0 0 0 0
0 0 0 0 0 0 0 0 0
0 0 0 0 0 0 0 0 0
0 0 0 0 0 0 0 0 0
0 0 0 0 0 0 0 0 0
0 0 0 0 0 0 0 0 0
0 0 0 0 0 0 0 0 0
1
32
1,2,3,4,5,6,7,8,9,10,11,12,13,14,15,16,17,18,19,20,21,22,23,24,25,26,27,28,29,30,31,32
21
0 0 0 0 0 0 0 0 0
0 0 0 0 0 0 0 0 0
0 0 0 0 0 0 0 0 0
0 0 0 0 0 0 0 0 0
0 0 0 0 0 0 0 0 0
0 0 0 0 0 0 0 0 0
0 0 0 0 0 0 0 0 0
0 0 0 0 0 0 0 0 0
0 0 0 0 0 0 0 0 0
0 0 0 0 0 0 0 0 0
0 0 0 0 0 0 0 0 0
0 0 0 0 0 0 0 0 0
0 0 0 0 0 0 0 0 0
0 0 0 0 0 0 0 0 0
0 0 0 0 0 0 0 0 0
0 0 0 0 0 0 0 0 0
0 0 0 0 0 0 0 0 0
0 0 0 0 0 0 0 0 0
```

```
0 0 0 0 0 0 0 0
0 0 0 0 0 0 0 0
0 0 0 0 0 0 0 0
0 0 0 0 0 0 0 0
0 0 0 0 0 0 0 0
0 0 0 0 0 0 0 0
0 0 0 0 0 0 0 0
0 0 0 0 0 0 0 0
0 0 0 0 0 0 0 0
0 0 0 0 0 0 0 0
0 0 0 0 0 0 0 0
0 0 0 0 0 0 0 0
0 0 0 0 0 0 0 0
0 0 0 0 0 0 0 0
1
32
1,2,3,4,5,6,7,8,9,10,11,12,13,14,15,16,17,18,19,20,21,22,23,24,25,26,27,28,29,30,31,32
22
0 0 0 0 0 0 0 0
0 0 0 0 0 0 0 0
0 0 0 0 0 0 0 0
0 0 0 0 0 0 0 0
0 0 0 0 0 0 0 0
0 0 0 0 0 0 0 0
0 0 0 0 0 0 0 0
0 0 0 0 0 0 0 0
0 0 0 0 0 0 0 0
0 0 0 0 0 0 0 0
0 0 0 0 0 0 0 0
0 0 0 0 0 0 0 0
0 0 0 0 0 0 0 0
0 0 0 0 0 0 0 0
0 0 0 0 0 0 0 0
0 0 0 0 0 0 0 0
0 0 0 0 0 0 0 0
0 0 0 0 0 0 0 0
0 0 0 0 0 0 0 0
0 0 0 0 0 0 0 0
0 0 0 0 0 0 0 0
0 0 0 0 0 0 0 0
0 0 0 0 0 0 0 0
0 0 0 0 0 0 0 0
0 0 0 0 0 0 0 0
0 0 0 0 0 0 0 0
0 0 0 0 0 0 0 0
0 0 0 0 0 0 0 0
0 0 0 0 0 0 0 0
0 0 0 0 0 0 0 0
0 0 0 0 0 0 0 0
0 0 0 0 0 0 0 0
1
32
1,2,3,4,5,6,7,8,9,10,11,12,13,14,15,16,17,18,19,20,21,22,23,24,25,26,27,28,29,30,31,32
23
0 0 0 0 0 0 0 0
0 0 0 0 0 0 0 0
0 0 0 0 0 0 0 0
0 0 0 0 0 0 0 0
0 0 0 0 0 0 0 0
0 0 0 0 0 0 0 0
```

0 0 0 0 0 0 0 0 0
0 0 0 0 0 0 0 0 0
0 0 0 0 0 0 0 0 0
0 0 0 0 0 0 0 0 0
0 0 0 0 0 0 0 0 0
0 0 0 0 0 0 0 0 0
0 0 0 0 0 0 0 0 0
0 0 0 0 0 0 0 0 0
0 0 0 0 0 0 0 0 0
0 0 0 0 0 0 0 0 0
0 0 0 0 0 0 0 0 0
0 0 0 0 0 0 0 0 0
0 0 0 0 0 0 0 0 0
0 0 0 0 0 0 0 0 0
0 0 0 0 0 0 0 0 0
0 0 0 0 0 0 0 0 0
0 0 0 0 0 0 0 0 0
0 0 0 0 0 0 0 0 0
0 0 0 0 0 0 0 0 0
0 0 0 0 0 0 0 0 0
0 0 0 0 0 0 0 0 0
0 0 0 0 0 0 0 0 0
0 0 0 0 0 0 0 0 0
0 0 0 0 0 0 0 0 0
0 0 0 0 0 0 0 0 0
0 0 0 0 0 0 0 0 0
1
32
1,2,3,4,5,6,7,8,9,10,11,12,13,14,15,16,17,18,19,20,21,22,23,24,25,26,27,28,29,30,31,32
24
0 0 0 0 0 0 0 0 0
0 0 0 0 0 0 0 0 0
0 0 0 0 0 0 0 0 0
0 0 0 0 0 0 0 0 0
0 0 0 0 0 0 0 0 0
0 0 0 0 0 0 0 0 0
0 0 0 0 0 0 0 0 0
0 0 0 0 0 0 0 0 0
0 0 0 0 0 0 0 0 0
0 0 0 0 0 0 0 0 0
0 0 0 0 0 0 0 0 0
0 0 0 0 0 0 0 0 0
0 0 0 0 0 0 0 0 0
0 0 0 0 0 0 0 0 0
0 0 0 0 0 0 0 0 0
0 0 0 0 0 0 0 0 0
0 0 0 0 0 0 0 0 0
0 0 0 0 0 0 0 0 0
0 0 0 0 0 0 0 0 0
0 0 0 0 0 0 0 0 0
0 0 0 0 0 0 0 0 0
0 0 0 0 0 0 0 0 0
0 0 0 0 0 0 0 0 0
0 0 0 0 0 0 0 0 0
0 0 0 0 0 0 0 0 0
0 0 0 0 0 0 0 0 0
0 0 0 0 0 0 0 0 0
0 0 0 0 0 0 0 0 0
0 0 0 0 0 0 0 0 0
0 0 0 0 0 0 0 0 0

0 0 0 0 0 0 0 0
0 0 0 0 0 0 0 0
1
32
1,2,3,4,5,6,7,8,9,10,11,12,13,14,15,16,17,18,19,20,21,22,23,24,25,26,27,28,29,30,31,32
0
OP,INTI
10,7,128.14,134.94,130.57,131.29 !EXP1
127,128,129,130,131,132,133,134,135,136
129.0,129.5,130.0,130.5,131.0,131.5,132.0
10,7,128.14,134.94,131.38,132.13 !EXP2
127,128,129,130,131,132,133,134,135,136
130.5,131.0,131.5,132.0,132.5,133.0,133.5
10,7,128.14,134.94,132.21,132.99 !EXP3
127,128,129,130,131,132,133,134,135,136
131.5,132.0,132.5,133.0,133.5,134.0,134.5
10,7,128.14,134.94,133.08,133.88 !EXP4
127,128,129,130,131,132,133,134,135,136
132.5,133.0,133.5,134.0,134.5,135.0,135.5
10,7,128.14,134.94,133.97,134.80 !EXP5
127,128,129,130,131,132,133,134,135,136
133.0,133.5,134.0,134.5,135.0,135.5,136.0
10,7,128.14,134.94,134.89,135.75 !EXP6
127,128,129,130,131,132,133,134,135,136
133.5,134.0,134.5,135.0,135.5,136.0,136.5
10,7,128.14,134.94,135.84,136.73 !EXP7
127,128,129,130,131,132,133,134,135,136
134.5,135.0,135.5,136.0,136.5,137.0,137.5
10,7,128.14,134.94,136.83,137.74 !EXP8
127,128,129,130,131,132,133,134,135,136
135.5,136.0,136.5,137.0,137.5,138.0,138.5
10,7,128.14,134.94,137.85,138.79 !EXP9
127,128,129,130,131,132,133,134,135,136
136.5,137.0,137.5,138.0,138.5,139.0,139.5
10,7,128.14,134.94,138.90,139.88 !EXP10
127,128,129,130,131,132,133,134,135,136
137.5,138.0,138.5,139.0,139.5,140.0,140.5
10,7,128.14,134.94,139.99,140.99 !EXP11
127,128,129,130,131,132,133,134,135,136
138.5,139.0,139.5,140.0,140.5,141.0,141.5
10,7,128.14,134.94,141.11,142.15 !EXP12
127,128,129,130,131,132,133,134,135,136
140.5,141.0,141.5,142.0,142.5,143.0,143.5
10,7,128.14,134.94,142.27,143.34 !EXP13
127,128,129,130,131,132,133,134,135,136
141.5,142.0,142.5,143.0,143.5,144.0,144.5
10,7,128.14,134.94,143.47,144.57 !EXP14
127,128,129,130,131,132,133,134,135,136
142.5,143.0,143.5,144.0,144.5,145.0,145.5
10,7,128.14,134.94,144.70,145.84 !EXP15
127,128,129,130,131,132,133,134,135,136
143.5,144.0,144.5,145.0,145.5,146.0,146.5
10,7,128.14,134.94,145.98,147.15 !EXP16
127,128,129,130,131,132,133,134,135,136
145.0,145.5,146.0,146.5,147.0,147.5,148.0
10,7,128.14,134.94,147.29,148.50 !EXP17
127,128,129,130,131,132,133,134,135,136
146.5,147.0,147.5,148.0,148.5,149.0,149.5
10,7,128.14,134.94,148.64,149.89 !EXP18
127,128,129,130,131,132,133,134,135,136

147.5,148.0,148.5,149.0,149.5,150.0,150.5
10,7,128.14,134.94,150.04,151.32 !EXP19
127,128,129,130,131,132,133,134,135,136
149.0,149.5,150.0,150.5,151.0,151.5,152.0
10,7,128.14,134.94,151.47,152.79 !EXP20
127,128,129,130,131,132,133,134,135,136
150.5,151.0,151.5,152.0,152.5,153.0,153.5
10,7,128.14,134.94,152.94,154.30 !EXP21
127,128,129,130,131,132,133,134,135,136
152.0,152.5,153.0,153.5,154.0,154.5,155.0
10,7,128.14,134.94,154.46,155.85 !EXP22
127,128,129,130,131,132,133,134,135,136
153.5,154.0,154.5,155.0,155.5,156.0,156.5
10,7,128.14,134.94,156.01,157.44 !EXP23
127,128,129,130,131,132,133,134,135,136
155.0,155.5,156.0,156.5,157.0,157.5,158.0
10,7,128.14,134.94,157.60,159.06 !EXP24
127,128,129,130,131,132,133,134,135,136
156.8,157.3,157.8,158.3,158.8,159.3,159.8
10 !No of stopping powers (dE/dx) at different energies 1
127,128,129,130,131,132,133,134,135,136
6.885,6.874,6.863,6.852,6.841,6.830,6.819,6.808,6.797,6.786
10,10
10
!No of stopping powers (dE/dx) at different energies 2
127,128,129,130,131,132,133,134,135,136
6.885,6.874,6.863,6.852,6.841,6.830,6.819,6.808,6.797,6.786
10,10
10 !No of stopping powers (dE/dx) at different energies 3
127,128,129,130,131,132,133,134,135,136
6.885,6.874,6.863,6.852,6.841,6.830,6.819,6.808,6.797,6.786
10,10
10 !No of stopping powers (dE/dx) at different energies 4
127,128,129,130,131,132,133,134,135,136
6.885,6.874,6.863,6.852,6.841,6.830,6.819,6.808,6.797,6.786
10,10
10 !No of stopping powers (dE/dx) at different energies 5
127,128,129,130,131,132,133,134,135,136
6.885,6.874,6.863,6.852,6.841,6.830,6.819,6.808,6.797,6.786
10,10
10 !No of stopping powers (dE/dx) at different energies 6
127,128,129,130,131,132,133,134,135,136
6.885,6.874,6.863,6.852,6.841,6.830,6.819,6.808,6.797,6.786
10,10
10 !No of stopping powers (dE/dx) at different energies 7
127,128,129,130,131,132,133,134,135,136
6.885,6.874,6.863,6.852,6.841,6.830,6.819,6.808,6.797,6.786
10,10
10 !No of stopping powers (dE/dx) at different energies 8
127,128,129,130,131,132,133,134,135,136
6.885,6.874,6.863,6.852,6.841,6.830,6.819,6.808,6.797,6.786
10,10
10 !No of stopping powers (dE/dx) at different energies 9
127,128,129,130,131,132,133,134,135,136
6.885,6.874,6.863,6.852,6.841,6.830,6.819,6.808,6.797,6.786
10,10
10 !No of stopping powers (dE/dx) at different energies 10
127,128,129,130,131,132,133,134,135,136
6.885,6.874,6.863,6.852,6.841,6.830,6.819,6.808,6.797,6.786
10,10

10 !No of stopping powers (dE/dx) at different energies 11
127,128,129,130,131,132,133,134,135,136
6.885,6.874,6.863,6.852,6.841,6.830,6.819,6.808,6.797,6.786
10,10
10 !No of stopping powers (dE/dx) at different energies 12
127,128,129,130,131,132,133,134,135,136
6.885,6.874,6.863,6.852,6.841,6.830,6.819,6.808,6.797,6.786
10,10
10 !No of stopping powers (dE/dx) at different energies 13
127,128,129,130,131,132,133,134,135,136
6.885,6.874,6.863,6.852,6.841,6.830,6.819,6.808,6.797,6.786
10,10
10 !No of stopping powers (dE/dx) at different energies 14
127,128,129,130,131,132,133,134,135,136
6.885,6.874,6.863,6.852,6.841,6.830,6.819,6.808,6.797,6.786
10,10
10 !No of stopping powers (dE/dx) at different energies 15
127,128,129,130,131,132,133,134,135,136
6.885,6.874,6.863,6.852,6.841,6.830,6.819,6.808,6.797,6.786
10,10
10 !No of stopping powers (dE/dx) at different energies 16
127,128,129,130,131,132,133,134,135,136
6.885,6.874,6.863,6.852,6.841,6.830,6.819,6.808,6.797,6.786
10,10
10 !No of stopping powers (dE/dx) at different energies 17
127,128,129,130,131,132,133,134,135,136
6.885,6.874,6.863,6.852,6.841,6.830,6.819,6.808,6.797,6.786
10,10
10 !No of stopping powers (dE/dx) at different energies 18
127,128,129,130,131,132,133,134,135,136
6.885,6.874,6.863,6.852,6.841,6.830,6.819,6.808,6.797,6.786
10,10
10 !No of stopping powers (dE/dx) at different energies 19
127,128,129,130,131,132,133,134,135,136
6.885,6.874,6.863,6.852,6.841,6.830,6.819,6.808,6.797,6.786
10,10
10 !No of stopping powers (dE/dx) at different energies 20
127,128,129,130,131,132,133,134,135,136
6.885,6.874,6.863,6.852,6.841,6.830,6.819,6.808,6.797,6.786
10,10
10 !No of stopping powers (dE/dx) at different energies 21
127,128,129,130,131,132,133,134,135,136
6.885,6.874,6.863,6.852,6.841,6.830,6.819,6.808,6.797,6.786
10,10
10 !No of stopping powers (dE/dx) at different energies 22
127,128,129,130,131,132,133,134,135,136
6.885,6.874,6.863,6.852,6.841,6.830,6.819,6.808,6.797,6.786
10,10
10 !No of stopping powers (dE/dx) at different energies 23
127,128,129,130,131,132,133,134,135,136
6.885,6.874,6.863,6.852,6.841,6.830,6.819,6.808,6.797,6.786
10,10
10 !No of stopping powers (dE/dx) at different energies 24
127,128,129,130,131,132,133,134,135,136
6.885,6.874,6.863,6.852,6.841,6.830,6.819,6.808,6.797,6.786
10,10
OP,EXIT

B.2 ^{194}Pt Input File (Target)

```
OP,FILE
22,3,1
194Pt.out
9,3,1
det194Pt.gdt
8,3,1
det194Pt.raw
0,0,0
OP,TITL
40Ar+194Pt@134.94 Mev beam excitation
OP,GOSI
LEVE
1,1,0,0
2,1,2,0.3285
3,1,2,0.622
4,1,4,0.8113
0,0,0,0
ME
2,0,0,0,0
1,2,1.2811,-0.5,1.2
1,4,0.09853,-0.1,1.4
2,2,0.83121,-0.6,1.9
2,3,2.2591,0.5,2.9
2,4,1.7236,0.2,2.1
0,0,0,0,0
EXPT
24,78,194
18,40,134.94,130.9,4,1,0,0,360,0,1 !R1
18,40,134.94,131.8,4,1,0,0,360,0,2 !R2
18,40,134.94,132.6,4,1,0,0,360,0,3 !R3
18,40,134.94,133.5,4,1,0,0,360,0,4 !R4
18,40,134.94,134.4,4,1,0,0,360,0,5 !R5
18,40,134.94,135.3,4,1,0,0,360,0,6 !R6
18,40,134.94,136.3,4,1,0,0,360,0,7 !R7
18,40,134.94,137.3,4,1,0,0,360,0,8 !R8
18,40,134.94,138.3,4,1,0,0,360,0,9 !R9
18,40,134.94,139.4,4,1,0,0,360,0,10 !R10
18,40,134.94,140.5,4,1,0,0,360,0,11 !R11
18,40,134.94,141.6,4,1,0,0,360,0,12 !R12
18,40,134.94,142.8,4,1,0,0,360,0,13 !R13
18,40,134.94,144.0,4,1,0,0,360,0,14 !R14
18,40,134.94,145.3,4,1,0,0,360,0,15 !R15
18,40,134.94,146.6,4,1,0,0,360,0,16 !R16
18,40,134.94,147.9,4,1,0,0,360,0,17 !R17
18,40,134.94,149.3,4,1,0,0,360,0,18 !R18
18,40,134.94,150.7,4,1,0,0,360,0,19 !R19
18,40,134.94,152.1,4,1,0,0,360,0,20 !R20
18,40,134.94,153.6,4,1,0,0,360,0,21 !R21
18,40,134.94,155.2,4,1,0,0,360,0,22 !R22
18,40,134.94,156.7,4,1,0,0,360,0,23 !R23
18,40,134.94,158.3,4,1,0,0,360,0,24 !R24
CONT
SPL,1.
INT,24.
1,1000
2,1000
3,1000
```

4,1000
5,1000
6,1000
7,1000
8,1000
9,1000
10,1000
11,1000
12,1000
13,1000
14,1000
15,1000
16,1000
17,1000
18,1000
19,1000
20,1000
21,1000
22,1000
23,1000
24,1000
PRT,0.
1,-1
2,0
4,0
5,1
11,1
12,0
14,0
16,0
18,1
0,0
END,

OP,YIEL
0
8,1
1.0,1.5,2.0,2.5,3.0,3.5,4.0,4.5 !Energy mesh points
2
0.00547,0.00259,0.001754,0.001493,0.00144,0.001474,0.001548,0.001639 !Electron conversion coefficients
32,32,32,32,32,32,32,32,32,32,32,32,32,32,32,32,32,32,32,32,32,32,32,32 ! 24 experiments and 32 gamma detectors per experiment
1,1,1,1,1,1,1,1,1,1,1,1,1,1,1,1,1,1,1,1,1,1,1,1,1,1,1,1,1,1,1,1 ! up to 32
84.8,95.1,95.1,84.8,84.8,95.1,95.1,84.8,84.8,95.1,95.1,84.8,84.8,95.1,95.1,84.8,130.1,140.4,140.4, 130.1,130.1,140.4,140.4,130.1,130.1,140.4,140.4,130.1,8
!theta angles
95.1,95.1,84.8,84.8,49.8,49.8,39.5,39.5,230.3,230.3,220.0,220.0,320.3,320.3,310.0,310.0,5.2,5.2, 354.7,354.7,275.0,275.0,264.7,264.7,49.8,49.8,39.5,39.5,2
!phi angles
1,1,1,1,1,1,1,1,1,1,1,1,1,1,1,1,1,1,1,1,1,1,1,1,1,1,1,1,1,1,1,1
84.8,95.1,95.1,84.8,84.8,95.1,95.1,84.8,84.8,95.1,95.1,84.8,84.8,95.1,95.1,84.8,130.1,140.4,140.4,
130.1,130.1,140.4,140.4,130.1,130.1,140.4,140.4,130.1,84.8,95.1,95.1,84.8
95.1,95.1,84.8,84.8,49.8,49.8,39.5,39.5,230.3,230.3,220.0,220.0,320.3,320.3,310.0,310.0,5.2,5.2,
354.7,354.7,275.0,275.0,264.7,264.7,49.8,49.8,39.5,39.5,275.0,275.0,264.7,264.7
1,1,1,1,1,1,1,1,1,1,1,1,1,1,1,1,1,1,1,1,1,1,1,1,1,1,1,1,1,1,1,1
84.8,95.1,95.1,84.8,84.8,95.1,95.1,84.8,84.8,95.1,95.1,84.8,84.8,95.1,95.1,84.8,130.1,140.4,140.4,
130.1,130.1,140.4,140.4,130.1,130.1,140.4,140.4,130.1,84.8,95.1,95.1,84.8
95.1,95.1,84.8,84.8,49.8,49.8,39.5,39.5,230.3,230.3,220.0,220.0,320.3,320.3,310.0,310.0,5.2,5.2,
354.7,354.7,275.0,275.0,264.7,264.7,49.8,49.8,39.5,39.5,275.0,275.0,264.7,264.7
1,1,1,1,1,1,1,1,1,1,1,1,1,1,1,1,1,1,1,1,1,1,1,1,1,1,1,1,1,1,1,1

```
84.8,95.1,95.1,84.8,84.8,95.1,95.1,84.8,84.8,95.1,95.1,84.8,84.8,95.1,95.1,84.8,130.1,140.4,140.4,
130.1,130.1,140.4,140.4,130.1,130.1,140.4,140.4,130.1,84.8,95.1,95.1,84.8
95.1,95.1,84.8,84.8,49.8,49.8,39.5,39.5,230.3,230.3,220.0,220.0,320.3,320.3,310.0,310.0,5.2,5.2,
354.7,354.7,275.0,275.0,264.7,264.7,49.8,49.8,39.5,39.5,275.0,275.0,264.7,264.7
1,1,1,1,1,1,1,1,1,1,1,1,1,1,1,1,1,1,1,1,1,1,1,1,1,1,1,1,1,1,1,1
84.8,95.1,95.1,84.8,84.8,95.1,95.1,84.8,84.8,95.1,95.1,84.8,84.8,95.1,95.1,84.8,130.1,140.4,140.4,
130.1,130.1,140.4,140.4,130.1,130.1,140.4,140.4,130.1,84.8,95.1,95.1,84.8
95.1,95.1,84.8,84.8,49.8,49.8,39.5,39.5,230.3,230.3,220.0,220.0,320.3,320.3,310.0,310.0,5.2,5.2,
354.7,354.7,275.0,275.0,264.7,264.7,49.8,49.8,39.5,39.5,275.0,275.0,264.7,264.7
1,1,1,1,1,1,1,1,1,1,1,1,1,1,1,1,1,1,1,1,1,1,1,1,1,1,1,1,1,1,1,1
84.8,95.1,95.1,84.8,84.8,95.1,95.1,84.8,84.8,95.1,95.1,84.8,84.8,95.1,95.1,84.8,130.1,140.4,140.4,
130.1,130.1,140.4,140.4,130.1,130.1,140.4,140.4,130.1,84.8,95.1,95.1,84.8
95.1,95.1,84.8,84.8,49.8,49.8,39.5,39.5,230.3,230.3,220.0,220.0,320.3,320.3,310.0,310.0,5.2,5.2,
354.7,354.7,275.0,275.0,264.7,264.7,49.8,49.8,39.5,39.5,275.0,275.0,264.7,264.7
1,1,1,1,1,1,1,1,1,1,1,1,1,1,1,1,1,1,1,1,1,1,1,1,1,1,1,1,1,1,1,1
84.8,95.1,95.1,84.8,84.8,95.1,95.1,84.8,84.8,95.1,95.1,84.8,84.8,95.1,95.1,84.8,130.1,140.4,140.4,
130.1,130.1,140.4,140.4,130.1,130.1,140.4,140.4,130.1,84.8,95.1,95.1,84.8
95.1,95.1,84.8,84.8,49.8,49.8,39.5,39.5,230.3,230.3,220.0,220.0,320.3,320.3,310.0,310.0,5.2,5.2,
354.7,354.7,275.0,275.0,264.7,264.7,49.8,49.8,39.5,39.5,275.0,275.0,264.7,264.7
1,1,1,1,1,1,1,1,1,1,1,1,1,1,1,1,1,1,1,1,1,1,1,1,1,1,1,1,1,1,1,1
84.8,95.1,95.1,84.8,84.8,95.1,95.1,84.8,84.8,95.1,95.1,84.8,84.8,95.1,95.1,84.8,130.1,140.4,140.4,
130.1,130.1,140.4,140.4,130.1,130.1,140.4,140.4,130.1,84.8,95.1,95.1,84.8
95.1,95.1,84.8,84.8,49.8,49.8,39.5,39.5,230.3,230.3,220.0,220.0,320.3,320.3,310.0,310.0,5.2,5.2,
354.7,354.7,275.0,275.0,264.7,264.7,49.8,49.8,39.5,39.5,275.0,275.0,264.7,264.7
1,1,1,1,1,1,1,1,1,1,1,1,1,1,1,1,1,1,1,1,1,1,1,1,1,1,1,1,1,1,1,1
84.8,95.1,95.1,84.8,84.8,95.1,95.1,84.8,84.8,95.1,95.1,84.8,84.8,95.1,95.1,84.8,130.1,140.4,140.4,
130.1,130.1,140.4,140.4,130.1,130.1,140.4,140.4,130.1,84.8,95.1,95.1,84.8
95.1,95.1,84.8,84.8,49.8,49.8,39.5,39.5,230.3,230.3,220.0,220.0,320.3,320.3,310.0,310.0,5.2,5.2,
354.7,354.7,275.0,275.0,264.7,264.7,49.8,49.8,39.5,39.5,275.0,275.0,264.7,264.7
1,1,1,1,1,1,1,1,1,1,1,1,1,1,1,1,1,1,1,1,1,1,1,1,1,1,1,1,1,1,1,1
84.8,95.1,95.1,84.8,84.8,95.1,95.1,84.8,84.8,95.1,95.1,84.8,84.8,95.1,95.1,84.8,130.1,140.4,140.4,
130.1,130.1,140.4,140.4,130.1,130.1,140.4,140.4,130.1,84.8,95.1,95.1,84.8
95.1,95.1,84.8,84.8,49.8,49.8,39.5,39.5,230.3,230.3,220.0,220.0,320.3,320.3,310.0,310.0,5.2,5.2,
354.7,354.7,275.0,275.0,264.7,264.7,49.8,49.8,39.5,39.5,275.0,275.0,264.7,264.7
1,1,1,1,1,1,1,1,1,1,1,1,1,1,1,1,1,1,1,1,1,1,1,1,1,1,1,1,1,1,1,1
84.8,95.1,95.1,84.8,84.8,95.1,95.1,84.8,84.8,95.1,95.1,84.8,84.8,95.1,95.1,84.8,130.1,140.4,140.4,
130.1,130.1,140.4,140.4,130.1,130.1,140.4,140.4,130.1,84.8,95.1,95.1,84.8
95.1,95.1,84.8,84.8,49.8,49.8,39.5,39.5,230.3,230.3,220.0,220.0,320.3,320.3,310.0,310.0,5.2,5.2,
354.7,354.7,275.0,275.0,264.7,264.7,49.8,49.8,39.5,39.5,275.0,275.0,264.7,264.7
1,1,1,1,1,1,1,1,1,1,1,1,1,1,1,1,1,1,1,1,1,1,1,1,1,1,1,1,1,1,1,1
84.8,95.1,95.1,84.8,84.8,95.1,95.1,84.8,84.8,95.1,95.1,84.8,84.8,95.1,95.1,84.8,130.1,140.4,140.4,
130.1,130.1,140.4,140.4,130.1,130.1,140.4,140.4,130.1,84.8,95.1,95.1,84.8
95.1,95.1,84.8,84.8,49.8,49.8,39.5,39.5,230.3,230.3,220.0,220.0,320.3,320.3,310.0,310.0,5.2,5.2,
354.7,354.7,275.0,275.0,264.7,264.7,49.8,49.8,39.5,39.5,275.0,275.0,264.7,264.7
1,1,1,1,1,1,1,1,1,1,1,1,1,1,1,1,1,1,1,1,1,1,1,1,1,1,1,1,1,1,1,1
84.8,95.1,95.1,84.8,84.8,95.1,95.1,84.8,84.8,95.1,95.1,84.8,84.8,95.1,95.1,84.8,130.1,140.4,140.4,
130.1,130.1,140.4,140.4,130.1,130.1,140.4,140.4,130.1,84.8,95.1,95.1,84.8
95.1,95.1,84.8,84.8,49.8,49.8,39.5,39.5,230.3,230.3,220.0,220.0,320.3,320.3,310.0,310.0,5.2,5.2,
354.7,354.7,275.0,275.0,264.7,264.7,49.8,49.8,39.5,39.5,275.0,275.0,264.7,264.7
1,1,1,1,1,1,1,1,1,1,1,1,1,1,1,1,1,1,1,1,1,1,1,1,1,1,1,1,1,1,1,1
84.8,95.1,95.1,84.8,84.8,95.1,95.1,84.8,84.8,95.1,95.1,84.8,84.8,95.1,95.1,84.8,130.1,140.4,140.4,
130.1,130.1,140.4,140.4,130.1,130.1,140.4,140.4,130.1,84.8,95.1,95.1,84.8,
95.1,95.1,84.8,84.8,49.8,49.8,39.5,39.5,230.3,230.3,220.0,220.0,320.3,320.3,310.0,310.0,5.2,5.2,
354.7,354.7,275.0,275.0,264.7,264.7,49.8,49.8,39.5,39.5,275.0,275.0,264.7,264.7
1,1,1,1,1,1,1,1,1,1,1,1,1,1,1,1,1,1,1,1,1,1,1,1,1,1,1,1,1,1,1,1
84.8,95.1,95.1,84.8,84.8,95.1,95.1,84.8,84.8,95.1,95.1,84.8,84.8,95.1,95.1,84.8,130.1,140.4,140.4,
130.1,130.1,140.4,140.4,130.1,130.1,140.4,140.4,130.1,84.8,95.1,95.1,84.8
95.1,95.1,84.8,84.8,49.8,49.8,39.5,39.5,230.3,230.3,220.0,220.0,320.3,320.3,310.0,310.0,5.2,5.2,
354.7,354.7,275.0,275.0,264.7,264.7,49.8,49.8,39.5,39.5,275.0,275.0,264.7,264.7
1,1,1,1,1,1,1,1,1,1,1,1,1,1,1,1,1,1,1,1,1,1,1,1,1,1,1,1,1,1,1,1
```

```
84.8,95.1,95.1,84.8,84.8,95.1,95.1,84.8,84.8,95.1,95.1,84.8,84.8,95.1,95.1,84.8,130.1,140.4,140.4,
130.1,130.1,140.4,140.4,130.1,130.1,140.4,140.4,130.1,84.8,95.1,95.1,84.8
95.1,95.1,84.8,84.8,49.8,49.8,39.5,39.5,230.3,230.3,220.0,220.0,320.3,320.3,310.0,310.0,5.2,5.2,
354.7,354.7,275.0,275.0,264.7,264.7,49.8,49.8,39.5,39.5,275.0,275.0,264.7,264.7
1,1,1,1,1,1,1,1,1,1,1,1,1,1,1,1,1,1,1,1,1,1,1,1,1,1,1,1,1,1,1,1
84.8,95.1,95.1,84.8,84.8,95.1,95.1,84.8,84.8,95.1,95.1,84.8,84.8,95.1,95.1,84.8,130.1,140.4,140.4,
130.1,130.1,140.4,140.4,130.1,130.1,140.4,140.4,130.1,84.8,95.1,95.1,84.8
95.1,95.1,84.8,84.8,49.8,49.8,39.5,39.5,230.3,230.3,220.0,220.0,320.3,320.3,310.0,310.0,5.2,5.2,
354.7,354.7,275.0,275.0,264.7,264.7,49.8,49.8,39.5,39.5,275.0,275.0,264.7,264.7
1,1,1,1,1,1,1,1,1,1,1,1,1,1,1,1,1,1,1,1,1,1,1,1,1,1,1,1,1,1,1,1
84.8,95.1,95.1,84.8,84.8,95.1,95.1,84.8,84.8,95.1,95.1,84.8,84.8,95.1,95.1,84.8,130.1,140.4,140.4,
130.1,130.1,140.4,140.4,130.1,130.1,140.4,140.4,130.1,84.8,95.1,95.1,84.8
95.1,95.1,84.8,84.8,49.8,49.8,39.5,39.5,230.3,230.3,220.0,220.0,320.3,320.3,310.0,310.0,5.2,5.2,
354.7,354.7,275.0,275.0,264.7,264.7,49.8,49.8,39.5,39.5,275.0,275.0,264.7,264.7
1,1,1,1,1,1,1,1,1,1,1,1,1,1,1,1,1,1,1,1,1,1,1,1,1,1,1,1,1,1,1,1
84.8,95.1,95.1,84.8,84.8,95.1,95.1,84.8,84.8,95.1,95.1,84.8,84.8,95.1,95.1,84.8,130.1,140.4,140.4,
130.1,130.1,140.4,140.4,130.1,130.1,140.4,140.4,130.1,84.8,95.1,95.1,84.8
95.1,95.1,84.8,84.8,49.8,49.8,39.5,39.5,230.3,230.3,220.0,220.0,320.3,320.3,310.0,310.0,5.2,5.2,
354.7,354.7,275.0,275.0,264.7,264.7,49.8,49.8,39.5,39.5,275.0,275.0,264.7,264.7
1,1,1,1,1,1,1,1,1,1,1,1,1,1,1,1,1,1,1,1,1,1,1,1,1,1,1,1,1,1,1,1
84.8,95.1,95.1,84.8,84.8,95.1,95.1,84.8,84.8,95.1,95.1,84.8,84.8,95.1,95.1,84.8,130.1,140.4,140.4,
130.1,130.1,140.4,140.4,130.1,130.1,140.4,140.4,130.1,84.8,95.1,95.1,84.8
95.1,95.1,84.8,84.8,49.8,49.8,39.5,39.5,230.3,230.3,220.0,220.0,320.3,320.3,310.0,310.0,5.2,5.2,
354.7,354.7,275.0,275.0,264.7,264.7,49.8,49.8,39.5,39.5,275.0,275.0,264.7,264.7
1,1,1,1,1,1,1,1,1,1,1,1,1,1,1,1,1,1,1,1,1,1,1,1,1,1,1,1,1,1,1,1
84.8,95.1,95.1,84.8,84.8,95.1,95.1,84.8,84.8,95.1,95.1,84.8,84.8,95.1,95.1,84.8,130.1,140.4,140.4,
130.1,130.1,140.4,140.4,130.1,130.1,140.4,140.4,130.1,84.8,95.1,95.1,84.8
95.1,95.1,84.8,84.8,49.8,49.8,39.5,39.5,230.3,230.3,220.0,220.0,320.3,320.3,310.0,310.0,5.2,5.2,
354.7,354.7,275.0,275.0,264.7,264.7,49.8,49.8,39.5,39.5,275.0,275.0,264.7,264.7
1,1,1,1,1,1,1,1,1,1,1,1,1,1,1,1,1,1,1,1,1,1,1,1,1,1,1,1,1,1,1,1
84.8,95.1,95.1,84.8,84.8,95.1,95.1,84.8,84.8,95.1,95.1,84.8,84.8,95.1,95.1,84.8,130.1,140.4,140.4,
130.1,130.1,140.4,140.4,130.1,130.1,140.4,140.4,130.1,84.8,95.1,95.1,84.8
95.1,95.1,84.8,84.8,49.8,49.8,39.5,39.5,230.3,230.3,220.0,220.0,320.3,320.3,310.0,310.0,5.2,5.2,
354.7,354.7,275.0,275.0,264.7,264.7,49.8,49.8,39.5,39.5,275.0,275.0,264.7,264.7
1,1,1,1,1,1,1,1,1,1,1,1,1,1,1,1,1,1,1,1,1,1,1,1,1,1,1,1,1,1,1,1
84.8,95.1,95.1,84.8,84.8,95.1,95.1,84.8,84.8,95.1,95.1,84.8,84.8,95.1,95.1,84.8,130.1,140.4,140.4,
130.1,130.1,140.4,140.4,130.1,130.1,140.4,140.4,130.1,84.8,95.1,95.1,84.8
95.1,95.1,84.8,84.8,49.8,49.8,39.5,39.5,230.3,230.3,220.0,220.0,320.3,320.3,310.0,310.0,5.2,5.2,
354.7,354.7,275.0,275.0,264.7,264.7,49.8,49.8,39.5,39.5,275.0,275.0,264.7,264.7
1,1,1,1,1,1,1,1,1,1,1,1,1,1,1,1,1,1,1,1,1,1,1,1,1,1,1,1,1,1,1,1
84.8,95.1,95.1,84.8,84.8,95.1,95.1,84.8,84.8,95.1,95.1,84.8,84.8,95.1,95.1,84.8,130.1,140.4,140.4,
130.1,130.1,140.4,140.4,130.1,130.1,140.4,140.4,130.1,84.8,95.1,95.1,84.8
95.1,95.1,84.8,84.8,49.8,49.8,39.5,39.5,230.3,230.3,220.0,220.0,320.3,320.3,310.0,310.0,5.2,5.2,
354.7,354.7,275.0,275.0,264.7,264.7,49.8,49.8,39.5,39.5,275.0,275.0,264.7,264.7
2,1
1
1111. !1
1
1
1111. !2
1
1
1111. !3
1
1
1111. !4
1
1
1111. !5
1
```

1
1111. !6
1
1
1111. !7
1
1
1111. !8
1
1
1111. !9
1
1
1111. !10
1
1
1111. !11
1
1
1111. !12
1
1
1111. !13
1
1
1111. !14
1
1
1111. !15
1
1
1111. !16
1
1
1111. !17
1
1
1111. !18
1
1
1111. !19
1
1
1111. !20
1
1
1111. !21
1
1
1111. !22
1
1
1111. !23
1
1
1111. !24
1
0
0,0
3,1.0 !Lifetimes

```
2,60.494,8.656
3,50.494,5.771
4,5.338,2.883
0,0
0,0
OP,RAW
1
0 0 0 0 0 0 0 0
0 0 0 0 0 0 0 0
0 0 0 0 0 0 0 0
0 0 0 0 0 0 0 0
0 0 0 0 0 0 0 0
0 0 0 0 0 0 0 0
0 0 0 0 0 0 0 0
0 0 0 0 0 0 0 0
0 0 0 0 0 0 0 0
0 0 0 0 0 0 0 0
0 0 0 0 0 0 0 0
0 0 0 0 0 0 0 0
0 0 0 0 0 0 0 0
0 0 0 0 0 0 0 0
0 0 0 0 0 0 0 0
0 0 0 0 0 0 0 0
0 0 0 0 0 0 0 0
0 0 0 0 0 0 0 0
0 0 0 0 0 0 0 0
0 0 0 0 0 0 0 0
0 0 0 0 0 0 0 0
0 0 0 0 0 0 0 0
0 0 0 0 0 0 0 0
0 0 0 0 0 0 0 0
0 0 0 0 0 0 0 0
0 0 0 0 0 0 0 0
0 0 0 0 0 0 0 0
0 0 0 0 0 0 0 0
0 0 0 0 0 0 0 0
0 0 0 0 0 0 0 0
0 0 0 0 0 0 0 0
0 0 0 0 0 0 0 0
1
32
1,2,3,4,5,6,7,8,9,10,11,12,13,14,15,16,17,18,19,20,21,22,23,24,25,26,27,28,29,30,31,32
2
0 0 0 0 0 0 0 0
0 0 0 0 0 0 0 0
0 0 0 0 0 0 0 0
0 0 0 0 0 0 0 0
0 0 0 0 0 0 0 0
0 0 0 0 0 0 0 0
0 0 0 0 0 0 0 0
0 0 0 0 0 0 0 0
0 0 0 0 0 0 0 0
0 0 0 0 0 0 0 0
0 0 0 0 0 0 0 0
0 0 0 0 0 0 0 0
0 0 0 0 0 0 0 0
0 0 0 0 0 0 0 0
0 0 0 0 0 0 0 0
0 0 0 0 0 0 0 0
0 0 0 0 0 0 0 0
```

```
0 0 0 0 0 0 0 0
0 0 0 0 0 0 0 0
0 0 0 0 0 0 0 0
0 0 0 0 0 0 0 0
0 0 0 0 0 0 0 0
0 0 0 0 0 0 0 0
0 0 0 0 0 0 0 0
0 0 0 0 0 0 0 0
0 0 0 0 0 0 0 0
0 0 0 0 0 0 0 0
0 0 0 0 0 0 0 0
0 0 0 0 0 0 0 0
0 0 0 0 0 0 0 0
0 0 0 0 0 0 0 0
0 0 0 0 0 0 0 0
1
32
1,2,3,4,5,6,7,8,9,10,11,12,13,14,15,16,17,18,19,20,21,22,23,24,25,26,27,28,29,30,31,32
3
0 0 0 0 0 0 0 0
0 0 0 0 0 0 0 0
0 0 0 0 0 0 0 0
0 0 0 0 0 0 0 0
0 0 0 0 0 0 0 0
0 0 0 0 0 0 0 0
0 0 0 0 0 0 0 0
0 0 0 0 0 0 0 0
0 0 0 0 0 0 0 0
0 0 0 0 0 0 0 0
0 0 0 0 0 0 0 0
0 0 0 0 0 0 0 0
0 0 0 0 0 0 0 0
0 0 0 0 0 0 0 0
0 0 0 0 0 0 0 0
0 0 0 0 0 0 0 0
0 0 0 0 0 0 0 0
0 0 0 0 0 0 0 0
0 0 0 0 0 0 0 0
0 0 0 0 0 0 0 0
0 0 0 0 0 0 0 0
0 0 0 0 0 0 0 0
0 0 0 0 0 0 0 0
0 0 0 0 0 0 0 0
0 0 0 0 0 0 0 0
0 0 0 0 0 0 0 0
0 0 0 0 0 0 0 0
0 0 0 0 0 0 0 0
0 0 0 0 0 0 0 0
0 0 0 0 0 0 0 0
0 0 0 0 0 0 0 0
0 0 0 0 0 0 0 0
1
32
1,2,3,4,5,6,7,8,9,10,11,12,13,14,15,16,17,18,19,20,21,22,23,24,25,26,27,28,29,30,31,32
4
0 0 0 0 0 0 0 0
0 0 0 0 0 0 0 0
0 0 0 0 0 0 0 0
0 0 0 0 0 0 0 0
0 0 0 0 0 0 0 0
```

```
0 0 0 0 0 0 0 0
0 0 0 0 0 0 0 0
0 0 0 0 0 0 0 0
0 0 0 0 0 0 0 0
0 0 0 0 0 0 0 0
0 0 0 0 0 0 0 0
0 0 0 0 0 0 0 0
0 0 0 0 0 0 0 0
0 0 0 0 0 0 0 0
0 0 0 0 0 0 0 0
0 0 0 0 0 0 0 0
0 0 0 0 0 0 0 0
0 0 0 0 0 0 0 0
0 0 0 0 0 0 0 0
0 0 0 0 0 0 0 0
0 0 0 0 0 0 0 0
0 0 0 0 0 0 0 0
0 0 0 0 0 0 0 0
0 0 0 0 0 0 0 0
0 0 0 0 0 0 0 0
0 0 0 0 0 0 0 0
0 0 0 0 0 0 0 0
0 0 0 0 0 0 0 0
0 0 0 0 0 0 0 0
0 0 0 0 0 0 0 0
0 0 0 0 0 0 0 0
0 0 0 0 0 0 0 0
1
32
1,2,3,4,5,6,7,8,9,10,11,12,13,14,15,16,17,18,19,20,21,22,23,24,25,26,27,28,29,30,31,32
5
0 0 0 0 0 0 0 0
0 0 0 0 0 0 0 0
0 0 0 0 0 0 0 0
0 0 0 0 0 0 0 0
0 0 0 0 0 0 0 0
0 0 0 0 0 0 0 0
0 0 0 0 0 0 0 0
0 0 0 0 0 0 0 0
0 0 0 0 0 0 0 0
0 0 0 0 0 0 0 0
0 0 0 0 0 0 0 0
0 0 0 0 0 0 0 0
0 0 0 0 0 0 0 0
0 0 0 0 0 0 0 0
0 0 0 0 0 0 0 0
0 0 0 0 0 0 0 0
0 0 0 0 0 0 0 0
0 0 0 0 0 0 0 0
0 0 0 0 0 0 0 0
0 0 0 0 0 0 0 0
0 0 0 0 0 0 0 0
0 0 0 0 0 0 0 0
0 0 0 0 0 0 0 0
0 0 0 0 0 0 0 0
0 0 0 0 0 0 0 0
0 0 0 0 0 0 0 0
0 0 0 0 0 0 0 0
0 0 0 0 0 0 0 0
0 0 0 0 0 0 0 0
```

```
0 0 0 0 0 0 0 0 0
0 0 0 0 0 0 0 0 0
0 0 0 0 0 0 0 0 0
1
32
1,2,3,4,5,6,7,8,9,10,11,12,13,14,15,16,17,18,19,20,21,22,23,24,25,26,27,28,29,30,31,32
6
0 0 0 0 0 0 0 0 0
0 0 0 0 0 0 0 0 0
0 0 0 0 0 0 0 0 0
0 0 0 0 0 0 0 0 0
0 0 0 0 0 0 0 0 0
0 0 0 0 0 0 0 0 0
0 0 0 0 0 0 0 0 0
0 0 0 0 0 0 0 0 0
0 0 0 0 0 0 0 0 0
0 0 0 0 0 0 0 0 0
0 0 0 0 0 0 0 0 0
0 0 0 0 0 0 0 0 0
0 0 0 0 0 0 0 0 0
0 0 0 0 0 0 0 0 0
0 0 0 0 0 0 0 0 0
0 0 0 0 0 0 0 0 0
0 0 0 0 0 0 0 0 0
0 0 0 0 0 0 0 0 0
0 0 0 0 0 0 0 0 0
0 0 0 0 0 0 0 0 0
0 0 0 0 0 0 0 0 0
0 0 0 0 0 0 0 0 0
0 0 0 0 0 0 0 0 0
0 0 0 0 0 0 0 0 0
0 0 0 0 0 0 0 0 0
0 0 0 0 0 0 0 0 0
0 0 0 0 0 0 0 0 0
0 0 0 0 0 0 0 0 0
0 0 0 0 0 0 0 0 0
0 0 0 0 0 0 0 0 0
0 0 0 0 0 0 0 0 0
0 0 0 0 0 0 0 0 0
1
32
1,2,3,4,5,6,7,8,9,10,11,12,13,14,15,16,17,18,19,20,21,22,23,24,25,26,27,28,29,30,31,32
7
0 0 0 0 0 0 0 0 0
0 0 0 0 0 0 0 0 0
0 0 0 0 0 0 0 0 0
0 0 0 0 0 0 0 0 0
0 0 0 0 0 0 0 0 0
0 0 0 0 0 0 0 0 0
0 0 0 0 0 0 0 0 0
0 0 0 0 0 0 0 0 0
0 0 0 0 0 0 0 0 0
0 0 0 0 0 0 0 0 0
0 0 0 0 0 0 0 0 0
0 0 0 0 0 0 0 0 0
0 0 0 0 0 0 0 0 0
0 0 0 0 0 0 0 0 0
0 0 0 0 0 0 0 0 0
0 0 0 0 0 0 0 0 0
0 0 0 0 0 0 0 0 0
```

```
0 0 0 0 0 0 0 0
0 0 0 0 0 0 0 0
0 0 0 0 0 0 0 0
0 0 0 0 0 0 0 0
0 0 0 0 0 0 0 0
0 0 0 0 0 0 0 0
0 0 0 0 0 0 0 0
0 0 0 0 0 0 0 0
0 0 0 0 0 0 0 0
0 0 0 0 0 0 0 0
0 0 0 0 0 0 0 0
0 0 0 0 0 0 0 0
0 0 0 0 0 0 0 0
0 0 0 0 0 0 0 0
0 0 0 0 0 0 0 0
1
32
1,2,3,4,5,6,7,8,9,10,11,12,13,14,15,16,17,18,19,20,21,22,23,24,25,26,27,28,29,30,31,32
8
0 0 0 0 0 0 0 0
0 0 0 0 0 0 0 0
0 0 0 0 0 0 0 0
0 0 0 0 0 0 0 0
0 0 0 0 0 0 0 0
0 0 0 0 0 0 0 0
0 0 0 0 0 0 0 0
0 0 0 0 0 0 0 0
0 0 0 0 0 0 0 0
0 0 0 0 0 0 0 0
0 0 0 0 0 0 0 0
0 0 0 0 0 0 0 0
0 0 0 0 0 0 0 0
0 0 0 0 0 0 0 0
0 0 0 0 0 0 0 0
0 0 0 0 0 0 0 0
0 0 0 0 0 0 0 0
0 0 0 0 0 0 0 0
0 0 0 0 0 0 0 0
0 0 0 0 0 0 0 0
0 0 0 0 0 0 0 0
0 0 0 0 0 0 0 0
0 0 0 0 0 0 0 0
0 0 0 0 0 0 0 0
0 0 0 0 0 0 0 0
0 0 0 0 0 0 0 0
0 0 0 0 0 0 0 0
0 0 0 0 0 0 0 0
0 0 0 0 0 0 0 0
0 0 0 0 0 0 0 0
0 0 0 0 0 0 0 0
0 0 0 0 0 0 0 0
1
32
1,2,3,4,5,6,7,8,9,10,11,12,13,14,15,16,17,18,19,20,21,22,23,24,25,26,27,28,29,30,31,32
9
0 0 0 0 0 0 0 0
0 0 0 0 0 0 0 0
0 0 0 0 0 0 0 0
0 0 0 0 0 0 0 0
0 0 0 0 0 0 0 0
```

```
0 0 0 0 0 0 0 0 0
0 0 0 0 0 0 0 0 0
0 0 0 0 0 0 0 0 0
0 0 0 0 0 0 0 0 0
0 0 0 0 0 0 0 0 0
0 0 0 0 0 0 0 0 0
0 0 0 0 0 0 0 0 0
0 0 0 0 0 0 0 0 0
0 0 0 0 0 0 0 0 0
0 0 0 0 0 0 0 0 0
0 0 0 0 0 0 0 0 0
0 0 0 0 0 0 0 0 0
0 0 0 0 0 0 0 0 0
0 0 0 0 0 0 0 0 0
0 0 0 0 0 0 0 0 0
0 0 0 0 0 0 0 0 0
0 0 0 0 0 0 0 0 0
0 0 0 0 0 0 0 0 0
0 0 0 0 0 0 0 0 0
0 0 0 0 0 0 0 0 0
0 0 0 0 0 0 0 0 0
0 0 0 0 0 0 0 0 0
0 0 0 0 0 0 0 0 0
0 0 0 0 0 0 0 0 0
0 0 0 0 0 0 0 0 0
0 0 0 0 0 0 0 0 0
0 0 0 0 0 0 0 0 0
1
32
1,2,3,4,5,6,7,8,9,10,11,12,13,14,15,16,17,18,19,20,21,22,23,24,25,26,27,28,29,30,31,32
10
0 0 0 0 0 0 0 0 0
0 0 0 0 0 0 0 0 0
0 0 0 0 0 0 0 0 0
0 0 0 0 0 0 0 0 0
0 0 0 0 0 0 0 0 0
0 0 0 0 0 0 0 0 0
0 0 0 0 0 0 0 0 0
0 0 0 0 0 0 0 0 0
0 0 0 0 0 0 0 0 0
0 0 0 0 0 0 0 0 0
0 0 0 0 0 0 0 0 0
0 0 0 0 0 0 0 0 0
0 0 0 0 0 0 0 0 0
0 0 0 0 0 0 0 0 0
0 0 0 0 0 0 0 0 0
0 0 0 0 0 0 0 0 0
0 0 0 0 0 0 0 0 0
0 0 0 0 0 0 0 0 0
0 0 0 0 0 0 0 0 0
0 0 0 0 0 0 0 0 0
0 0 0 0 0 0 0 0 0
0 0 0 0 0 0 0 0 0
0 0 0 0 0 0 0 0 0
0 0 0 0 0 0 0 0 0
0 0 0 0 0 0 0 0 0
0 0 0 0 0 0 0 0 0
0 0 0 0 0 0 0 0 0
0 0 0 0 0 0 0 0 0
0 0 0 0 0 0 0 0 0
```

```
0 0 0 0 0 0 0 0 0
0 0 0 0 0 0 0 0 0
0 0 0 0 0 0 0 0 0
1
32
1,2,3,4,5,6,7,8,9,10,11,12,13,14,15,16,17,18,19,20,21,22,23,24,25,26,27,28,29,30,31,32
11
0 0 0 0 0 0 0 0 0
0 0 0 0 0 0 0 0 0
0 0 0 0 0 0 0 0 0
0 0 0 0 0 0 0 0 0
0 0 0 0 0 0 0 0 0
0 0 0 0 0 0 0 0 0
0 0 0 0 0 0 0 0 0
0 0 0 0 0 0 0 0 0
0 0 0 0 0 0 0 0 0
0 0 0 0 0 0 0 0 0
0 0 0 0 0 0 0 0 0
0 0 0 0 0 0 0 0 0
0 0 0 0 0 0 0 0 0
0 0 0 0 0 0 0 0 0
0 0 0 0 0 0 0 0 0
0 0 0 0 0 0 0 0 0
0 0 0 0 0 0 0 0 0
0 0 0 0 0 0 0 0 0
0 0 0 0 0 0 0 0 0
0 0 0 0 0 0 0 0 0
0 0 0 0 0 0 0 0 0
0 0 0 0 0 0 0 0 0
0 0 0 0 0 0 0 0 0
0 0 0 0 0 0 0 0 0
0 0 0 0 0 0 0 0 0
0 0 0 0 0 0 0 0 0
0 0 0 0 0 0 0 0 0
0 0 0 0 0 0 0 0 0
0 0 0 0 0 0 0 0 0
0 0 0 0 0 0 0 0 0
0 0 0 0 0 0 0 0 0
0 0 0 0 0 0 0 0 0
1
32
1,2,3,4,5,6,7,8,9,10,11,12,13,14,15,16,17,18,19,20,21,22,23,24,25,26,27,28,29,30,31,32
12
0 0 0 0 0 0 0 0 0
0 0 0 0 0 0 0 0 0
0 0 0 0 0 0 0 0 0
0 0 0 0 0 0 0 0 0
0 0 0 0 0 0 0 0 0
0 0 0 0 0 0 0 0 0
0 0 0 0 0 0 0 0 0
0 0 0 0 0 0 0 0 0
0 0 0 0 0 0 0 0 0
0 0 0 0 0 0 0 0 0
0 0 0 0 0 0 0 0 0
0 0 0 0 0 0 0 0 0
0 0 0 0 0 0 0 0 0
0 0 0 0 0 0 0 0 0
0 0 0 0 0 0 0 0 0
0 0 0 0 0 0 0 0 0
0 0 0 0 0 0 0 0 0
```

```
0 0 0 0 0 0 0 0 0
0 0 0 0 0 0 0 0 0
0 0 0 0 0 0 0 0 0
0 0 0 0 0 0 0 0 0
0 0 0 0 0 0 0 0 0
0 0 0 0 0 0 0 0 0
0 0 0 0 0 0 0 0 0
0 0 0 0 0 0 0 0 0
0 0 0 0 0 0 0 0 0
0 0 0 0 0 0 0 0 0
0 0 0 0 0 0 0 0 0
0 0 0 0 0 0 0 0 0
0 0 0 0 0 0 0 0 0
0 0 0 0 0 0 0 0 0
0 0 0 0 0 0 0 0 0
1
32
1,2,3,4,5,6,7,8,9,10,11,12,13,14,15,16,17,18,19,20,21,22,23,24,25,26,27,28,29,30,31,32
13
0 0 0 0 0 0 0 0 0
0 0 0 0 0 0 0 0 0
0 0 0 0 0 0 0 0 0
0 0 0 0 0 0 0 0 0
0 0 0 0 0 0 0 0 0
0 0 0 0 0 0 0 0 0
0 0 0 0 0 0 0 0 0
0 0 0 0 0 0 0 0 0
0 0 0 0 0 0 0 0 0
0 0 0 0 0 0 0 0 0
0 0 0 0 0 0 0 0 0
0 0 0 0 0 0 0 0 0
0 0 0 0 0 0 0 0 0
0 0 0 0 0 0 0 0 0
0 0 0 0 0 0 0 0 0
0 0 0 0 0 0 0 0 0
0 0 0 0 0 0 0 0 0
0 0 0 0 0 0 0 0 0
0 0 0 0 0 0 0 0 0
0 0 0 0 0 0 0 0 0
0 0 0 0 0 0 0 0 0
0 0 0 0 0 0 0 0 0
0 0 0 0 0 0 0 0 0
0 0 0 0 0 0 0 0 0
0 0 0 0 0 0 0 0 0
0 0 0 0 0 0 0 0 0
0 0 0 0 0 0 0 0 0
0 0 0 0 0 0 0 0 0
0 0 0 0 0 0 0 0 0
0 0 0 0 0 0 0 0 0
0 0 0 0 0 0 0 0 0
0 0 0 0 0 0 0 0 0
1
32
1,2,3,4,5,6,7,8,9,10,11,12,13,14,15,16,17,18,19,20,21,22,23,24,25,26,27,28,29,30,31,32
14
0 0 0 0 0 0 0 0 0
0 0 0 0 0 0 0 0 0
0 0 0 0 0 0 0 0 0
0 0 0 0 0 0 0 0 0
0 0 0 0 0 0 0 0 0
```

```
0 0 0 0 0 0 0 0 0
0 0 0 0 0 0 0 0 0
0 0 0 0 0 0 0 0 0
0 0 0 0 0 0 0 0 0
0 0 0 0 0 0 0 0 0
0 0 0 0 0 0 0 0 0
0 0 0 0 0 0 0 0 0
0 0 0 0 0 0 0 0 0
0 0 0 0 0 0 0 0 0
0 0 0 0 0 0 0 0 0
0 0 0 0 0 0 0 0 0
0 0 0 0 0 0 0 0 0
0 0 0 0 0 0 0 0 0
0 0 0 0 0 0 0 0 0
0 0 0 0 0 0 0 0 0
0 0 0 0 0 0 0 0 0
0 0 0 0 0 0 0 0 0
0 0 0 0 0 0 0 0 0
0 0 0 0 0 0 0 0 0
0 0 0 0 0 0 0 0 0
0 0 0 0 0 0 0 0 0
0 0 0 0 0 0 0 0 0
0 0 0 0 0 0 0 0 0
0 0 0 0 0 0 0 0 0
0 0 0 0 0 0 0 0 0
0 0 0 0 0 0 0 0 0
0 0 0 0 0 0 0 0 0
1
32
1,2,3,4,5,6,7,8,9,10,11,12,13,14,15,16,17,18,19,20,21,22,23,24,25,26,27,28,29,30,31,32
15
0 0 0 0 0 0 0 0 0
0 0 0 0 0 0 0 0 0
0 0 0 0 0 0 0 0 0
0 0 0 0 0 0 0 0 0
0 0 0 0 0 0 0 0 0
0 0 0 0 0 0 0 0 0
0 0 0 0 0 0 0 0 0
0 0 0 0 0 0 0 0 0
0 0 0 0 0 0 0 0 0
0 0 0 0 0 0 0 0 0
0 0 0 0 0 0 0 0 0
0 0 0 0 0 0 0 0 0
0 0 0 0 0 0 0 0 0
0 0 0 0 0 0 0 0 0
0 0 0 0 0 0 0 0 0
0 0 0 0 0 0 0 0 0
0 0 0 0 0 0 0 0 0
0 0 0 0 0 0 0 0 0
0 0 0 0 0 0 0 0 0
0 0 0 0 0 0 0 0 0
0 0 0 0 0 0 0 0 0
0 0 0 0 0 0 0 0 0
0 0 0 0 0 0 0 0 0
0 0 0 0 0 0 0 0 0
0 0 0 0 0 0 0 0 0
0 0 0 0 0 0 0 0 0
0 0 0 0 0 0 0 0 0
0 0 0 0 0 0 0 0 0
0 0 0 0 0 0 0 0 0
```

```
0 0 0 0 0 0 0 0 0
0 0 0 0 0 0 0 0 0
0 0 0 0 0 0 0 0 0
1
32
1,2,3,4,5,6,7,8,9,10,11,12,13,14,15,16,17,18,19,20,21,22,23,24,25,26,27,28,29,30,31,32
16
0 0 0 0 0 0 0 0 0
0 0 0 0 0 0 0 0 0
0 0 0 0 0 0 0 0 0
0 0 0 0 0 0 0 0 0
0 0 0 0 0 0 0 0 0
0 0 0 0 0 0 0 0 0
0 0 0 0 0 0 0 0 0
0 0 0 0 0 0 0 0 0
0 0 0 0 0 0 0 0 0
0 0 0 0 0 0 0 0 0
0 0 0 0 0 0 0 0 0
0 0 0 0 0 0 0 0 0
0 0 0 0 0 0 0 0 0
0 0 0 0 0 0 0 0 0
0 0 0 0 0 0 0 0 0
0 0 0 0 0 0 0 0 0
0 0 0 0 0 0 0 0 0
0 0 0 0 0 0 0 0 0
0 0 0 0 0 0 0 0 0
0 0 0 0 0 0 0 0 0
0 0 0 0 0 0 0 0 0
0 0 0 0 0 0 0 0 0
0 0 0 0 0 0 0 0 0
0 0 0 0 0 0 0 0 0
0 0 0 0 0 0 0 0 0
0 0 0 0 0 0 0 0 0
0 0 0 0 0 0 0 0 0
0 0 0 0 0 0 0 0 0
0 0 0 0 0 0 0 0 0
0 0 0 0 0 0 0 0 0
0 0 0 0 0 0 0 0 0
0 0 0 0 0 0 0 0 0
1
32
1,2,3,4,5,6,7,8,9,10,11,12,13,14,15,16,17,18,19,20,21,22,23,24,25,26,27,28,29,30,31,32
17
0 0 0 0 0 0 0 0 0
0 0 0 0 0 0 0 0 0
0 0 0 0 0 0 0 0 0
0 0 0 0 0 0 0 0 0
0 0 0 0 0 0 0 0 0
0 0 0 0 0 0 0 0 0
0 0 0 0 0 0 0 0 0
0 0 0 0 0 0 0 0 0
0 0 0 0 0 0 0 0 0
0 0 0 0 0 0 0 0 0
0 0 0 0 0 0 0 0 0
0 0 0 0 0 0 0 0 0
0 0 0 0 0 0 0 0 0
0 0 0 0 0 0 0 0 0
0 0 0 0 0 0 0 0 0
0 0 0 0 0 0 0 0 0
0 0 0 0 0 0 0 0 0
```

```
0 0 0 0 0 0 0 0 0
0 0 0 0 0 0 0 0 0
0 0 0 0 0 0 0 0 0
0 0 0 0 0 0 0 0 0
0 0 0 0 0 0 0 0 0
0 0 0 0 0 0 0 0 0
0 0 0 0 0 0 0 0 0
0 0 0 0 0 0 0 0 0
0 0 0 0 0 0 0 0 0
0 0 0 0 0 0 0 0 0
0 0 0 0 0 0 0 0 0
0 0 0 0 0 0 0 0 0
0 0 0 0 0 0 0 0 0
0 0 0 0 0 0 0 0 0
0 0 0 0 0 0 0 0 0
1
32
1,2,3,4,5,6,7,8,9,10,11,12,13,14,15,16,17,18,19,20,21,22,23,24,25,26,27,28,29,30,31,32
18
0 0 0 0 0 0 0 0 0
0 0 0 0 0 0 0 0 0
0 0 0 0 0 0 0 0 0
0 0 0 0 0 0 0 0 0
0 0 0 0 0 0 0 0 0
0 0 0 0 0 0 0 0 0
0 0 0 0 0 0 0 0 0
0 0 0 0 0 0 0 0 0
0 0 0 0 0 0 0 0 0
0 0 0 0 0 0 0 0 0
0 0 0 0 0 0 0 0 0
0 0 0 0 0 0 0 0 0
0 0 0 0 0 0 0 0 0
0 0 0 0 0 0 0 0 0
0 0 0 0 0 0 0 0 0
0 0 0 0 0 0 0 0 0
0 0 0 0 0 0 0 0 0
0 0 0 0 0 0 0 0 0
0 0 0 0 0 0 0 0 0
0 0 0 0 0 0 0 0 0
0 0 0 0 0 0 0 0 0
0 0 0 0 0 0 0 0 0
0 0 0 0 0 0 0 0 0
0 0 0 0 0 0 0 0 0
0 0 0 0 0 0 0 0 0
0 0 0 0 0 0 0 0 0
0 0 0 0 0 0 0 0 0
0 0 0 0 0 0 0 0 0
0 0 0 0 0 0 0 0 0
0 0 0 0 0 0 0 0 0
0 0 0 0 0 0 0 0 0
0 0 0 0 0 0 0 0 0
1
32
1,2,3,4,5,6,7,8,9,10,11,12,13,14,15,16,17,18,19,20,21,22,23,24,25,26,27,28,29,30,31,32
19
0 0 0 0 0 0 0 0 0
0 0 0 0 0 0 0 0 0
0 0 0 0 0 0 0 0 0
0 0 0 0 0 0 0 0 0
0 0 0 0 0 0 0 0 0
```

0 0 0 0 0 0 0 0 0
0 0 0 0 0 0 0 0 0
0 0 0 0 0 0 0 0 0
0 0 0 0 0 0 0 0 0
0 0 0 0 0 0 0 0 0
0 0 0 0 0 0 0 0 0
0 0 0 0 0 0 0 0 0
0 0 0 0 0 0 0 0 0
0 0 0 0 0 0 0 0 0
0 0 0 0 0 0 0 0 0
0 0 0 0 0 0 0 0 0
0 0 0 0 0 0 0 0 0
0 0 0 0 0 0 0 0 0
0 0 0 0 0 0 0 0 0
0 0 0 0 0 0 0 0 0
0 0 0 0 0 0 0 0 0
0 0 0 0 0 0 0 0 0
0 0 0 0 0 0 0 0 0
0 0 0 0 0 0 0 0 0
0 0 0 0 0 0 0 0 0
0 0 0 0 0 0 0 0 0
0 0 0 0 0 0 0 0 0
0 0 0 0 0 0 0 0 0
0 0 0 0 0 0 0 0 0
0 0 0 0 0 0 0 0 0
0 0 0 0 0 0 0 0 0
0 0 0 0 0 0 0 0 0
1
32
1,2,3,4,5,6,7,8,9,10,11,12,13,14,15,16,17,18,19,20,21,22,23,24,25,26,27,28,29,30,31,32
20
0 0 0 0 0 0 0 0 0
0 0 0 0 0 0 0 0 0
0 0 0 0 0 0 0 0 0
0 0 0 0 0 0 0 0 0
0 0 0 0 0 0 0 0 0
0 0 0 0 0 0 0 0 0
0 0 0 0 0 0 0 0 0
0 0 0 0 0 0 0 0 0
0 0 0 0 0 0 0 0 0
0 0 0 0 0 0 0 0 0
0 0 0 0 0 0 0 0 0
0 0 0 0 0 0 0 0 0
0 0 0 0 0 0 0 0 0
0 0 0 0 0 0 0 0 0
0 0 0 0 0 0 0 0 0
0 0 0 0 0 0 0 0 0
0 0 0 0 0 0 0 0 0
0 0 0 0 0 0 0 0 0
0 0 0 0 0 0 0 0 0
0 0 0 0 0 0 0 0 0
0 0 0 0 0 0 0 0 0
0 0 0 0 0 0 0 0 0
0 0 0 0 0 0 0 0 0
0 0 0 0 0 0 0 0 0
0 0 0 0 0 0 0 0 0
0 0 0 0 0 0 0 0 0
0 0 0 0 0 0 0 0 0
0 0 0 0 0 0 0 0 0
0 0 0 0 0 0 0 0 0

```
0 0 0 0 0 0 0 0 0
0 0 0 0 0 0 0 0 0
0 0 0 0 0 0 0 0 0
1
32
1,2,3,4,5,6,7,8,9,10,11,12,13,14,15,16,17,18,19,20,21,22,23,24,25,26,27,28,29,30,31,32
21
0 0 0 0 0 0 0 0 0
0 0 0 0 0 0 0 0 0
0 0 0 0 0 0 0 0 0
0 0 0 0 0 0 0 0 0
0 0 0 0 0 0 0 0 0
0 0 0 0 0 0 0 0 0
0 0 0 0 0 0 0 0 0
0 0 0 0 0 0 0 0 0
0 0 0 0 0 0 0 0 0
0 0 0 0 0 0 0 0 0
0 0 0 0 0 0 0 0 0
0 0 0 0 0 0 0 0 0
0 0 0 0 0 0 0 0 0
0 0 0 0 0 0 0 0 0
0 0 0 0 0 0 0 0 0
0 0 0 0 0 0 0 0 0
0 0 0 0 0 0 0 0 0
0 0 0 0 0 0 0 0 0
0 0 0 0 0 0 0 0 0
0 0 0 0 0 0 0 0 0
0 0 0 0 0 0 0 0 0
0 0 0 0 0 0 0 0 0
0 0 0 0 0 0 0 0 0
0 0 0 0 0 0 0 0 0
0 0 0 0 0 0 0 0 0
0 0 0 0 0 0 0 0 0
0 0 0 0 0 0 0 0 0
0 0 0 0 0 0 0 0 0
0 0 0 0 0 0 0 0 0
0 0 0 0 0 0 0 0 0
0 0 0 0 0 0 0 0 0
0 0 0 0 0 0 0 0 0
1
32
1,2,3,4,5,6,7,8,9,10,11,12,13,14,15,16,17,18,19,20,21,22,23,24,25,26,27,28,29,30,31,32
22
0 0 0 0 0 0 0 0 0
0 0 0 0 0 0 0 0 0
0 0 0 0 0 0 0 0 0
0 0 0 0 0 0 0 0 0
0 0 0 0 0 0 0 0 0
0 0 0 0 0 0 0 0 0
0 0 0 0 0 0 0 0 0
0 0 0 0 0 0 0 0 0
0 0 0 0 0 0 0 0 0
0 0 0 0 0 0 0 0 0
0 0 0 0 0 0 0 0 0
0 0 0 0 0 0 0 0 0
0 0 0 0 0 0 0 0 0
0 0 0 0 0 0 0 0 0
0 0 0 0 0 0 0 0 0
0 0 0 0 0 0 0 0 0
0 0 0 0 0 0 0 0 0
```

```
0 0 0 0 0 0 0 0
0 0 0 0 0 0 0 0
0 0 0 0 0 0 0 0
0 0 0 0 0 0 0 0
0 0 0 0 0 0 0 0
0 0 0 0 0 0 0 0
0 0 0 0 0 0 0 0
0 0 0 0 0 0 0 0
0 0 0 0 0 0 0 0
0 0 0 0 0 0 0 0
0 0 0 0 0 0 0 0
0 0 0 0 0 0 0 0
0 0 0 0 0 0 0 0
0 0 0 0 0 0 0 0
0 0 0 0 0 0 0 0
1
32
1,2,3,4,5,6,7,8,9,10,11,12,13,14,15,16,17,18,19,20,21,22,23,24,25,26,27,28,29,30,31,32
23
0 0 0 0 0 0 0 0
0 0 0 0 0 0 0 0
0 0 0 0 0 0 0 0
0 0 0 0 0 0 0 0
0 0 0 0 0 0 0 0
0 0 0 0 0 0 0 0
0 0 0 0 0 0 0 0
0 0 0 0 0 0 0 0
0 0 0 0 0 0 0 0
0 0 0 0 0 0 0 0
0 0 0 0 0 0 0 0
0 0 0 0 0 0 0 0
0 0 0 0 0 0 0 0
0 0 0 0 0 0 0 0
0 0 0 0 0 0 0 0
0 0 0 0 0 0 0 0
0 0 0 0 0 0 0 0
0 0 0 0 0 0 0 0
0 0 0 0 0 0 0 0
0 0 0 0 0 0 0 0
0 0 0 0 0 0 0 0
0 0 0 0 0 0 0 0
0 0 0 0 0 0 0 0
0 0 0 0 0 0 0 0
0 0 0 0 0 0 0 0
0 0 0 0 0 0 0 0
0 0 0 0 0 0 0 0
0 0 0 0 0 0 0 0
0 0 0 0 0 0 0 0
0 0 0 0 0 0 0 0
0 0 0 0 0 0 0 0
0 0 0 0 0 0 0 0
1
32
1,2,3,4,5,6,7,8,9,10,11,12,13,14,15,16,17,18,19,20,21,22,23,24,25,26,27,28,29,30,31,32
24
0 0 0 0 0 0 0 0
0 0 0 0 0 0 0 0
0 0 0 0 0 0 0 0
0 0 0 0 0 0 0 0
0 0 0 0 0 0 0 0
```

```
0 0 0 0 0 0 0 0
0 0 0 0 0 0 0 0
0 0 0 0 0 0 0 0
0 0 0 0 0 0 0 0
0 0 0 0 0 0 0 0
0 0 0 0 0 0 0 0
0 0 0 0 0 0 0 0
0 0 0 0 0 0 0 0
0 0 0 0 0 0 0 0
0 0 0 0 0 0 0 0
0 0 0 0 0 0 0 0
0 0 0 0 0 0 0 0
0 0 0 0 0 0 0 0
0 0 0 0 0 0 0 0
0 0 0 0 0 0 0 0
0 0 0 0 0 0 0 0
0 0 0 0 0 0 0 0
0 0 0 0 0 0 0 0
0 0 0 0 0 0 0 0
0 0 0 0 0 0 0 0
0 0 0 0 0 0 0 0
0 0 0 0 0 0 0 0
0 0 0 0 0 0 0 0
0 0 0 0 0 0 0 0
0 0 0 0 0 0 0 0
0 0 0 0 0 0 0 0
0 0 0 0 0 0 0 0
1
32
1,2,3,4,5,6,7,8,9,10,11,12,13,14,15,16,17,18,19,20,21,22,23,24,25,26,27,28,29,30,31,32
0
OP,INTI
10,7,128.14,134.94,130.57,131.29 !EXP1
127,128,129,130,131,132,133,134,135,136
129.0,129.5,130.0,130.5,131.0,131.5,132.0
10,7,128.14,134.94,131.38,132.13 !EXP2
127,128,129,130,131,132,133,134,135,136
130.5,131.0,131.5,132.0,132.5,133.0,133.5
10,7,128.14,134.94,132.21,132.99 !EXP3
127,128,129,130,131,132,133,134,135,136
131.5,132.0,132.5,133.0,133.5,134.0,134.5
10,7,128.14,134.94,133.08,133.88 !EXP4
127,128,129,130,131,132,133,134,135,136
132.5,133.0,133.5,134.0,134.5,135.0,135.5
10,7,128.14,134.94,133.97,134.80 !EXP5
127,128,129,130,131,132,133,134,135,136
133.0,133.5,134.0,134.5,135.0,135.5,136.0
10,7,128.14,134.94,134.89,135.75 !EXP6
127,128,129,130,131,132,133,134,135,136
133.5,134.0,134.5,135.0,135.5,136.0,136.5
10,7,128.14,134.94,135.84,136.73 !EXP7
127,128,129,130,131,132,133,134,135,136
134.5,135.0,135.5,136.0,136.5,137.0,137.5
10,7,128.14,134.94,136.83,137.74 !EXP8
127,128,129,130,131,132,133,134,135,136
135.5,136.0,136.5,137.0,137.5,138.0,138.5
10,7,128.14,134.94,137.85,138.79 !EXP9
127,128,129,130,131,132,133,134,135,136
136.5,137.0,137.5,138.0,138.5,139.0,139.5
10,7,128.14,134.94,138.90,139.88 !EXP10
```

127,128,129,130,131,132,133,134,135,136
137.5,138.0,138.5,139.0,139.5,140.0,140.5
10,7,128.14,134.94,139.99,140.99 !EXP11
127,128,129,130,131,132,133,134,135,136
138.5,139.0,139.5,140.0,140.5,141.0,141.5
10,7,128.14,134.94,141.11,142.15 !EXP12
127,128,129,130,131,132,133,134,135,136
140.5,141.0,141.5,142.0,142.5,143.0,143.5
10,7,128.14,134.94,142.27,143.34 !EXP13
127,128,129,130,131,132,133,134,135,136
141.5,142.0,142.5,143.0,143.5,144.0,144.5
10,7,128.14,134.94,143.47,144.57 !EXP14
127,128,129,130,131,132,133,134,135,136
142.5,143.0,143.5,144.0,144.5,145.0,145.5
10,7,128.14,134.94,144.70,145.84 !EXP15
127,128,129,130,131,132,133,134,135,136
143.5,144.0,144.5,145.0,145.5,146.0,146.5
10,7,128.14,134.94,145.98,147.15 !EXP16
127,128,129,130,131,132,133,134,135,136
145.0,145.5,146.0,146.5,147.0,147.5,148.0
10,7,128.14,134.94,147.29,148.50 !EXP17
127,128,129,130,131,132,133,134,135,136
146.5,147.0,147.5,148.0,148.5,149.0,149.5
10,7,128.14,134.94,148.64,149.89 !EXP18
127,128,129,130,131,132,133,134,135,136
147.5,148.0,148.5,149.0,149.5,150.0,150.5
10,7,128.14,134.94,150.04,151.32 !EXP19
127,128,129,130,131,132,133,134,135,136
149.0,149.5,150.0,150.5,151.0,151.5,152.0
10,7,128.14,134.94,151.47,152.79 !EXP20
127,128,129,130,131,132,133,134,135,136
150.5,151.0,151.5,152.0,152.5,153.0,153.5
10,7,128.14,134.94,152.94,154.30 !EXP21
127,128,129,130,131,132,133,134,135,136
152.0,152.5,153.0,153.5,154.0,154.5,155.0
10,7,128.14,134.94,154.46,155.85 !EXP22
127,128,129,130,131,132,133,134,135,136
153.5,154.0,154.5,155.0,155.5,156.0,156.5
10,7,128.14,134.94,156.01,157.44 !EXP23
127,128,129,130,131,132,133,134,135,136
155.0,155.5,156.0,156.5,157.0,157.5,158.0
10,7,128.14,134.94,157.60,159.06 !EXP24
127,128,129,130,131,132,133,134,135,136
156.8,157.3,157.8,158.3,158.8,159.3,159.8
10 !No of stopping powers (dE/dx) at different energies 1
127,128,129,130,131,132,133,134,135,136
6.885,6.874,6.863,6.852,6.841,6.830,6.819,6.808,6.797,6.786
10,10
10
!No of stopping powers (dE/dx) at different energies 2
127,128,129,130,131,132,133,134,135,136
6.885,6.874,6.863,6.852,6.841,6.830,6.819,6.808,6.797,6.786
10,10
10 !No of stopping powers (dE/dx) at different energies 3
127,128,129,130,131,132,133,134,135,136
6.885,6.874,6.863,6.852,6.841,6.830,6.819,6.808,6.797,6.786
10,10
10 !No of stopping powers (dE/dx) at different energies 4
127,128,129,130,131,132,133,134,135,136
6.885,6.874,6.863,6.852,6.841,6.830,6.819,6.808,6.797,6.786

10,10
10 !No of stopping powers (dE/dx) at different energies 5
127,128,129,130,131,132,133,134,135,136
6.885,6.874,6.863,6.852,6.841,6.830,6.819,6.808,6.797,6.786
10,10
10 !No of stopping powers (dE/dx) at different energies 6
127,128,129,130,131,132,133,134,135,136
6.885,6.874,6.863,6.852,6.841,6.830,6.819,6.808,6.797,6.786
10,10
10 !No of stopping powers (dE/dx) at different energies 7
127,128,129,130,131,132,133,134,135,136
6.885,6.874,6.863,6.852,6.841,6.830,6.819,6.808,6.797,6.786
10,10
10 !No of stopping powers (dE/dx) at different energies 8
127,128,129,130,131,132,133,134,135,136
6.885,6.874,6.863,6.852,6.841,6.830,6.819,6.808,6.797,6.786
10,10
10 !No of stopping powers (dE/dx) at different energies 9
127,128,129,130,131,132,133,134,135,136
6.885,6.874,6.863,6.852,6.841,6.830,6.819,6.808,6.797,6.786
10,10
10 !No of stopping powers (dE/dx) at different energies 10
127,128,129,130,131,132,133,134,135,136
6.885,6.874,6.863,6.852,6.841,6.830,6.819,6.808,6.797,6.786
10,10
10 !No of stopping powers (dE/dx) at different energies 11
127,128,129,130,131,132,133,134,135,136
6.885,6.874,6.863,6.852,6.841,6.830,6.819,6.808,6.797,6.786
10,10
10 !No of stopping powers (dE/dx) at different energies 12
127,128,129,130,131,132,133,134,135,136
6.885,6.874,6.863,6.852,6.841,6.830,6.819,6.808,6.797,6.786
10,10
10 !No of stopping powers (dE/dx) at different energies 13
127,128,129,130,131,132,133,134,135,136
6.885,6.874,6.863,6.852,6.841,6.830,6.819,6.808,6.797,6.786
10,10
10 !No of stopping powers (dE/dx) at different energies 14
127,128,129,130,131,132,133,134,135,136
6.885,6.874,6.863,6.852,6.841,6.830,6.819,6.808,6.797,6.786
10,10
10 !No of stopping powers (dE/dx) at different energies 15
127,128,129,130,131,132,133,134,135,136
6.885,6.874,6.863,6.852,6.841,6.830,6.819,6.808,6.797,6.786
10,10
10 !No of stopping powers (dE/dx) at different energies 16
127,128,129,130,131,132,133,134,135,136
6.885,6.874,6.863,6.852,6.841,6.830,6.819,6.808,6.797,6.786
10,10
10 !No of stopping powers (dE/dx) at different energies 17
127,128,129,130,131,132,133,134,135,136
6.885,6.874,6.863,6.852,6.841,6.830,6.819,6.808,6.797,6.786
10,10
10 !No of stopping powers (dE/dx) at different energies 18
127,128,129,130,131,132,133,134,135,136
6.885,6.874,6.863,6.852,6.841,6.830,6.819,6.808,6.797,6.786
10,10
10 !No of stopping powers (dE/dx) at different energies 19
127,128,129,130,131,132,133,134,135,136
6.885,6.874,6.863,6.852,6.841,6.830,6.819,6.808,6.797,6.786

10,10
10 !No of stopping powers (dE/dx) at different energies 20
127,128,129,130,131,132,133,134,135,136
6.885,6.874,6.863,6.852,6.841,6.830,6.819,6.808,6.797,6.786
10,10
10 !No of stopping powers (dE/dx) at different energies 21
127,128,129,130,131,132,133,134,135,136
6.885,6.874,6.863,6.852,6.841,6.830,6.819,6.808,6.797,6.786
10,10
10 !No of stopping powers (dE/dx) at different energies 22
127,128,129,130,131,132,133,134,135,136
6.885,6.874,6.863,6.852,6.841,6.830,6.819,6.808,6.797,6.786
10,10
10 !No of stopping powers (dE/dx) at different energies 23
127,128,129,130,131,132,133,134,135,136
6.885,6.874,6.863,6.852,6.841,6.830,6.819,6.808,6.797,6.786
10,10
10 !No of stopping powers (dE/dx) at different energies 24
127,128,129,130,131,132,133,134,135,136
6.885,6.874,6.863,6.852,6.841,6.830,6.819,6.808,6.797,6.786
10,10
OP,EXIT

Appendix C

Sort Code

C.1 MTsort-MIDAS Sorting Code

```
 *formats
clover[1:8](e1, e2, e3, e4, x1, x2, x3, x4)
sect[21:52](e1, x1)
ring[53:77](e1, x1)

 *data
! ##################_CLOVER_CALIBRATION_ ############
Gainarray SegA
1 (1.83394 0.408693 0.000)
2 (1.70136 0.557025 0.000)
3 (1.18043 0.389165 0.000)
4 (0.886919 0.384527 0.000)
5 (0.331059 0.365618 0.000)
6 (1.39831 0.37031 0.000)
7 (1.59156 0.570186 0.000)
8 (0.992269 0.368534 0.000)

Gainarray SegB
1 (0.673453 0.380931 0.000)
2 (0.212467 0.538783 0.000)
3 (-0.188039 0.372385 0.000)
```

```
4 (1.69734 0.393348 0.000)
5 (1.90463 0.378482 0.000)
6 (2.42458 0.371312 0.000)
7 (1.42867 0.541504 0.000)
8 (0.792749 0.38332 0.000)

Gainarray SegC
1 (1.80567 0.413765 0.000)
2 (0.722882 0.377488 0.000)
3 (0.5081 0.468408 0.000)
4 (1.96008 0.671295 0.000)
5 (2.2955 0.360906 0.000)
6 (0.267175 0.165661 0.000)
7 (0.558599 0.356025 0.000)
8 (0.856782 0.590274 0.000)

Gainarray SegD
1 (0.783868 0.414408 0.000)
2 (0.649476 0.424103 0.000)
3 (0.444089 0.400237 0.000)
4 (-0.950817 0.385935 0.000)
5 (1.97191 0.362656 0.000)
6 (2.07927 0.361093 0.000)
7 (0.855453 0.525096 0.000)
8 (0.707279 0.358627 0.000)

! #############_RING_AND SECTOR_CALIBRATION_ #######

Gainarray ring
53 (-1480.51 55.96 0.000)
54 (-1386.30 55.56 0.000)
55 (-1463.04 55.43 0.000)
56 (-1630.03 55.33 0.000)
57 (-1425.59 53.78 0.000)
58 (-1401.63 53.92 0.000)
59 (-1378.37 53.64 0.000)
60 (-1370.08 53.97 0.000)
61 (-1315.35 52.77 0.000)
62 (-1305.59 51.68 0.000)
63 (-1324.73 51.42 0.000)
64 (-1268.14 50.29 0.000)
65 (-1260.23 50.71 0.000)
66 (-1263.90 50.25 0.000)
67 (-1219.31 50.29 0.000)
```

```
68 (-1196.17 49.76 0.000)
69 (-1183.95 47.94 0.000)
70 (-1169.82 48.11 0.000)
71 (-1154.12 48.75 0.000)
72 (-1135.16 48.74 0.000)
73 (-1112.48 48.71 0.000)
74 (-1097.21 47.11 0.000)
75 (-1028.39 46.36 0.000)
76 (-1098.76 46.86 0.000)
77 (0.00 0.00 0.000)

Gainarray sect
21 (-1432.76 13.57 0.000)
22 (-1424.86 13.59 0.000)
23 (-1452.52 13.73 0.000)
24 (-1407.39 13.55 0.000)
25 (-1402.48 13.37 0.000)
26 (-1392.92 13.43 0.000)
27 (-1377.02 13.18 0.000)
28 (-1364.38 13.53 0.000)
29 (-1358.33 13.03 0.000)
30 (-1354.24 13.26 0.000)
31 (-1346.28 13.33 0.000)
32 (-1363.99 13.16 0.000)
33 (-1345.68 13.29 0.000)
34 (-1349.20 13.19 0.000)
35 (-1364.05 13.30 0.000)
36 (-1355.87 13.65 0.000)
37 (-1359.88 13.03 0.000)
38 (-1371.67 13.16 0.000)
39 (-1381.07 13.10 0.000)
40 (-1396.49 13.20 0.000)
41 (-1403.94 13.52 0.000)
42 (-1415.33 13.33 0.000)
43 (-1421.40 13.72 0.000)
44 (-1471.96 13.83 0.000)
45 (-1440.50 13.37 0.000)
46 (-1488.10 13.62 0.000)
47 (-1447.95 13.94 0.000)
48 (-1450.28 13.92 0.000)
49 (-1447.45 13.56 0.000)
50 (-1445.58 13.50 0.000)
51 (-1444.84 13.32 0.000)
52 (0.00 0.00 0.000)
```

```
! ##############_VARIABLE_DECLARATIONS_ #############

longlong tg = 0, ts = 0, tr = 0, td = 0, tga = 0, tgb = 0, tgc = 0, tgd = 0, tdr = 0, tds = 0
longlong tss1 = 0, trr1 = 0, tdgr = 0,  tdgs = 0, tdddd = 0
float  xa, xbb, xc, xd, xb, ya, ybb, yc, yd, yb, za, zbb, zc, zd, zb, caa, cab, cac, cad
valuearray tg1[1:8]
0 0 0 0 0 0 0 0
valuearray energyg1[1:8]
0 0 0 0 0 0 0 0
valuearray tg2[1:8]
0 0 0 0 0 0 0 0
valuearray energyg2[1:8]
0 0 0 0 0 0 0 0
valuearray tg3[1:8]
0 0 0 0 0 0 0 0
valuearray energyg3[1:8]
0 0 0 0 0 0 0 0
valuearray tg4[1:8]
0 0 0 0 0 0 0 0
valuearray energyg4[1:8]
0 0 0 0 0 0 0 0
valuearray sum[1:8]
0 0 0 0 0 0 0 0
valuearray nrr[1:24]
0 0 0 0 0 0 0 0
0 0 0 0 0 0 0 0
0 0 0 0 0 0 0 0
valuearray nss[1:32]
0 0 0 0 0 0 0 0
0 0 0 0 0 0 0 0
0 0 0 0 0 0 0 0
0 0 0 0 0 0 0 0
valuearray energyr[1:24]
0 0 0 0 0 0 0 0
0 0 0 0 0 0 0 0
0 0 0 0 0 0 0 0
valuearray energys[1:32]
0 0 0 0 0 0 0 0
0 0 0 0 0 0 0 0
0 0 0 0 0 0 0 0
0 0 0 0 0 0 0 0
valuearray tr1[1:24]
0 0 0 0 0 0 0 0
```

```
0 0 0 0 0 0 0 0
0 0 0 0 0 0 0 0
valuearray ts1[1:32]
0 0 0 0 0 0 0 0
0 0 0 0 0 0 0 0
0 0 0 0 0 0 0 0
0 0 0 0 0 0 0 0
valuearray  sumdop[1:8]
0 0 0 0 0 0 0 0
valuearray  sumdopx[1:8]
0 0 0 0 0 0 0 0
valuearray  sumnodop[1:8]
0 0 0 0 0 0 0 0
valuearray  sumnodopx[1:8]
0 0 0 0 0 0 0 0
valuearray  e11ca[1:8]
0 0 0 0 0 0 0 0
valuearray  e11cb[1:8]
0 0 0 0 0 0 0 0
valuearray  e11cc[1:8]
0 0 0 0 0 0 0 0
valuearray  e11cd[1:8]
0 0 0 0 0 0 0 0
valuearray  x_1[1:8]
0 0 0 0 0 0 0 0
valuearray  x_2[1:8]
0 0 0 0 0 0 0 0
valuearray  x_3[1:8]
0 0 0 0 0 0 0 0
valuearray  x_4[1:8]
0 0 0 0 0 0 0 0
valuearray  y_1[1:8]
0 0 0 0 0 0 0 0
valuearray  y_2[1:8]
0 0 0 0 0 0 0 0
valuearray  y_3[1:8]
0 0 0 0 0 0 0 0
valuearray  y_4[1:8]
0 0 0 0 0 0 0 0
valuearray  z_1[1:8]
0 0 0 0 0 0 0 0
valuearray  z_2[1:8]
0 0 0 0 0 0 0 0
valuearray  z_3[1:8]
```

```
0 0 0 0 0 0 0 0
valuearray  z_4[1:8]
0 0 0 0 0 0 0 0
valuearray sumdr[1:24]
0 0 0 0 0 0 0 0
0 0 0 0 0 0 0 0
0 0 0 0 0 0 0 0
valuearray sumndr[1:24]
0 0 0 0 0 0 0 0
0 0 0 0 0 0 0 0
0 0 0 0 0 0 0 0
valuearray sumdrab[1:24]
0 0 0 0 0 0 0 0
0 0 0 0 0 0 0 0
0 0 0 0 0 0 0 0
valuearray eegdop[1:9]
0 0 0 0 0 0 0 0 0
float  pi = 3.14

! #######_DETECTOR_DISTANCES_FROM_TARGET_ #########

float  d_target2ge = 19.60, d_target2s3 = -3.00

! ############_THETA_ANGLE_OF_CLOVERS_ ##############

valuearray ge_theta[1:8]
1.57080 1.57080 1.57080 1.57080 2.35620 2.35620 2.35620 1.57080

! #############_PHI_ANGLE_OF_CLOVERS_ ###############

valuearray ge_phi[1:8]
1.57080 0.78540 3.92700 5.49779 0.00000 4.71239 0.78540 4.71239

! #############_THETA_ANGLE_OF_RINGS_ ###############

valuearray angdis[1:24]
2.7391 2.70968 2.68103 2.65317 2.62612 2.59986
2.57442 2.54977 2.52591 2.50282 2.48051 2.45894
2.4381 2.41798 2.39854 2.37978 2.36166 2.34417
2.32729 2.31098 2.29524 2.28005 2.26537 2.25119

! ######################_BETA_ ######################

valuearray beta[1:24]
```

```
0.061 0.061 0.061 0.061 0.061 0.061
0.061 0.061 0.061 0.061 0.061 0.061
0.061 0.061 0.061 0.061 0.061 0.061
0.061 0.061 0.061 0.061 0.061 0.061

! ##############_PHI_ANGLE_OF_SECTORS_ ##############

valuearray sec_phi[1:32]
0.09817 0.29452 0.49087 0.68722 0.88357 1.07992 1.27627 1.47262
1.66897 1.86532 2.06167 2.25802 2.45437 2.65072 2.84707 3.04342
3.23977 3.43612 3.63247 3.82882 4.02516 4.22152 4.41786 4.61421
4.81056 5.00691 5.20326 5.39961 5.59596 5.79231 5.98866 6.18501

! ############_THETA_ANGLE_OF_CRISTALS_ #############

valuearray crys_a_theta[1:8]
1.48 1.48 1.48 1.48 2.27 2.27 2.27 1.48
valuearray crys_b_theta[1:8]
1.66 1.66 1.66 1.66 2.45 2.45 2.45 1.66
valuearray crys_d_theta[1:8]
1.66 1.66 1.66 1.66 2.45 2.45 2.45 1.66
valuearray crys_c_theta[1:8]
1.48 1.48 1.48 1.48 2.27 2.27 2.27 1.48

! #############_PHI_ANGLE_OF_CRISTALS_ ##############

valuearray crys_a_phi[1:8]
1.66 0.87 4.02 5.59 0.09 4.80 0.87 4.80
valuearray crys_c_phi[1:8]
1.66 0.87 4.02 5.59 0.09 4.80 0.87 4.80
valuearray crys_b_phi[1:8]
1.48 0.69 3.84 5.41 6.19 4.62 0.69 4.62
valuearray crys_d_phi[1:8]
1.48 0.69 3.84 5.41 6.19 4.62 0.69 4.62

! #################_INELASTIC_GATES_ ################

valuearray inelas_max[1:24]
15494 15298 15354 15354 15214 15186
15046 15102 15074 15046 15906 14878
14617 14661 14550 14572 14572 14528
14572 14550 14350 14394 14528 14261
valuearray inelas_min[1:24]
6224 6275 6552 6249 6501 6602
```

```
6048 6375 6527 5796 5451 6249
5794 5741 5426 5479 5374 5321
5164 5032 5006 5269 4849 5059

*spectra
! ###############_SPECTRUM_DEFINITIONS_ ############

!rclovera: gamma spectra for crystal a
!rcloverb: gamma spectra for crystal b
!rcloverc: gamma spectra for crystal c
!rcloverd: gamma spectra for crystal  d
!sectors: particle energy spectra for sectors
!ring:particle energy spectra for sectors
!hitpatg: hitpattern for Ge detectors
!hitpatr: hitpattern for rings
!hitpats: hitpattern for sectors
!timesi: ring and time difference spectrum
!timeg1: ring and gamma time difference spectrum
!timeg2: sector and gamma time difference spectrum
!ge_sum_no_dopplerr: non Doppler corrected gamma spectra for
 individual rings and all clovers (after conditions)
!ge_sum_no_doppler: non Doppler corrected gamma spectra for all
 rings and all clovers (after conditions)
!ge_sum_no_dopplerr2: non Doppler corrected gamma spectra for
individual rings (after conditions)
!ge_sum_no_doppler2: non Doppler corrected gamma spectra for all
 rings (after conditions)
!ge_sum_dopplerr: Doppler corrected gamma spectra for individual
 rings and all clovers (after conditions)
!ge_sum_doppler: Doppler corrected gamma spectra for all rings and
 all clovers (after conditions)
!ge_sum_dopplerr2: Doppler corrected gamma spectra for individual
rings (after conditions)
!ge_sum_doppler2: Doppler corrected gamma spectra for all
rings (after conditions)
!ge_sum_doppleraddbb[1:24]: Doppler corrected gamma spectra for
 each ring (after conditions)
!ge_sum_doppleraddb:add back Doppler corrected gamma spectra for
 all rings (after conditions)
!2D ring-gamma histogram (ring-gamma time difference (x-axis) & sum
 of all clover energies (y-axis))
!2D sector-gamma histogram (sector-gamma time difference (x-axis) &
sum of all clover energies (y-axis))
!si_mat: 2d si matrix (sector energy (x axis) & ring energy (y axis))
```

```
rclovera[1:8] 16384
rcloverb[1:8] 16384
rcloverc[1:8] 16384
rcloverd[1:8] 16384
sectors[1:32] 65536
rings[1:24] 65536
hitpatg 108 32
hitpatr 108 32
hitpats 64 32
timesi 4096 32
timeg1 4096 32
timeg2 4096 32
ge_sum_no_dopplerr[1:24] 16384 32
ge_sum_no_doppler 16384 32
ge_sum_no_dopplerr2[1:24] 16384 32
ge_sum_no_doppler2 16384 32
ge_sum_dopplerr[1:24] 16384 32
ge_sum_doppler 16384 32
ge_sum_dopplerr2[1:24] 16384 32
ge_sum_doppler2 16384 32
ge_sum_doppleraddbb[1:24] 16384 32
ge_sum_doppleraddb 16384 32
matdgr  2048 2d
matdgs  2048 2d
si_mat  4096 2d
eeg 4096 32
eegdc 4096 32
si_matdc 4096 2d

*commands
! ##################_COMMANDS_ ####################

doloop i from 1  to 32 step +1
{
 energys(i) =  0
 ts1(i) =  0
}
 doloop i from 1  to 24 step +1
{
 energyr(i) =  0
 tr1(i) =  0
 sumndr(i) =  0
 sumdr(i) =  0
```

```
 sumdrab(i) =  0
}
 doloop i from 1  to 8 step +1
{
 sum(i) =  0
 sumnodop(i) =  0
 sumdop(i) =  0
 eegdop(i) =  0
energyg1(i)=0
 tg1(i) = 0
 e11ca(i) =  0
 e11cb(i) =  0
 e11cc(i) =  0
 e11cd(i) =  0
energyg2(i)=0
 tg2(i) = 0
 x_1(i) =  0
 x_2(i) =  0
 x_3(i) =  0
 x_4(i) =  0
energyg3(i)=0
 tg3(i) = 0
 y_1(i) =  0
 y_2(i) =  0
 y_3(i) =  0
 y_4(i) =  0
energyg4(i)=0
 tg4(i) = 0
 z_1(i) =  0
 z_2(i) =  0
 z_3(i) =  0
 z_4(i) =  0
}
 ns  =  0
 nr  =  0
 nga  =  0
 ngb  =  0
 ngc  =  0
 ngd  =  0

createlist glist from clover
createlist slist from sect
createlist rlist from ring
```

```
gain glist.e1 segA factor 1.00
gain glist.e2 segB factor 1.00
gain glist.e3 segC factor 1.00
gain glist.e4 segD factor 1.00

loopif $g1=glist.e1 gt 0
{
  g = group($g1)
  inc hitpatg(g)
  energyg1(g)=$g1.e1
  inc rclovera($g1.e1) indexed g
  tg=timestampof($g1.e1)
  tg1(g) = timestampof($g1.e1)
  sum(g) = sum(g) + $g1.e1
}
loopif $g2=glist.e2 gt 0
{
  g = group($g2)
  inc hitpatg(g)
  energyg2(g)=$g2.e2
  inc rcloverb($g2.e2) indexed g
  tg=timestampof($g2.e2)
  tg2(g) = timestampof($g2.e2)
  sum(g) = sum(g) + $g2.e2
}
loopif $g3=glist.e3 gt 0
{
  g = group($g3)
  inc hitpatg(g)
  energyg3(g)=$g3.e3
  inc rcloverc($g3.e3) indexed g
  tg=timestampof($g3.e3)
  tg3(g) = timestampof($g3.e3)
  sum(g) = sum(g) + $g3.e3
}
loopif $g4=glist.e4 gt 0
{
  g = group($g4)
  inc hitpatg(g)
  energyg4(g)=$g4.e4
  inc rcloverd($g4.e4) indexed g
  tg=timestampof($g4.e4)
  tg4(g) = timestampof($g4.e4)
  sum(g) = sum(g) + $g4.e4
```

```
}

gain slist.e1 sect factor 1.00
gain rlist.e1 ring factor 1.00

!*******_BROAD_ENERGY_GATES_CONDITION_**********

loopif $r=rlist.e1 passes (5500,16384)
{
  g = group($r) - 52
  inc hitpatr(g)
  energyr(g) = $r.e1
  inc rings($r.e1) indexed g
  tr = timestampof($r.e1)
  tr1(g) = timestampof($r.e1)
  trr1 = tr1(g)
  nr=nr + 1
}
loopif $s=slist.e1 passes (5497,17671)
{
  g = group($s) - 20
  inc hitpats(g)
  energys(g) = $s.e1
  inc sectors($s.e1) indexed g
  ts = timestampof($s.e1)
  ts1(g) = timestampof($s.e1)
  tss1 = ts1(g)
  ns=ns + 1
}
td=(ts-tr)+1024
inc timesi(td)
td=(tg-tr)+1024
inc timeg1(td)
td=(tg-ts)+1024
inc timeg2(td)
doloop iii from 1  to 32 step +1
{
 es  =  energys(iii)
 tss  =  ts
 nsss  =  nss(iii)
if es gt 10
 {
 ss  =  iii
 es1  =  energys(ss)
```

```
 }
}
if ns eq 1
 {
 nsss  =  ns
 }
doloop ii from 1  to 24 step +1
{
 er  =  energyr(ii)
 trr  =  tr
 nrrr  =  nrr(ii)
if er gt 10
 {
 rr  =  ii
 imax  =  inelas_max(ii)
 imin  =  inelas_min(ii)
 er1  =  energyr(rr)
 }
}
if nr eq 1
 {
 nrrr  =  nr
 }
c_si  =  nr + ns
td = (tss-trr) +1024

!******_PARTICLE_COINCIDENCE_CONDITION_**********

if td passes (976,1082)
 {
if c_si eq 2
 {
inc si_mat(es1/4,er1/4)
ee = ABS(es1-er1)
inc eeg(ee)

!**********_ENERGY_SHARE_CONDITION_****

if ee lt  1461     !2500
{
inc si_matdc(es1/4,er1/4)

!*********_INELASTIC_GATE_CONDITION_***
```

```
!if er1 lt  imax
! {
! if er1 gt  imin
!  {

!--------------------------_DOPPLER_CORRECTION_-----------------------------

 ee123  =  0
 ecad  =  0
 ee312  =  0
 ecbd  =  0
 ee321  =  0
 eccd  =  0
 ee213  =  0
 ecdd  =  0
doloop i from 1 to 8 step +1
{

!-------------- -_TRANSFORMATION_MATRIX_FOR_S3_DETECTOR_CRISTAL_A_-----------

xb = d_target2s3*sin(sec_phi(ss))*sin(angdis(rr))
yb = d_target2s3*sin(angdis(rr))
zb = d_target2s3*cos(sec_phi(ss))*sin(angdis(rr))
ee123  =  energyg1(i)
if ee123 gt 0
{

!---------------_TRANSFORMATION_MATRIX_FOR_GE_DETECTOR_CRISTAL_A_-------------

x_1(i)=d_target2ge*sin(crys_a_phi(i))*sin(crys_a_theta(i))
 xa  =  x_1(i)
y_1(i)=d_target2ge*cos(crys_a_theta(i))
 ya  =  y_1(i)
z_1(i)=d_target2ge*cos(crys_a_phi(i))*sin(crys_a_theta(i))
 za  =  z_1(i)
}
caa=(xa*xb+ya*yb+za*zb)/(sqrt(xa*xa+ya*ya+za*za)*sqrt(xb*xb+yb*yb+zb*zb))

!---------------_ENERGY_DOPPLER_CORRECTED_CRYSTAL_A_--------------------------

e11ca(i)=energyg1(i)*(1-beta(rr)*caa)/sqrt(1-beta(rr)*beta(rr))
ecad=e11ca(i)
 tgg  =  tg1(i)
 trr  =  tr1(rr)
```

```
 tss  =  ts1(ss)
 tdgs  =  (tgg - tss) +1024
 tddd  =  (tgg - trr) +1024

!**********_PARTICLE_GAMMA_COINCIDENCE_CONDITION_CRYSTAL_A_**********

if tdgs passes (1142,1247)
 {
if tddd passes (1142,1247)
 {
sumdr(rr)=sumdr(rr)+ecad
sumndr(rr)=sumndr(rr)+ee123
sumnodop(i)=sumnodop(i)+ee123
sumdop(i)=sumdop(i)+ecad
 }
}
 ee312  =  energyg2(i)
if ee312 gt 0
{
x_2(i)=d_target2ge*sin(crys_b_phi(i))*sin(crys_b_theta(i))
 xbb  =  x_2(i)
y_2(i)=d_target2ge*cos(crys_b_theta(i))
 ybb  =  y_2(i)
z_2(i)=d_target2ge*cos(crys_b_phi(i))*sin(crys_b_theta(i))
 zbb  =  z_2(i)
}
cab=(xbb*xb+ybb*yb+zbb*zb)/(sqrt(xbb*xbb+ybb*ybb+zbb*zbb)*sqrt(xb*xb+yb*yb+zb*zb))
e11cb(i)=energyg2(i)*(1-beta(rr)*cab)/sqrt(1-beta(rr)*beta(rr))
ecbd=e11cb(i)
 tgg  =  tg2(i)
 trr  =  tr1(rr)
 tss  =  ts1(ss)
 tdgs  =  (tgg - tss) +1024
 tddd  =  (tgg - trr) +1024
if tdgs passes (1142,1247)
 {
if tddd passes (1142,1247)
 {
sumdr(rr)=sumdr(rr)+ecbd
sumndr(rr)=sumndr(rr)+ee312
sumnodop(i)=sumnodop(i)+ee312
sumdop(i)=sumdop(i)+ecbd
 }
}
```

```
 ee321  =  energyg3(i)
if ee321 gt 0
{
x_3(i)=d_target2ge*sin(crys_c_phi(i))*sin(crys_c_theta(i))
 xc  =  x_3(i)
y_3(i)=d_target2ge*cos(crys_c_theta(i))
 yc  =  y_3(i)
z_3(i)=d_target2ge*cos(crys_c_phi(i))*sin(crys_c_theta(i))
 zc  =  z_3(i)
}
cac=(xc*xb+yc*yb+zc*zb)/(sqrt(xc*xc+yc*yc+zc*zc)*sqrt(xb*xb+yb*yb+zb*zb))
e11cc(i)=energyg3(i)*(1-beta(rr)*cac)/sqrt(1-beta(rr)*beta(rr))
eccd=e11cc(i)
 tgg  =  tg3(i)
 trr  =  tr1(rr)
 tss  =  ts1(ss)
 tdgs  =  (tgg - tss) +1024
 tddd  =  (tgg - trr) +1024
if tdgs passes (1142,1247)
 {
if tddd passes (1142,1247)
 {
sumdr(rr)=sumdr(rr)+eccd
sumndr(rr)=sumndr(rr)+ee321
sumnodop(i)=sumnodop(i)+ee321
sumdop(i)=sumdop(i)+eccd
 }
}
 ee213  =  energyg4(i)
if ee213 gt 0
{
x_4(i)=d_target2ge*sin(crys_d_phi(i))*sin(crys_d_theta(i))
 xd  =  x_4(i)
y_4(i)=d_target2ge*cos(crys_d_theta(i))
 yd  =  y_4(i)
z_4(i)=d_target2ge*cos(crys_d_phi(i))*sin(crys_d_theta(i))
 zd  =  z_4(i)
}
cad=(xd*xb+yd*yb+zd*zb)/(sqrt(xd*xd+yd*yd+zd*zd)*sqrt(xb*xb+yb*yb+zb*zb))
e11cd(i)=energyg4(i)*(1-beta(rr)*cad)/sqrt(1-beta(rr)*beta(rr))
ecdd=e11cd(i)
 tgg  =  tg4(i)
 trr  =  tr1(rr)
 tss  =  ts1(ss)
```

```
 tdgs  =  (tgg - tss) +1024
 tddd  =  (tgg - trr) +1024
if tdgs passes (1142,1247)
 {
if tddd passes (1142,1247)
 {
sumdr(rr)=sumdr(rr)+ecdd
sumndr(rr)=sumndr(rr)+ee213
sumnodop(i)=sumnodop(i)+ee213
sumdop(i)=sumdop(i)+ecdd
 }
}
 sndop  =  sumnodop(i)
 sndopr  =  sumndr(rr)
 sdop  =  sumdop(i)
 sdopr  =  sumdr(rr)
if sndop passes (1,16384)
 {
inc   ge_sum_no_dopplerr(sndop) indexed rr
inc   ge_sum_no_doppler(sndop)
 }
if sndopr passes (1,16384)
 {
inc   ge_sum_no_dopplerr2(sndopr) indexed rr
inc   ge_sum_no_doppler2(sndopr)
 }
if sdop passes (1,16384)
 {
inc   ge_sum_dopplerr(sdop) indexed rr
inc   ge_sum_doppler(sdop)
inc   eegdc(ee)
 }
if sdopr passes (1,16384)
 {
inc   ge_sum_dopplerr2(sdopr) indexed rr
inc   ge_sum_doppler2(sdopr)
 }
eegdop(i)=e11ca(i) + e11cb(i) + e11cc(i) + e11cd(i)
 eegdop1  =  eegdop(i)
 tddd  =  (tg - trr) +1024
 tddd2  =  (tg - tss) +1024
sumdrab(rr)=sumdrab(rr)+eegdop1
 sdopaddb  =  sumdrab(rr)
if sdopaddb passes (1,16364)
```

```
 {
inc   matdgr(tddd,sdopaddb)
inc   matdgs(tddd2,sdopaddb)
inc   ge_sum_doppleraddbb(sdopaddb)  indexed rr
inc   ge_sum_doppleraddb(sdopaddb)
 }
 }
 }
 }
}
!}
!}

*runfiles
! ##################_RUN_FILES_ ####################

DISC /home/hornam/Desktop/masters/run_files/R6_0
DISC /home/hornam/Desktop/masters/run_files/R8_0
DISC /home/hornam/Desktop/masters/run_files/R9_0
DISC /home/hornam/Desktop/masters/run_files/R12_0
DISC /home/hornam/Desktop/masters/run_files/R13_0
DISC /home/hornam/Desktop/masters/run_files/R18_0
DISC /home/hornam/Desktop/masters/run_files/R19_0
DISC /home/hornam/Desktop/masters/run_files/R21_0

*finish
```

Appendix D

iThemba LABS Accelerator Facility

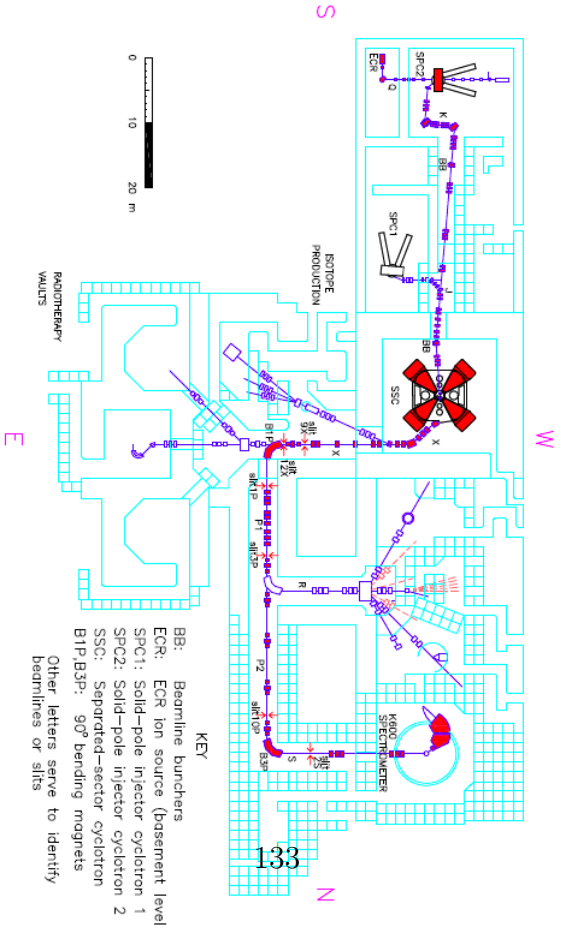

Figure D.1

Bibliography

[1] V. F. Weisskopf, Phys. Rev. **53**, 1018 (1938).

[2] C. L. McClelland and C. Goodman, Phys. Rev. **91**, 760 (1953).

[3] K. Alder, A. Bohr, T. Huus, B. Mottelson and A. Winther, Phys. Rev. Modern Phys. **28**, 432 (1956).

[4] P. E. Garrett and J. L. Wood, J. Phys. G: Nucl. Part. Phys. **37** 064028 (2010).

[5] John Lilley, *Nuclear Physics Principles and Applications*, Wiley (2005).

[6] H. D. Young, R. A. Freedman, *University Physics*, 11^{th} edition, Pearson (2004).

[7] https://physics.tutorvista.com/modern-physics/rutherford-s-gold-foil-experiment.html.

[8] F. Jourdan, D. F. Mark, and C. Verati. Advances in $^{40}Ar/^{39}Ar$ dating: from archaeology to planetary sciences–introduction (2014).

[9] http://www.rsc.org/periodic-table/element/18/argon.

[10] https://www.iopscience.iop.org/article/10.1088/0954-3899/43/6/064001.

[11] E. Clement *et al.*, Phys. Rev. C **75**, (2007).

[12] http://www.riken.jp/en/research/rikenresearch/highlights/7240/.

[13] R. H. Spear, Phys. Rep. **7**3, 369 (1981).

[14] C. Mehl, *Developing a sorting code for Coulomb excitation data analysis*, UWC (2015).

[15] M. J. Mokgolobotho, *Determining the Spectroscopic Quadrupole*, UWC (2017).

[16] K. Nakai, I. L. Québert, F. S. Stephens and R. M. Diamond, Phys. Rev. Lett. **24**, 903 (1970).

[17] https://www.nndc.bnl.gov/.

[18] N. J. Stone, At. Data Nucl. Data Tables **90**, 75 (2005).

[19] T. Czosnyka, D. Cline and C. Y. Wu, GOSIA manual (2012) www.pas.rochester.edu/cline/Gosia/Gosia_Manual_20120510.pdf.

[20] D. C. Kean, Lecture Notes in Physics (Springer), Volume **92**, 80 (1976).

[21] J. Lilley, Nuclear Physics Principles and Applications, Wiley (2005).

[22] J. P. Elliott and B. H. Flowers, Proc. Ray. Soc. A **242** 57 (1957).

[23] A. Bohr and B R. Mottelson, Nuclear Structure (World Scientific, Singapore 1968, First Published 1969).

[24] K. S. Krane, *Introductory Nuclear Physics*, John Wiley and Sons (1988).

[25] J. L. Wood, K. Heyde, W. Nazarewicz, M. Huyse, and P. Van Duppen. Phys. Rep **215**, 101 (1992).

[26] K. Heyde and J. L. Wood, Rev. Mod. Phys. **83**, 1467 (2011).

[27] A. de Shalit, and I. Talmi, *Nuclear Shell Theory*, Academic Press, New York-London (1963).

[28] A. K. Mallik, Stability of Nuclei, The Himalayan Physics, Vol. II (2011).

[29] J. de Boer, J. Eichler (auth.), M. Baranger, Erich Vogt (eds.) Advances in Nuclear Physics (Springer) Volume 1 US, **1-73** (1968).

[30] K. Alder and A. Bohr, Study of Nuclear Structure by Electromagnetic Excitation with accelerated Ions, Rev. Mod. Phys. **28**, 433-437 (1967).

[31] K. Alder and A. Winther, Mat. Fys. 32, No. 5-8 (1960).

[32] O. Hausser, Nuclear Spectroscopy and Reactions, Part C, edited by J. Cerny (1974).

[33] K. Alder, A. Bohr, T. Huus, B. Mottelson, and A. Winther, Rev. Mod. Phys. **23**, 432 (1956).

[34] K. Alder and A. Winther, Coulomb Excitation, Academic Press, New York (1966).

[35] http://www.optique-ingenieur.org/en/courses/OPI_ang_M05_C02/co/Contenu_02.html.

[36] http://www.rsc.org/periodic-table/.

[37] http://www.micronsemiconductor.co.uk/multi-element-detectors-double-sided/.

[38] http://www.canberra.com/products/detectors/pdf/Clover-Detector-C39840.pdf.

[39] http://www.mesytec.com/datasheets/MHV4.pdf.

[40] http://www.mesytec.com/datasheets/MPR32.pdf.

[41] D. C. Radford, Nucl. Instrum. Meth. Phys. Rev. A **361**, 297 (1995).

[42] P. M. Jones, R. A. Bark, Development of the iThemba LABS Digital Data Acquisition System iThemba LABS annual report (2003).

[43] http://ns.ph.liv.ac.uk/MTsort-manual/MTsort.html.

[44] http://npsg.dl.ac.uk/MIDAS/.

[45] R. Neveling *et al.*, Nucl. Instrum. Meth. Phys. Rev. A **654** (2011) 29–39

[46] W. R. Leo, Techniques for nuclear and particle physics experiment, Springer (1867).

[47] SRIM - The stopping and Range of Ions in Matter ; http//www.srim.org.

[48] E. Storm, H. I. Israel, National Nuclear Data Table, **A7** (1970) 365.

[49] J. N. Orce *et al.*, Phys. Rev. C **86**, 041303(R) (2012).

[50] N. R. Erasmus, *Simulation of Silicon and Diamond detector systems by Geant4 simulation techniques*, UWC (2014).

[51] A. Al-Adili, *Simulations of Doppler Effects in Nuclear Reactions for AGATA Commissioning Experiments*, Uppsala, Sweden (2009).

[52] K. E. G. Löbner, The Electromagnetic Interaction in Nuclear Spectroscopy, edited by W. D. Hamilton.

[53] B. Pritychenko, M. Birch, B. Singh, M. Horoi, Tables of E2 transition probabilities from the first 2^+

[54] D. J. Rowe. Nuclear Collective Motion, Models and Theory (Methuen and Co. LTD, London), 6 - 12, 1970.